1978

Wind Turbine Blade Stress Analysis And Natural Frequencies

F. W. Perkins

Duane E. Cromack

PF 67025F
UC-60
UM-WF-TR-78-8

WIND TURBINE BLADE STRESS ANALYSIS AND NATURAL FREQUENCIES

Technical Report

by

F.W. Perkins and D.E. Cromack

Energy Alternatives Program
University of Massachusetts
Amherst, Massachusetts 01003

August 1978

Prepared for the United States Department of Energy and Rockwell International, Rocky Flats Plant Under Contract Number PF 67025F.

ABSTRACT

There are many problems to be addressed with respect to the design of wind turbine blades. Foremost among these are aerodynamic performance, structural integrity and cost. The subject of aerodynamic performance, at least in the steady state condition, has been dealt with at some length by various investigators. The cost of a blade system is beyond the scope of this paper.

The structural integrity of wind turbine blades must be insured in both the static and dynamic load cases. The critical static load has been determined to be a hurricane wind perpendicular to the blade planform. The dynamic loads include the fluctuating component due to the wind and all blade-support interactions.

Vital to an understanding of these structural problems is a description of the natural frequencies and mode shapes of the blades. These considerations are the subject of this paper. While these characteristics can be computed using existing programs (e.g. NASTRAN) the cost of the repetititve use of those codes is prohibitive for the general user. The enclosed codes are much less expensive to run, and are not as comprehensive. They are, however, closely matched to the needs of the Alternative Energy Program of the School of Engineerinf at the University of Massachusetts, and have been developed to be of use to the small wind energy conversion industry.

TABLE OF CONTENTS

TABLE OF CONTENTS (CONTINUED)

TABLE OF CONTENTS (Continued)

TABLE OF CONTENTS (Continued)

LIST OF TABLES

LIST OF FIGURES

CHAPTER I

RATIONALE

1.1 Description of WF-1 Blades

At the University of Massachusetts, there exists the Wind Furnace I. This machine is a prototype wind turbine which is intended to contribute a large portion of the heat energy required for space heating for the University's Solar Habitat I. The machine has a downwind, three bladed rotor. Each blade is inclined from the plane of rotation by the static coning angle of 10^{o}. Each blade is capable of being pitched through an arc of 93^{o} by the automatic pitch control mechanism.

The blade planform and geometry are described in Figure 1.1. The NACA 4415 airfoil shape was chosen as the exterior profile on each cross section. (The reasons for this choice are partly historical[1.1] and partly based on the popular use of the NACA 4415 airfoil in airplane propellers.) The blades are of 4 part construction (Figure 1.2). The skin is of a relatively low bending modulus composition fiberglass epoxy matrix. The spar is made of a relatively high modulus fiberglass epoxy matrix. The blade stock (Figure 1.1) is surrounded by a steel sleeve. (The intended cross section construction is described in Table 1.1.)

Measurements subsequent to blade construction showed that the cross sections varied considerably from the intended 15% thick airfoil (Table 1.2). Thicknesses as great as 22% were measured on the spare blade of te rotor system. The variation in the chord was slight. It is not, at this time, possible to measure the internal components of the blade to check for uniformity.

FIG.1.1

WF-1 PLANFORM AND TWIST

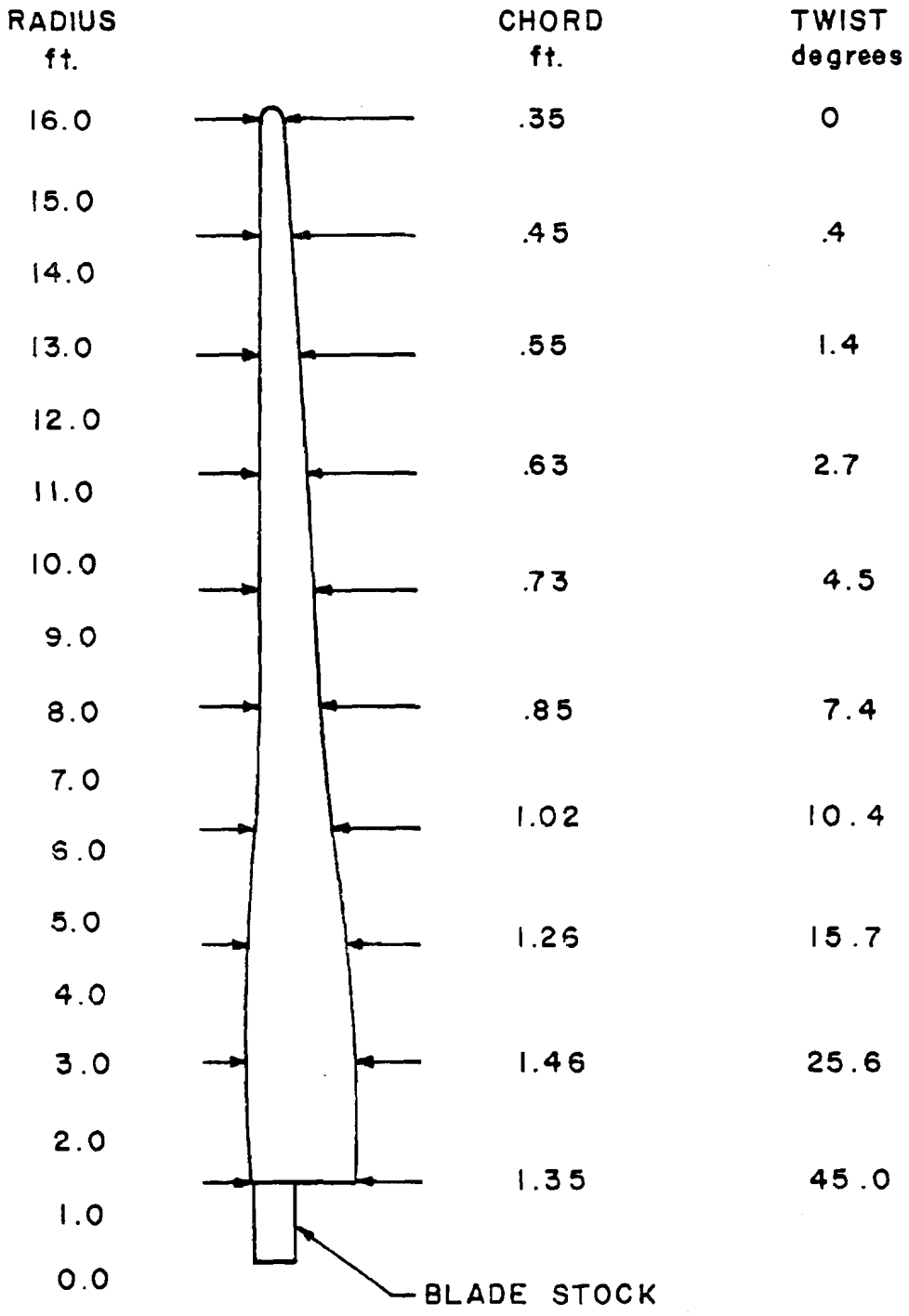

FIG. I.2

DESCRIPTION OF BLADE COMPONENTS

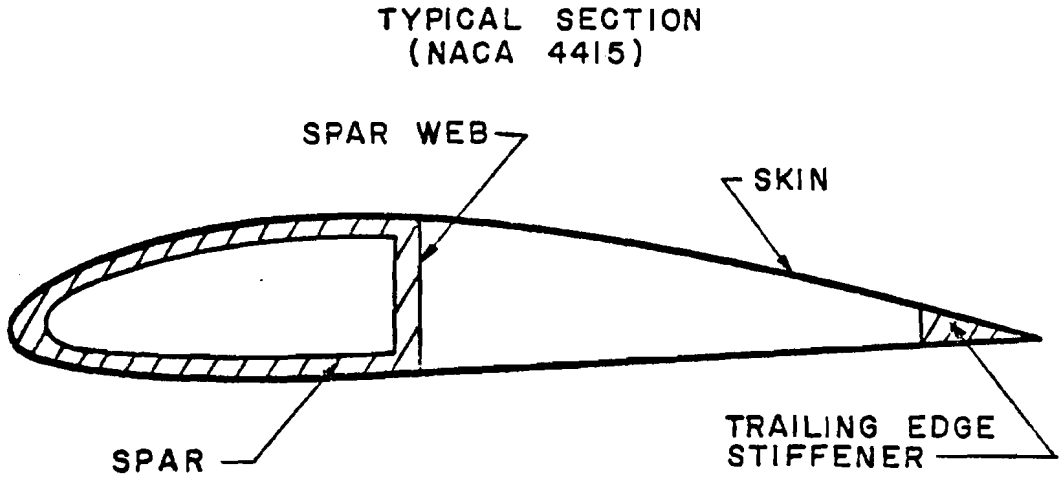

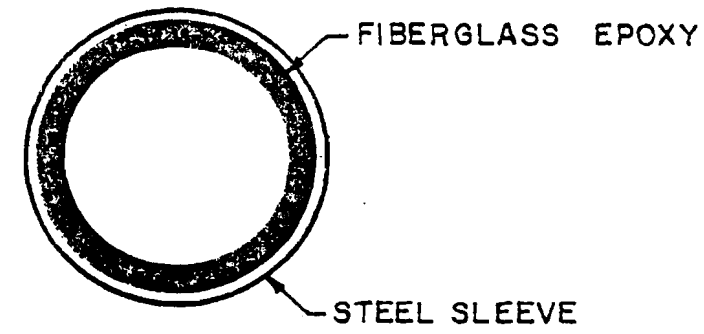

TABLE 1.1

BLADE DESIGN

WF-1 (Radius = 16.25 ft)

r/Radius (Station÷10)	Chord (ft)	Twist (degrees)	L.E. to Spar Web (ft)	Skin Thickness (in)	Spar Thickness (in)	Web Thickness (in)
.1	1.35	45	.54	.036	.238	.238
.2	1.46	25.6	.584	.036	.238	.238
.3	1.26	15.9	.504	.036	.205	.220
.4	1.02	10.4	.41	.036	.205	.150
.5	.85	7.4	.34	.036	.205	.050
.6	.73	4.5	.29	.027	.186	.050
.7	.63	2.7	.25	.027	.148	.050
.8	.55	1.4	.22	.018	.110	.050
.9	.45	.4	.18	.018	.072	.050
1.0	.35	0	.14	.018	.053	.050

$E_{skin} = 2.2 \times 10^6 psi$ $G_{skin} = .5 \times 10^6 psi$ $\rho_{skin} = .0555 \frac{lb}{in^3}$

$E_{spar} = 4.4 \times 10^6 psi$ $G_{spar} = .3 \times 10^6 psi$ $\rho_{spar} = .0501 \frac{lb}{in^3}$

TABLE 1.2

BLADE SHAPE

WF-1 (Radius = 16.25 ft)

	CHORD		AIRFOIL THICKNESS		
$\frac{r}{R}$	Design (in)	Result (in)	Design (in)	Result (in)	Error (%)
.1	16.2	15.8	2.4	5	108
.2	17.5	17.8	2.6	3.0	15.4
.3	15.1	15.5	2.3	2.6	13.0
.4	12.2	12.7	1.8	2.3	27.8
.5	10.2	10.5	1.5	2.0	33.3
.6	8.8	9.0	1.3	1.8	38.5
.7	7.6	7.9	1.1	1.5	36.4
.8	6.6	6.8	1.0	1.4	40.0
.9	5.4	5.5	.81	1.2	48.2
1.0	4.2	3.2	.63	.65	3.2

1.2 Observations on Design

It appears at this time that there is little if anything to be lost in terms of aerodynamic performance if thicker airfoils are used in design.[1.2] In fact, the observed thicknesses of the UMass WF-1 blades and the better than predicted performance tend to confirm this thought.

At this time however, there is no reason to expect that future blade designs will incorporate the same airfoil section at all radial points. It may turn out that specific parameters, e.g. low noise requirements or aeroelastic requirements, require blade shapes both highly twisted and tapered, as well as having various cross-sectional shapes.

The increasing availability of composite materials is a factor of great significance to the designer. Traditional structural materials will certainly continue to play a major role in blade construction. The likelihood of designs incorporating more than one material becoming commonplace is great. In fact, this is now standard practice in the military aircraft propeller industry.

1.3 Program Input Requirements

It is apparent from the foregoing that any comprehensive code for blade bending stress analysis must allow for the following inputs.

1) Cross section exterior shape
2) Cross section interior structure
3) Bending modulus distribution
4) Density distribution
5) Twist distribution
6) Radial spacing

7) Bending axis location

These inputs are sufficient for the bending stress analysis of the blade. (With the addition of the shear modulus, the input would be sufficient for a total stress analysis of the blade. The shear stress is ordinarily of secondary importance in the design of blades. Time does not allow its inclusion here.)

1.4 Program Output Requirements

The parameters of primary interest to the designer must be included in the output. These include

1) Bending stress distributions
2) Deflections under load
3) Mass of blade
4) Mass moment of inertia about axis of rotation
5) Natural frequencies of blade.

All of the above except for 4 and 5 can be uniquely specified. Number 4 is weakly dependent on the mode shape of the natural frequencies. Number 5 is strongly dependent on the means by which the blade is supported. The approach taken is to assume a cantilever beam and to compute the natural frequencies attendent to that configuration. From this point, the dynamacist should be able to predict most of the important system modes.[1.3,1.4]

CHAPTER II

DESCRIPTION OF PROBLEM

2.1 Historical Perspective

Traditionally, windmills have been designed to operate in the stalled aerodynamic mode. Figure 2.1 shows a plot of power versus RPM for a three bladed windmill. On the far left the region of stable stalled operation is indicated. In this mode of operation, all turbines have pretty much the same aerodynamic characteristics. The power output is dependent on the swept area of the rotor, the solidity of the blade system, rpm, etc. It is obvious that much more power can be delivered at the same wind speed by the same rotor if the rotational speed is allowed to increase. The rotor can then gain sufficient speed to allow the blades to "fly," that is to operate at a very low angle of attack with consequent high lift and low drag.

It was not until the early 20th century that airfoil knowledge had progressed sufficiently to allow the construction of efficient propellers and lifting surfaces.

These developments opened the way to powered flight and to the development of modern wind turbines. Since the introduction of airfoils into turbine technology, there have been two major thrusts in blade design.

The first approach, typified by the Smith-Putnam machine,[2.2] has been to de-emphasize aerodynamic sophistication with respect to the cost of untwisted, untapered blades. The penalities that are paid by using these simple blades are slightly (~10%) reduced performance with respect to aerodynamically optimum blades, noise of operation, and the investment of a relatively large amount of material in the blades per unit power. The

FIG. 2.1

POWER Vs. R.P.M.

ref. 2.1

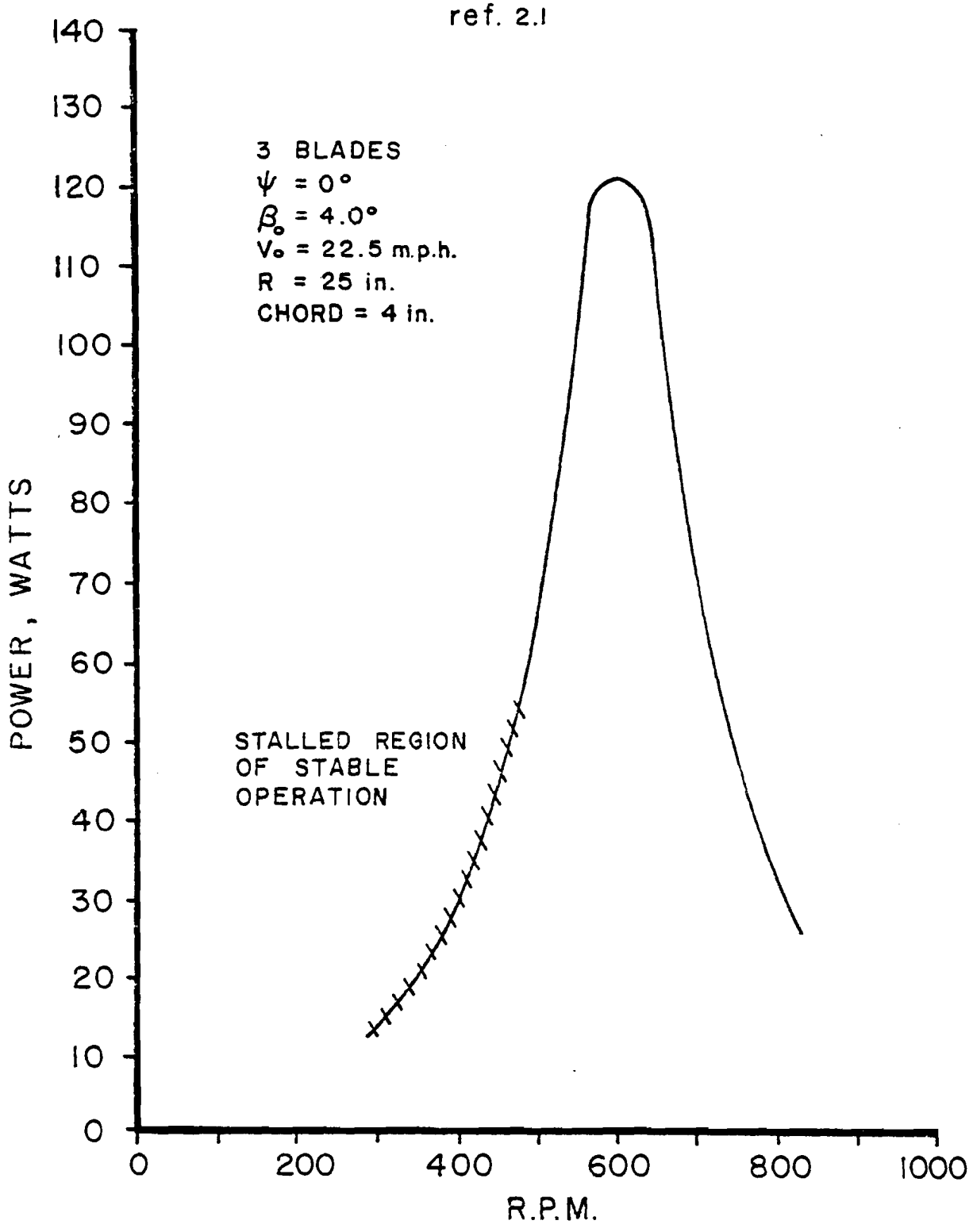

primary benefit is ease of fabrication and consequent low cost.

The second approach, as exemplified by the Hutter, Brace Institute, NASA MOD-0 and UMass machines, is to incorporate both twist and taper into the blade design in an attempt to optimize performance and reduce noise. Much work has been done to characterize the planforms required for optimum or nearly optimum performance over a wide range of design constraints. Recent work by Hutter[2.3], Wilson, Lissamann and Walker[2.4], and Cromack and Lefebvre[2.5] have elucidated these problems.

A serious objection to the above work is that the performance curves were generated using quasi-steady, high Reynold's Number airfoil data. Experience has shown that wind turbines almost never operate at their design point. The nature of the wind is such that the mean wind speed, with no other information, is only marginally adequate to characterize performance. The nature of practical turbines is such that, traditionally, airfoil data has been collected at from 3 to 10 times the Reynold's Number at which most of the power in a wind turbine is produced. (The Reynold's Number, Velocity x Chord ÷ Kinematic Viscosity, varies radially along blade. Most of the turbine's power is produced in the outbard 3/10 of the radius.) Work has yet to be done which will show which if any additional data are needed for adequate performance predictions, and how or if they can be included in existing performance codes.

2.2 Formal Description of Blade Problem

Rotating wings have traditionally been analyzed as beams with various boundary conditions. Depending on the detailed construction, these beams may be either hinged at the root, pinned at the root, or some combination. The outer edge is invariably free.

The simplest rotating winds, are of a rectangular planform and a single material. For example, extruded aluminum blades are now commercially available in various sizes. These are the simplest to analyze it will always be possible to find a set of axes which completely uncouples the bending deflections in one direction from those in the other. These are by definition the principal axes. They will have the same orientation for all sections and all loads and moments can be resolved about them.

The introduction of twist complicates the analysis. The twist will make it difficult or impossible to find axes for which the bending deflections are decoupled. However, the moments of inertia need only be calculated once. They can then be transformed by rotation into the correct orientation. At this point, the analysis requires the solution of the coupled bending equations (Appendix A) and the coupled bending stress equations.

The introduction of taper requires that the moments of inertia be computed at each station of interest. The equations which must be solved are then the same as in the case of a beam of rectangular planform with twist.

If the rotor blades are constructed of more than one material, for example aluminum and fiberglass or fiberglass of two or more different bending moduli, it is necessary that the so-called modulus weighted section properties be computed. This is a method by which the tensile properties of the different components of each cross-section are weighted in the accumulation of those quantities necessary for analysis. For example, the modulus weighted x and y centroid locations define the location of the tension center for the cross-section. (The tension center is that point at which an applied radial load gives no lateral deflections.)

The blades on the WF-1 are just such non-homogeneous, twisted, tapered beams. The solution of the bending and stress equations requires the incorporation of numerical techniques in some algorithms. The fact that the blade cross-sections are rather complex shapes (both externally and internally) indicates the need for some numerical methods for the computation of the section properties. (It turns out that many numerical techniques were required for the section property integrations.)

2.3 Description of Load

In the case of non-accelerated rotation the loads encountered are lift, drag, gravity loads and centrifugal loads. Performance codes[2.6] can predict the quasi-steady lift and drag operating on a blade section subject to the above restrictions. These loads can then be resolved about reference axes and the bending equations solved. The gravity load is both radial and flexural, depending on the blade orientation relative to the horizon. For each blade, gravity gives a one per revolution cyclic excitation. The centrifugal loads are constant if the angular speed is constant and deflections out of plane due to gravity are not too great.

Unsteady, accelerated motion introduces other loads. The tower shadow or wake may cause a cyclic variation in the applied wind loads. This will cause a change in the deflection pattern on a one per revolution per blade basis. The cyclic variation in deflection will cause the generation of so-called coriolis forces by the blade elements. The magnitude of these periodic loads is of considerable interest. They will determine the cyclic stresses, hence the fatigue properties of the blades. The periodic response of the blade to the tower wake is very poorly understood at this point. Ongoing investigations at the University of Massachusetts

and elsewhere may shed light on this area.

2.4 Other Dynamic Considerations

The effect of torsional coupling of vibrations has been neglected in the foregoing. The effect of the coupling between radial loads and vibrations has also been neglected. These effects are considered to be of marginal interest to the windmill designer because of the relatively low rotational speed of the rotor.

In a paper written by Ormiston[2.7], loads are scaled according to the radius of the wind machine under consideration. Ormiston shows that for very large machines, the one per revolution gravity loads may be the limiting design criterion. For moderately sized machines, the critical loads are flexural and are due to the aerodynamics of power production.

The random nature of the wind also provides a non-steady component in the air loads. This effect becomes more pronounced as the pitch at which peak power is produced is approached. This effect is presently thought secondary in importance to the tower wake and/or shadow with respect to cyclic loads. This is another area under active investigation.

2.5 Environmental Effects

The sun will degrade the strength of glass laminates which are not protected from it. The experience at the University of Massachusetts has been that significant erosion of the most exterior layer of resin took place in the first two years of operation. The blades were purposely not protected in order that structural defects would be easily seen. It is not

felt that this erosion had any effect on blade strength. No structural defects were found which can be unequivocally assigned to the design.

Metal-plastic composites may suffer from fatigue due to different coefficients of thermal expansion and the diurnal temperature cycle.

Metals are subject to corrosion in the environment of the wind turbine. There is presently great interest in the siting of windmills either on or near the ocean. The effects of salt spray on metal are fairly well understood. The fatigue properties of metals are quite well known, once the stress environment is prescribed. For inland locations, rain and windblown sand and dust are significant factors in the weathering of blades.

It seems at this time that the material properties of metals are better understood than are those of composites. However, the data base for composite fatigue is broadening.

CHAPTER III

GOVERNING EQUATIONS

3.1 Static Beam Bending

Beam theory for homogeneous prismatic beams is quite well developed. The dynamic characteristics of such beams are also well known. This is not the case with non-homogeneous, non-isotropic, or non-prismatic beams.

If we allow the existence of a coordinate system such that the x axis is parallel to the plane of rotation; the x axis points down the bending axis, and the y axis is inclined from the upwind direction by the coning angle (see Figure 1) with

u = unit deflection in the x direction

v = unit deflection in the y direction,

then the differential equations for beam bending are (see Appendix A)

$$\frac{d^2v}{dz^2}\ \frac{1}{\left(1-\left(\frac{dv}{dz}\right)^2\right)^{3/2}} = \frac{-1}{E_1}\frac{M_xI_{yy}+M_yI_{xy}}{I_{xx}I_{yy}-(I_{xy})^2} \tag{1}$$

$$\frac{d^2u}{dz^2} = \frac{1}{\left(1-\left(\frac{du}{dz}\right)^2\right)^{3/2}} = \frac{1}{E_1}\frac{M_yI_{xx}+M_xI_{xy}}{I_{xx}I_{yy}-(I_{xy})^2} \tag{2}$$

The general equations for bending stress at point (x,y) in some cross-section plane is

$$\sigma_{zz} = \frac{-E}{E_1}\ \frac{(M_xI_{yy}+M_yI_{xy})y-(M_yI_{xy}+M_xI_{xy})x}{I_{xx}I_{yy}-I_{xy}^2} \tag{3}$$

FIG. 3.1

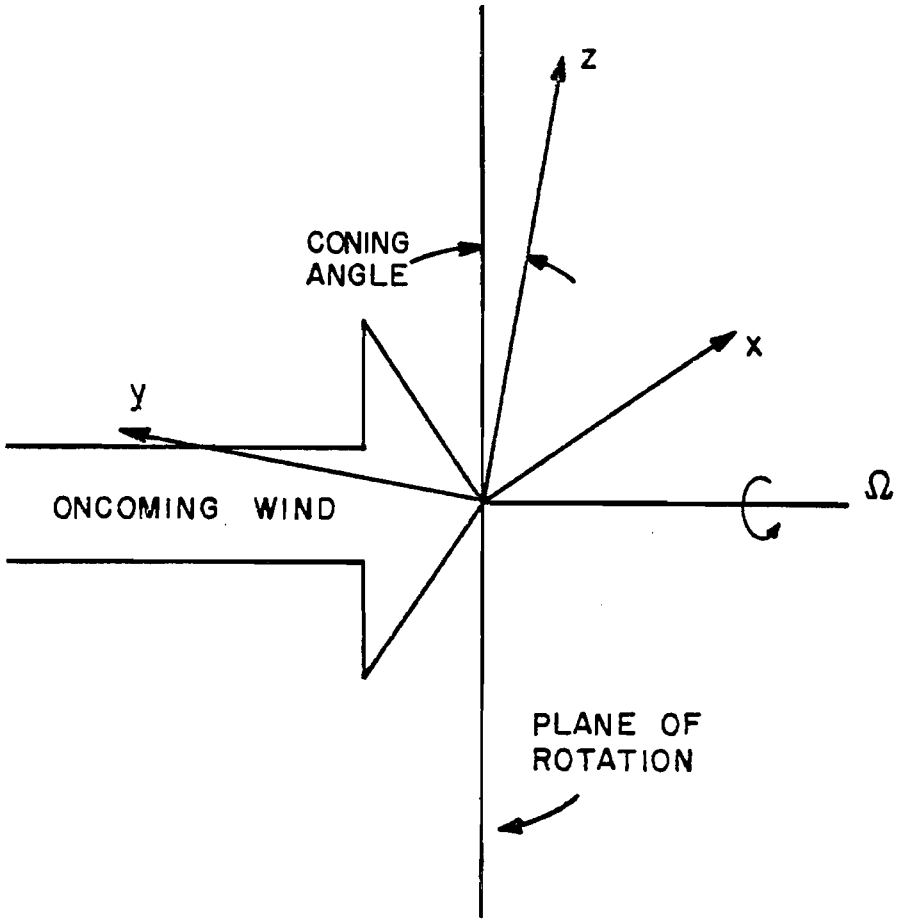

WINDMILL (ROTATING) CO-ORDINATE SYSTEM

These equations are solved in the enclosed codes. Because of the possibility of large deflections in a long, slender windmill blade, it was thought advisable to include the influence of slope in the deflection equations. The fact that many windmill blades are highly twisted and tapered required the allowance of bending about non-principal axes.

3.2 Equations of Motion for Small Flexural Vibrations

In general, the equations of motion of a rotating beam involve coupling between flexural, longitudinal, and torsional vibration . In many situations numerous simplifications may be made. Usually, however, numerical techniques must still be used for solution.

The equations of motion for the flexural vibrations of a beam allowing coupling between vibrations in orthogonal directions are (see Appendix B)

$$\ddot{v} = \frac{-E_1}{m} \frac{\partial^2}{\partial z^2} \left[I_{xx} \frac{\partial^2}{\partial z^2} v + I_{xy} \frac{\partial^2}{\partial z^2} u \right] \tag{4}$$

$$\ddot{u} = \frac{-E_1}{m} \frac{\partial^2}{\partial z^2} \left[I_{yy} \frac{\partial^2}{\partial z^2} u + I_{xy} \frac{\partial^2}{\partial z^2} v \right] \tag{5}$$

where $\ddot{v} = \frac{d^2}{dt^2} v$

$\ddot{u} = \frac{d^2}{dt^2} u$

m = lineal mass density.

CHAPTER IV

NUMERICAL TECHNIQUES

4.1 Integration of Section Properties

The axes used in all discussion of the section properties is as follows. Positive x has its origin at the leading edge and increases along the chord line. Positive y has its origin at the leading edge and is positive towards the low pressure surface.

The technique used in the computation of the section properties was the replacement of integrations with summations when the use of the direct integration was inappropriate. This procedure is accomplished by the functions. INDEX and INTEG (Appendices E and F respectively).

The function INDEX isolates three adjacent points on the periphery of the section being considered. It appends to this information the pertinent bending modulus and material thickness. (Thickness here refers to the minimum distance from the outside to the inside. If the listed thickness is zero the program assumes the section is solid.) It also appends the weight density. (Units used for the density are pounds per cubic inch.) This information is then used with function INTEG.

Function INTEG first fits the best parabola, in the least square sense, through the set of three points. The interval defined by these points is then divided into ten equal segments. Points on the periphery of each segment are then found by use of the least square coefficients,

$$(y_i = C_o + C_1 X_i + C_2 X_i^2, \quad i = 1, 2, \ldots, 10)$$

and the value of x at the midpoint of each section. Thus ten points are determined from the three input points. This has the effect of decreasing the error due to the replacement of the section integrations with summations at the expense of the error introduced by the use of a fit curve rather than the input data points.

If the section is solid, the section properties determined by the above ten intervals are solved for directly.

If the section is not solid, the algorithm accomplishes the following. For each value of y, another value is determined which is the former value minus the projected thickness. (The projected thickness is found by multiplying the thickness of the skin by the secant of the tangent at the point x, y. That is $t_{projected} = t[\cos \tan^{-1} (C_1 + 2C_2 X_i)]^{-1}$, where t is the skin thickness and C_1, C_2 are least square coefficients.) The midpoint values and the values X_i determine the area centroids of the load carrying material in this small interval.

The worth of this information can best be shown by examination of the following equations. If I_{xx}, I_{xy}, I_{yy} are the moments of inertia of some area about an arbitrary axis system xy, and I_{rr}, I_{rs}, I_{ss} are the moments of inertia of that same area about its own centroid axis system, then

$$I_{xx} = I_{rr} + Ay^2$$

$$I_{xy} = I_{rs} + Axy$$

$$I_{yy} = I_{ss} + Ax^2, \text{ where}$$

A = geometric area of the considered,

r is parallel to x,

s is parallel to y,

x,y are the coordinates of the centroid

I_{rr}, I_{rs}, I_{ss} can be made vanishingly small by the use of either a properly chosen coordinate system or a small area. Consider the following, a 1 inch square centered at x = y = 2 in.

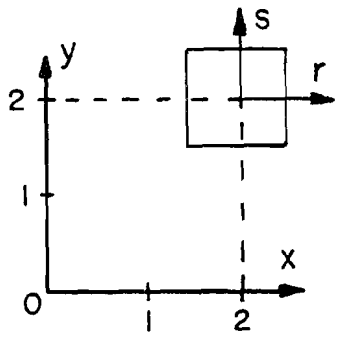

$$I_{rr} = I_{ss} = \frac{1}{12}$$

$$I_{rs} = 0$$

$$I_{xx} = \frac{1}{12} + 1\ (2)^2 = 4+\frac{1}{12}$$

$$I_{yy} = \frac{1}{12} + 1\ (2)^2 = 4+\frac{1}{12}$$

$$I_{xy} = 0 + 1\ (2)(2) = 4$$

For even so gross an example, the error in I_{xx} and I_{yy} introduced by neglecting the area's centroidal moment of inertia is only 2%.

When the cross section properties are computed, the small areas are weighted according to the local bending modulus, or by the local density.

The modulus weighting is a method whereby a composite cross section may be represented by a single total bending stiffness. This is done by dividing the local bending stiffness by an (arbitrary) reference modulus and multiplying the considered area by the result. This is done for all considered areas. Density weighting is accomplished by multiplying the considered area by the local density. (See Appendix F.) The results of the calculations are summed with the results of previous calculations for the cross section.

The quantities computed are the modulus weighted areas, first moments, and second moments, and the density weighted areas and first moments. In addition, the geometric areas of the cross section are computed. The modulus weighted area are used for the transposition of the section moments of inertia from the leading edge, the origin, to the bending axis. (The chordwise location of the bending axis is part of the program input. The logic assumes that the y coordinate of the bending axis is the same as the y coordinate of the tension axis.) The modulus weighted first moment is used to determine the location of the tension center. (The line connecting all tension centers is the tension axis.) The modulus weighted second moments are the section moments of inertia. They determine the flexural characteristics of the beam.

The density weighted first moments are used to determine the location of the centers of mass of the cross sections. The density weighted areas give the blade section weights.

In summary, when a solid section is considered, direct integration of the section properties is accomplished. When a non-solid section is considered, the following series replace the integrations.

$$I_{xx} = \int_A y^2 \, \phi \, dA \simeq \sum_i y_i^2 \, \phi_i \, \Delta A_i$$

$$I_{xy} = \int_A xy \, \phi \, dA \simeq \sum_i x_i \, y_i \, \phi_i \, \Delta A_i$$

$$I_{yy} = \int_A x_i^2 \, \phi \, dA \simeq \sum_i x_i^2 \, \phi_i \, \Delta A_i$$

$$\bar{x} = \frac{\int_A \phi \, x \, dA}{\int_A \phi \, dA} \simeq \frac{\sum_i \phi_i \, x_i \, \Delta A_i}{\sum_i d_i \, \Delta A_i}$$

$$\bar{y} = \frac{\int_A \phi \, y \, dA}{\int_A \phi \, dA} \simeq \frac{\sum_i \phi_i \, x_i \, \Delta A_i}{\sum_i \phi_i \, \Delta A_i}$$

$$\text{AREA} = \int_A \phi \, dA \simeq \sum_i \phi_i \, \Delta A_i ,$$

wherein

ϕ = weighting function,

$\bar{x}$, $\bar{y}$ = are centroid values dependent on the weighting function

AREA = either geometric or modulus weighted area of the load carrying material in the cross section.

4.2 Bending Deflections

The governing equations for beam bending, using the coordinate system of Chapter 1, where thermal stresses are not considered, are

$$\frac{d^2u}{dz^2}\frac{1}{(1-(\frac{du}{dz})^2)^{3/2}} = \frac{1}{EREF}\left(\frac{M_yI_{xx}+M_xI_{xy}}{I_{xx}I_{yy}-I_{yx}^2}\right)$$

$$\frac{d^2v}{dz^2}\frac{1}{(1-(\frac{dv}{dz})^2)^{3/2}} - \frac{1}{EREF}\left(\frac{M_xI_{yy}+M_yI_{xy}}{I_{xx}I_{yy}-I_{xy}^2}\right) .$$

These equations are non-linear. For small deflections, the non-linear term is customarily neglected. It is desirable that the non-linearity be included in an analysis of blade bending, however, because the blades are very long, thin, and flexible.

The method used for the solution of these equations is a fourth order Runge Kutta method.[4.1] This method uses the boundary conditions on a function and its derivatives to integrate the derivatives across some interval. The particular Runge-Kutta formulation chosen is the so-called classic method. Letting i be an index related to the position x, we have

$$\Phi_{i+1} = \Phi_i + \frac{1}{6}(k_1 + 2k_2 + 2k_3 + k_4), \text{ where}$$

$$k_1 = h\, f\,(x_i, y_i),$$

$$k_2 = h\, f\,(x_i + \frac{h}{2}, y_i + \frac{k_1}{2}),$$

$$k_3 = h\, f\,(x_i + \frac{h}{2}, y_i + \frac{k_2}{2}),$$

$$k_4 = h\, f\,(x_i + h, y_i + k_3),$$

$$h = x_{i+1} - x_i,$$

f is the integrand from which y is determined,

Φ is a derivative of some order 1 less than f.

By the use of this integration scheme, differential equations of any order may be solved. All of the derivatives of intermediate value must be carried in memory. (See APPENDIX G.) The precision available by the use of this method is quite high. If the precision is not acceptable, the integration interval may be shortened or higher order Runge Kutta methods used.

These equations could have been written in finite difference or finite element form as well. The finite element method led to unnecessary complication. The finite difference method required the introduction of new data points if the same resolution of displacements were required. Neither of these methods were considered uniquely superior to the Runge Kutta solution for this problem.

(One disadvantage of the Runge Kutta methods is that the application to partial differential equations is apparently unknown. This precludes their use for the solution of vibration problems in the time domain.)

4.3 Bending Stress

The expression for the bending stress at some point (x,y) is

$$\sigma_{zz} = \left(- \frac{M_y I_{xx} + M_x I_{xy}}{I_{xx} I_{yy} - I_{xy}^2} x + \frac{M_x I_{yy} + M_y I_{xy}}{I_{xx} I_{yy} - I_{xy}^2} y\right) .$$

There were no special techniques necessary for the solution of this problem. The multipliers of the coordinate components x and y are also computed in the solution of the bending equations. They are stored in memory and recalled where the stress distribution is reported.

The bending stress is resolved at each point listed in the first two inputs to the program, that is,on the high and low pressure aerodynamic surface skins. (APPENDIX D, INPUT.) If any other data are entered in their place, the stress will be resolved at the points entered. The input section is very versatile in that no special order of data entry is required (except CHORD, see APPENDIX D). The program output would not have to be modified in any way if the order of data entry is modified, as long as the operator keeps track of which data has been entered.

4.4 Flexural Vibrations

The governing equations for flexural vibrations of a twisted, nonprismatic beam are (APPENDIXB)

$$U = - \frac{E_r}{m} \frac{\partial^2}{\partial z^2} \left[I_{xx} \frac{\partial^2 v}{\partial z^2} + I_{xy} \frac{\partial^2 u}{\partial z^2} \right]$$

$$u = - \frac{E_r}{m} \frac{\partial^2}{\partial z^2} \left[I_{yy} \frac{\partial^2 u}{\partial z^2} + I_{xy} \frac{\partial^2 v}{\partial z^2} \right]$$

These equations cannot be solved in closed form without simplification. Their solution requires the use of numerical techniques. They may be solved in a number of ways. Obvious choices are the use of finite difference and finite element methods. The method used in this report is called Rayleigh's method.

The technique as used here (see APPENDIX I) differs slightly from the usual applications in that successive approximations are made to refine the determined mode shape, when possible. (For higher modes,

with twisted beams, the method does not always converge.) The technique is very versatile because only the response to an assumed load pattern need to be determined. Any response (axial, flexural, torsional) may be included. Any degree of simplification can be achieved by neglecting chosen parameters.

Rayleigh's method does not solve for the system behiavor in the time domain. Instead, the method resolves the natural frequencies and mode shapes of an oscillating system. This information can then be used in a modal analysis of the system.

The expression for the square of the natural frequency of an oscillating system is[4.2].

$$\omega^2 = \frac{\sum_i F_i \phi_i}{A \sum_i M_i \phi_i^2}$$

where

F_i is the imposed load at i,

ϕ_i is the mode shape at i,

A is the amplitude,

M_i is the mass at i.

The key to the method of successive approximations is that the inertial load is proportional to a mass times its displacement. Hence

$$F_i = k M_i \phi_i .$$

The constant k is of no interest, since the mode shapes are a property of the load patterns, not the loads themselves. This load pattern is used to compute another mode shape by calculating the deflections due to the imposed

loads. The magnitude of the deflection so computed at some one point is called the amplitude (A). The set of all deflections divided by this amplitude is the mode shape. When the inertial forces associated with some mode shape produce a deflection pattern having the same mode shape, the method has converged to the fundamental. At this point, the square of the circular frequency is the reciprocal of the amplitude. (See APPENDIX M for a sample calculation.)

The maximum kinetic energy for the system is

$$K = \sum_i \frac{1}{2} M_i \ (A \ \phi_i \ \omega)^2 \ .$$

The maximum potential energy is equal to the maximum kinetic energy and is given by

$$u = \sum_i \frac{1}{2} F_i \ (A \ \phi_i) = \sum_i \frac{1}{2} M_r \ \phi_i' \ A \ \phi_i \text{, where}$$

ϕ_i' is the mode shape from the last cycle of the iteration.

Setting these two expressions equal gives

$$\sum_i \frac{1}{2} M_i \ A^2 \ \phi_i^2 \ \omega^2 = \sum_i \frac{1}{2} M_i \ \phi_i' \ \phi_i \ A$$

or

$$\omega^2 = \frac{\sum_i \frac{1}{2} M_i \ \phi_i' \ \phi_i}{A \sum_i \frac{1}{2} M_i \ \phi_i^2} \qquad (2)$$

which is the same as equation 1 once the expansion of F_i has beem accomplished. If convergence of the mode shape has been achieved, then

$$\omega^2 = \frac{1}{A}$$

The introduction of twist in a beam, that is to say that the principal axes of all cross sections of a beam being non-parallel, introduces coupling between the loads in one plane and the deflections in another. If a beam is prismatic and not twisted, or at worst tapered, then the resonant vibrations of the beam will be aligned with one of the principal axes. This is a consequence of the deflections being uncoupled from each other. For a highly twisted beam, e.g. a windmill blade, the direction of resonant vibrations will, in general, vary from cross section to cross section. Any attempt at analysis, therefore, must allow two degrees of flexural freedom at each cross section. (A more complete analysis would also allow a torsional degree of freedom at each cross section. Since there was no observable torsional deflection of the tested blade under load, that component of the analysis was considered unimportant.) The same general results hold, however. The amplitude is chosen to be the magnitude of the tips deflection. The inertial forces are the mass per segment times the mode shape at the midpoint of each spanwise section. The deflections are computed using the function described above.

Rayleigh's method is usually used for a determination of the fundamental mode. There are various techniques available for the isolation of higher modes, however. The first such method is to impose a deflection in space oriented at 90° to the fundamental deflection pattern. (A free beam in space has the property that the fundamental mode shape follows a pattern which produces a maximum deflection for the given loads.) A load pattern 90° out of phase but equal in magnitude will produce much smaller deflections. (In fact, for a regular prismatic beam, the deflections so produced will be a minimum.) This deflection pattern can then be used to

compute the beam frequency. This frequency will be higher than the fundamental. It will often be the next highest frequency.

Another technique is known as Schmitt Orthogonalization (see APPENDIX K). (The following and much of the foregoing is taken from Biggs Structural Dynamics.) Any assumed deflection patten can be expressed as

$$\phi_{ia} = \sum_m \psi_m \phi_{im}$$

where

ϕ_{ia} = the assumed mode shape at i,

ψ_m = the participation factor of the m^{th} mode in ϕ_{ia} ,

ϕ_{im} = the mode shape of mode m at i.

Multiplying both sides by $m_i \phi_{in}$, we have

$$m_i \phi_{ia} \phi_{in} = \sum_m m_i \psi_m \phi_{im} \phi_{in},$$

where

m_i = mass at i

ϕ_{in} = mode shape at i for mode n

$$\sum_i m_i \phi_{ia} \phi_{in} = \sum_i \sum_m m_i \psi_m \phi_{im} \phi_{in} \qquad (3)$$

The orthogonality condition for normal modes is that

$$\sum_i m_i \phi_{im} \phi_{in} = 0$$

unless m = n. Equation 3 can now be rewritten

$$\sum_i m_i \phi_{ia} \phi_{in} = \sum_i m_i \psi_m \phi_{im}^2 .$$

The participation factor for the m^{th} mode is

$$\psi_m = \frac{\sum_i m_i \phi_{ia} \phi_{in}}{\sum_i m_i \phi_{im}^2}$$

Using this participation factor, the assumed mode shape can be swept clean of the influence of previously determined mode shapes. The assumed mode shape becomes

$$\phi_i = \phi_{ia} - \psi_1 \phi_{i1} - \psi_2 \phi_{i2} - \cdots - \psi_n \phi_{in}.$$

This procedure will converge to the next higher mode shape and frequency. (If an iterative process is used and the procedure is functioning correctly, the participation factors will all approach zero.)

Yet another procedure is to assume a number of mode shapes related to each other and look for a frequency minimum. Since the prescription of an incorrect mode shape does not excite resonant responses alone, the mode shape giving the maximum natural frequency is the most accurate.

C H A P T E R V

PROGRAM VERIFICATION

5.1 Section Properties

The functions which make up the programs as assembled were all subjected to verification. The functions INDEX and INTEG were used to compute the geometric properties of the sections shown in Fig. 5.1.

For the diamond shape, the modulus weighted calculated section properties, compared with the exact properties, are as follows:

	CALCULATED	EXACT	ERROR
I_{xx}	78.98 in^4	78.75 in^4	1%
I_{yy}	81.20 in^4	78.75 in^4	3.1%
I_{xy}	0.00	0.00	0
AREA	5.45 in^2	5.37 in^2	1.5%

Table 5.1

For the ellipse, the modulus weighted section properties calculated by the program compared with the exact values are as follows:

	CALCULATED	EXACT	ERROR
I_{xx}	190.7 in^4	190.4 in^4	1%
I_{yy}	337.4 in^4	357 in^4	5.6%
I_{xy}	0	0	
AREA	7.55 in^2	7.66 in^2	1.4%

Table 5.2

TEST SECTIONS

FIG. 5.1

ELLIPSE

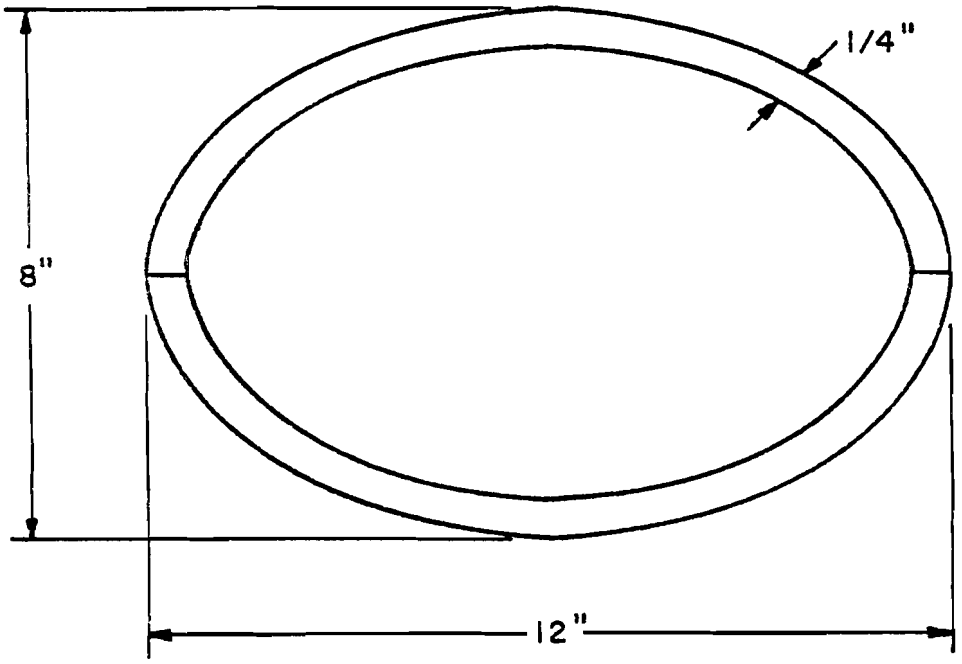

DIAMOND

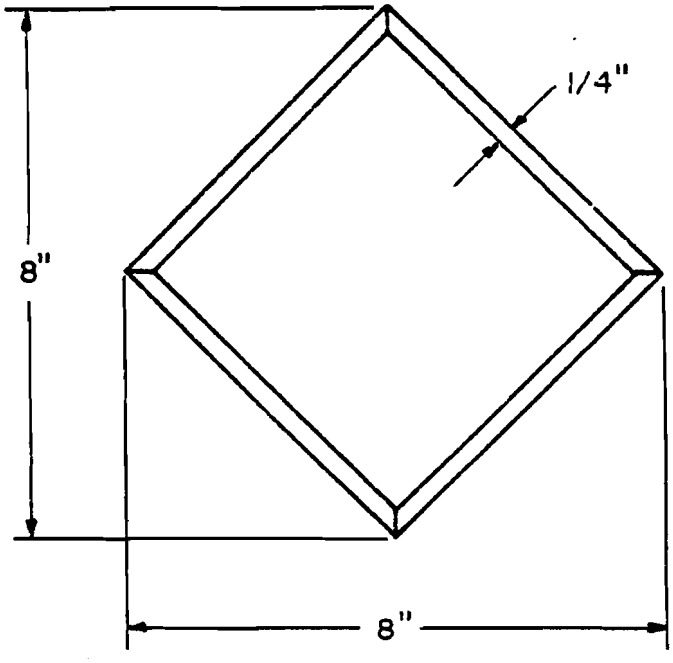

The relatively large error is due to the steep slope of the ellipse as it nears the leading and trailing edges. The most expedient way to improve the resolution of these rounded parts of the shape is to increase the number of points describing this region. (Airfoil section coordinates are usually listed in this way[5.1].

It was not possible to test the airfoil shapes directly, since the moments of inertia of airfoil shapes are not commonly available. From the foregoing, however, good results for the section properties can be expected.

5.2 Stress and Deflection

The elliptic cross section above was used as the cross section shape of a hypothetical cantilevered beam 10 feet long. The deflection predicted by the well known strength of materials formula is

$$\delta = \frac{PL^3}{3EI} = \frac{1000\ (120)^3}{3(3\times10^7)(63.45)} = .30 \text{ inches}$$

where

δ = deflection

P = load at 10 feet

L = length of the beam

E = Young's modulus (for steel)

$I = 63.45\ in^4$

The program calculated a deflection of .301 inches. The error is negligible.

The maximum stress predicted by the usual strength of materials formula for the above beam and load is

$$\sigma_{max} = \frac{PL}{I} y = \frac{(1000)(120)(4)}{63.45} = 7565 \text{ psi}$$

where y = maximum distance from the neutral axis.

The maximum predicted stress was 7551 psi. The error is negligible.

5.3 WF-1 Blade Stress and Deflection

As a final test of the static portion of the analysis, the geometry describing the WF-1 blade was entered. A hypothetical load of 15 lbs. 8 oz. was input at .95 R. An actual load of the same weight was placed on the test blade and the deflection and stress levels measured.

For the first trial, the published geometry of the WF-1 blade was used as program input. The observed deflections differed from the calculated deflections by approximately a factor of two. At this time, the blade geometry was established by measurement. The blade cross sections were discovered to have a great deal more depth than originally thought. The chord lengths of the cross sections were nearly at the specifications. (See Table 2.2).

New data files were established by multiplying the coordinates in the old files by the fractional difference between the observed and listed depths. (These data files are listed in APPENDIX M.) The new data files were used as input to the program.

Figure 5.2 shows the location of strain gages used for the test. The set of gages (1-10) around the circumferences of the blade at .475 R were 350 Ω Constantan BLH strain gages of various lots. The strain gages

FIG. 5.2

STRAIN GAGE LOCATION

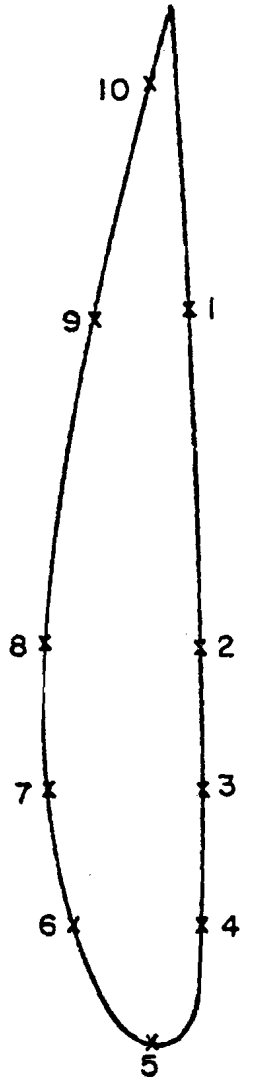

CROSS SECTION
AT .475 R

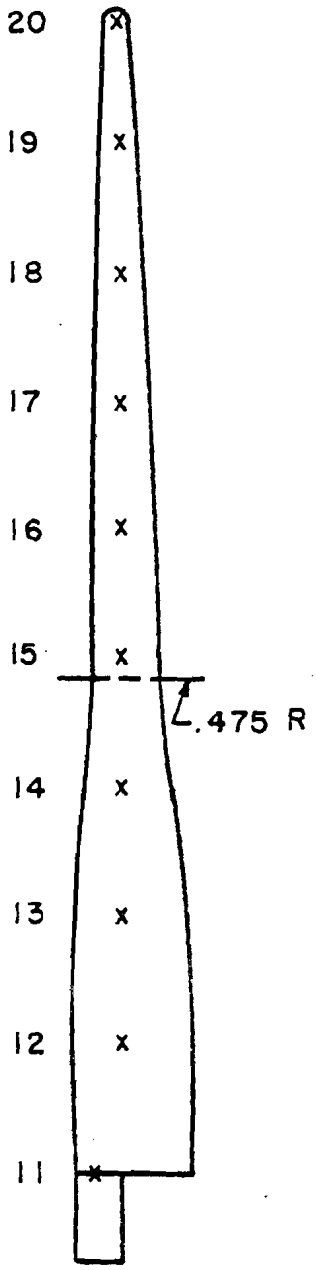

LOW PRESSURE
SURFACE FACING

organized radially (11-20) were 500 Ω Constantan BLH strain gages of the same lot. All bonds between gage and substrate were by Eastman 910 adhesive. The strains were detected and transduced by a shop built resistor bridge and amplifier.

Table 5.3 lists the observed and predicted values of stress for all gages. They are plotted in Figure 5.3 Agreement between predicted and measured values were good for all gages except number 17. The gage bond is suspect there, largely because of the good agreement between predicted and observed deflections.

Figure 5.4 shows the observed blade tip displacement due to the single 15 lb. 9 Oz. load at .95 R. This load was oriented at 90° to the chord line at the tip, towards the low pressure surface (towards the bottom of the page). The deflection in the lead direction (positive x direction according to the paper's sign convention) is due entirely to the coupling between the deflections in two planes. It is a consequence of the blade twist. The deflection values are as follows:

	Predicted	Measured
u	.57 in.	.36 $\pm$ .13 in.
v	2.99 in.	2.96 $\pm$ .06 in.

This agreement is acceptable. Uncertainties in the geometry of the trailing edge, particularly relative to the load carrying capacity of the roving bundle used to seal the trailing edge, make any more precise determination of the bending coupling unlikely.

TABLE 5.3

BENDING STRESS BY GAGE NUMBER

(Refer to Figure 5.2)

Gage Number	Stress, psi	
	Predicted	Observed ±33
1	267	264
2	398	386
3	462	448
4	466	402
5	203	141
6	- 360	356
7	- 520	478
8	- 563	540
9	- 342	-356
10	- 40.1	- 26.5
11	+ 143	- 94
12	- 323	-293
13	- 517	-351
14	- 557	-503
15	- 565	-550
16	- 634	-678
17	-1075	-585
18	- 610	-690
19	- 346	-421
20	0	0

FIG. 5.3

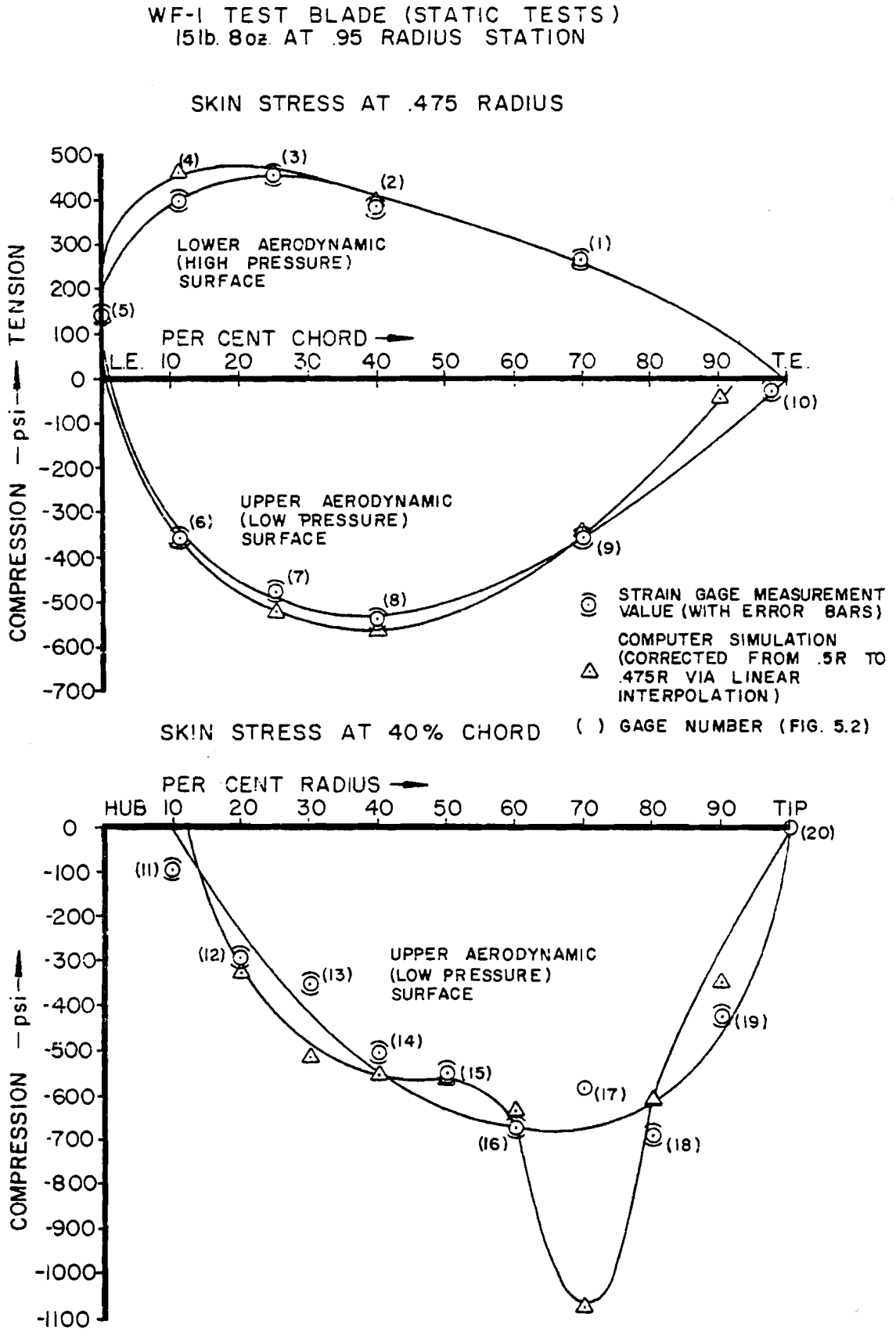
WF-1 TEST BLADE (STATIC TESTS)
15lb. 8oz. AT .95 RADIUS STATION
SKIN STRESS AT .475 RADIUS
COMPRESSION — psi — TENSION
500
400
300
200
100
0
-100
-200
-300
-400
-500
-600
-700
PER CENT CHORD →
L.E. 10 20 30 40 50 60 70 80 90 T.E.
LOWER AERODYNAMIC (HIGH PRESSURE) SURFACE
UPPER AERODYNAMIC (LOW PRESSURE) SURFACE
(1)
(2)
(3)
(4)
(5)
(6)
(7)
(8)
(9)
(10)
STRAIN GAGE MEASUREMENT VALUE (WITH ERROR BARS)
COMPUTER SIMULATION (CORRECTED FROM .5R TO .475R VIA LINEAR INTERPOLATION)
( ) GAGE NUMBER (FIG. 5.2)
SKIN STRESS AT 40% CHORD
PER CENT RADIUS →
HUB 10 20 30 40 50 60 70 80 90 TIP
COMPRESSION — psi —
0
-100
-200
-300
-400
-500
-600
-700
-800
-900
-1000
-1100
UPPER AERODYNAMIC (LOW PRESSURE) SURFACE
(11)
(12)
(13)
(14)
(15)
(16)
(17)
(18)
(19)
(20)

FIG. 5.4

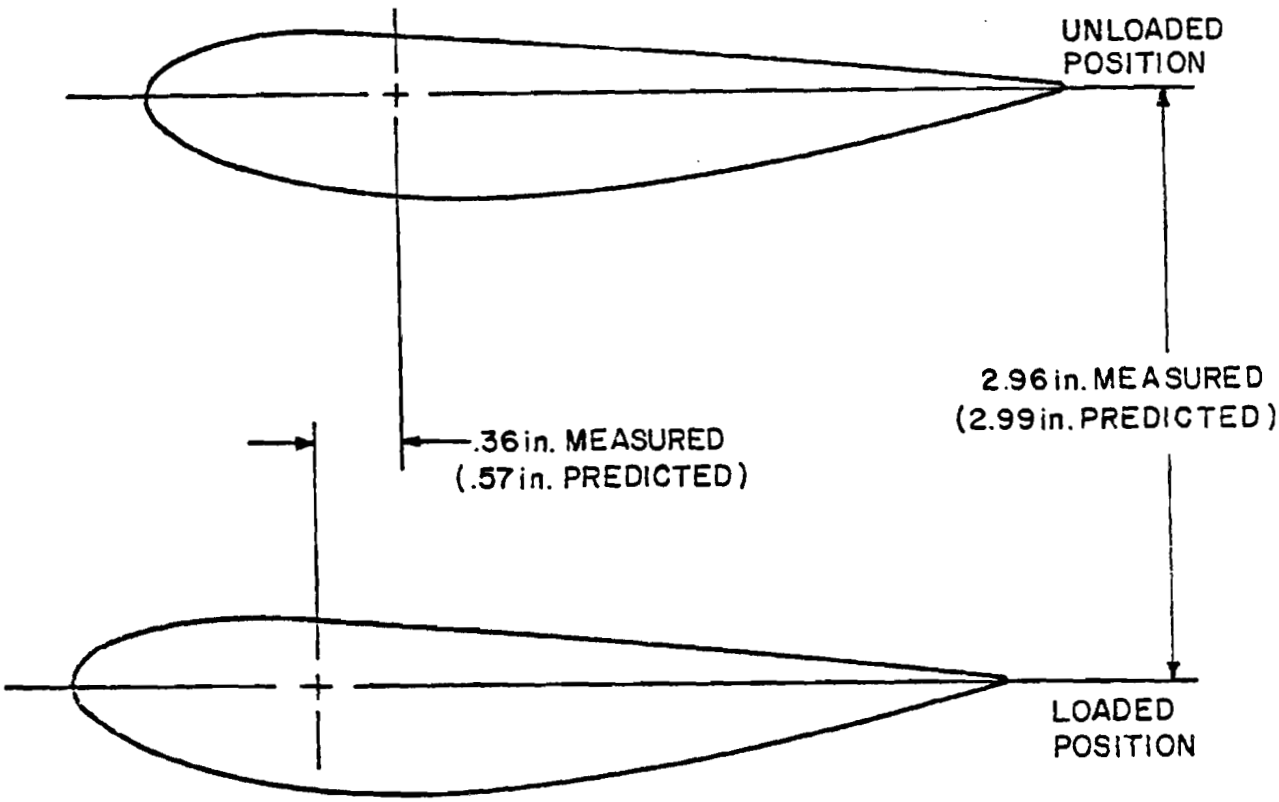

WIND FURNACE BLADE TIP DEFLECTION

5.4 Vibration

The Rayleigh Ritz method was used for the solution of the natural frequencies. The mode shapes were all normalized to the magnitude of the tip displacement vector (see APPENDIX I).

As a simple test of the program, the dimensions and section properties of a six foot long steel beam whose cross section was a one inch by four inch rectangle (Figure 5.5) were used. The three lowest frequencies of this beam are

$$\omega_1 = 39.8 \text{ radians/sec}$$

$$\omega_2 = 159 \text{ radians/sec}$$

$$\omega_3 = 251 \text{ radians/sec.}$$

The numbers predicted by program FREQ are

$$\omega_1 = 39.8 \text{ radians/sec}$$

$$\omega_2 = 159 \text{ radians/sec}$$

$$\omega_3 = 259 \text{ or } 260 \text{ radians/sec}$$

The agreement is seen to be quite good. The reason that two numbers are given for the highest predicted frequency is that the program FREQ contains two algorithms for the determination of this frequency. The first uses Schmitt orthogonalization for the solution. The second superimposes the function sin ($\pi x \div L$) over the fundamental mode shape and the value of x is varied.

On the spare wind furnace blade, a shaker was mounted for the isolation of resonant frequencies. The total weight of the shaker was 2.79 lbs. It was mounted at .35 R, 48.8 inches from the blade support. The rotor

FIG. 5.5

TEST BEAM

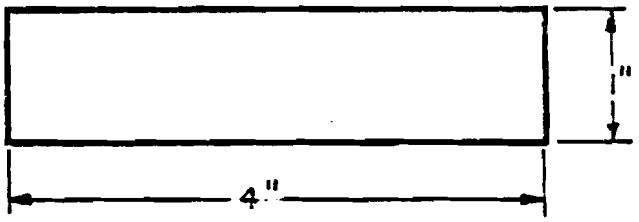

CROSS SECTION

STEEL BEAM
$E = 3 \times 10^7$ psi.
$m = \frac{.02095}{g}$ lb./in.

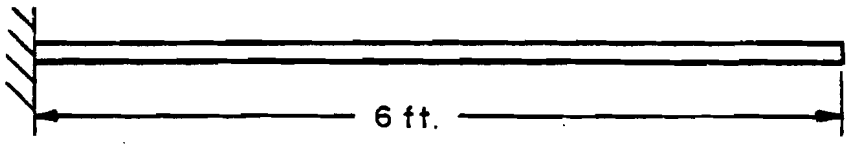

SIDE VIEW

weighed .40 lbs. and had an eccentricity of .38 in. The blade support was bolted atop a section of 8 inch diameter steam pipe 5 feet tall. The pipe was fixed to the concrete floor. The stand was stiffened by external supports in both bending and torsion.

The results of the frequency analysis of the WF-1 are shown below.

	Measured	Predicted
	(radians/sec)	
ω_1	25	28
ω_2	56	65
ω_3	84	93

The agreement is not extremely good. The primary reasons for the disagreement can be guessed at. First, the density of the blade's material is not known with any great precision. Second, the blade was balanced during construction (vis. a vis. the other similar blades) by the introduction of lead shot at unknown locations. Third, any remaining flexilibity in the support would lower the observed frequency. (Qualitatively, the support was quite rigid. A penny balanced on edge on the blade support did not tumble off during a vibration test.) Fourth, the apparatus available for the test, the rotor and a strobe light, do not allow tremendous resolution of the resonances, primarily because sympathetic vibrations in the blade will be caused by exciting forces not precisely at the resonant frequency.

The agreement between observed and predicted frequencies, although not tremendous, is considered acceptable. The predicted mode shapes are listed in Table 5.4. They appear to be correct, but measurement of these mode shapes was not possible with the instrumentation at hand.

TABLE 5.4

MODE SHAPES

ω = 26.8 radians/sec

u	0.0	0.0	-.01	-.02	-.05	-.08	-.12	-.17	-.23	-.30
v	0.0	.01	.03	.07	.15	.25	.38	.55	.75	.96

ω = 63.1

u	0.0	.01	.05	.11	.19	.30	.43	.60	.79	1.0
v	.00	.01	.02	.03	.05	.08	.13	.19	.26	.34

ω = 90.0

u	0.0	-.01	-.02	-.05	-.08	-.09	-.05	.05	.20
v	0.0	.02	.08	.17	.25	.27	.16	-.15	-.66

C H A P T E R V I

CONCLUSIONS

The object of this study was the development of computer programs useful to the wind turbine designer. Codes were developed which allow the resolution of bending stress in and natural frequencies of wind turbine blades. The codes are inexpensive to operate when compared with finite element codes of comparable sophistication.

Good agreement between the predicted and observed flexural deflections has been shown. Acceptable agreement between predicted and observed natural frequencies has also been shown. In short, the verification of the codes with respect to an existing wind turbine blade has been accomplished. This provides strong evidence that the application of Rayleigh's method to the problem of free vibration of a beam, allowing coupling between deflections in two directions, is valid. All other parts of the codes have also been verified.

The inclusion of the computer codes and documentation in the appendices should facilitate the use of these codes on other computer systems.

The extension of these codes to allow, for example, shear analysis and/or torsional coupling may be accomplished by subroutine modifications.

REFERENCES

1.1 Chilcott, R.E., The Design, Development, and Testing of a Low Cost 10 Hp Windmill Prime Mover; Brace Res. Inst. Publ. No. MT7, July, 1969.

1.2 Hutter, Ulrich; Optimum Wind Energy Conversion Systems, Ann. Rev. Fluid Mech., 1977, 9: 399-419.

1.3 Biggs, John M., Introduction to Structural Dynamics, McGraw-Hill, New York, 1964.

1.4 Shapiro, Jacob, Principles of Helicopter Engineering, Temple Press Limited, London, 1955.

2.1 Stoddard, Perkins, Cromack, Wind Tunnel Tests for Fixed Pitch Start-Up and Yaw Characteristics, UM-WT-TR-78-1.

2.2 Putnam, Palmer C., Power from the Wind, Van Nostrand Reinhold, New York, 1948.

2.3 Op. cit., Hutter.

2.4 Wilson, Robert E., et al., Aerodynamic Performance of Wind Turbines, Final Report, 1976, ERDA/NSF/04014-76/1.

2.5 Lefebvre, Paul L. and Cromack, Duane E., A Comparative Study of Optimized Blade Configurations for High Speed Wind Turbines, UM-WF-TR-77-0.

2.6 Wilson, Robert E. and Lissamann, Peter B.S., Applied Aerodynamics of Wind Power Machines, 1974, NTIS, PB-2385-95.

2.7 Ormiston, Robert A., Rotor Dynamic Considerations for Large Wind Power Generator Systems, WECS Workshop Proceedings, NSF/RA/W-73-006.

4.1 James, M.L., et al.; Applied Numerical Methods for Digital Computation, I.E.P. - A Dun Donnelley Publisher, New Yor, 1977.

REFERENCES (Continued)

4.2 Biggs

5.1 Abbott, I.A. and Von Doenhoff, A.E., Theory of Wind Sections, Dover Publications, 1959, New York, p. 407.

A.1 ibid.

BIBLIOGRAPHY

1. Burke, Barbara L., Meroney, Robert N.; Energy from the Wind, Annotated Bibliography, Libraries and Fluid Mechanics and Wind Engineering Program, Colorado State University, Ft. Collins, Colo.
2. Wilson, Robert E., and Lissaman, Peter B.S.; Applied Aerodynamics of Wind Power; NTIS, PB-238595, July, 1974.
3. Wilson, Robert E., et al.; Aerodynamic Performance of Wind Turbines, Final Report, ERDA/NSF/0401-76/1.
4. Chilcott, R.E.; The Design, Development, and Testing of a Low Cost 10 Hp Windmill Prime Mover, Brace Res. Inst. Publ. No. MT7, July, 1969.
5. Hütter, Ulrich; OPTIMUM WIND ENERGY CONVERSION SYSTEMS, Ann. Rev. Fluid Mech., 1977, 9: 399-419.
6. Biggs, John M.; Introduction to Structural Dynamics, McGraw-Hill, New York, 1964.
7. Shapiro, Jacob; Principles of Helicopter Engineering, TEMPLE PRESS Limited, London, 1955.
8. Putnam, Palmer C.; Power from the Wind, Van Nostrand Reinhold, New York, 1948.
9. Lefebvre, Paul L. and Cromack, Duane E.; A Comparative Study of Optimized Blade Configurations for High Speed Wind Turbines, UM-WF-TR-77-9.
10. Ormiston, Robert A.; Rotor Dynamic Considerations for Large Wind Turbine Power Generator Systems, WECS Workshop Proceedings, NSF/RA/W-73-006.
11. Rivello, Robert M; Theory and Analysis of Flight Structures, McGraw-Hill, New York, 1969.

12. Houbolt, John C. and Brooks, George W; Differential Equations of Motion for Combined Flapwise Bending, Chordwise Bending, and Torsion of Twisted Non-Uniform Rotor Blades, NACA TN 3905, 1957.

13. Harris, Cyril M and Crede, Charles E.; Shock and Vibration Handbook, McGraw Hill, New York, 1976.

14. James, M.L., et al.; Applied Numerical Methods for Digital Computation; I.E.P.-A Dun Donnelley Publisher, New York, 1977.

15. Abbott, Ira A. and Von Doenhoff, Albert E.; Theory of Wing Sections, Dover Publications, Inc., New York, 1959.

16. MIT; Wind Energy Conversion, U.S. Dept. of Commerce, PB-256198, 15 Feb., 1976.

17. Abramson, Norman H.; Dynamics of Airplanes, Ronald Press, New York, 1958.

18. Miles, Alfred and Newell, Joseph; Airplane Structures, Vol. 1, John Wiley and Sons, New York, 1954.

19. Ashley, Holt; Engineering Analysis of Flight Vehicles, Addison Wesley Publishing Co., Inc., Reading, Mass., 1974.

20. Williams, D; An Introduction to the Theory of Aircraft Structures, Edward Arnold (Publishers) Ltd., London, 1960.

21. Den Hartog; Mechanical Vibrations, McGraw Hill, New York, 1956.

22. Bisplinghoff, Raymond L., et al.; Aeroelasticity, Addison Wesley Publishing Co., Inc., Cambridge, Mass., 1955.

23. Fung, Y.C.; An Introduction to the Theory of Aeroelasticity, Dover Publications, New York, 1969.

24. Gessow, Alfred and Myers, Garry C. Jr.; Aerodynamics of the Helicopter, Frederick Ungar Publishing Co. Inc., New York, 1952.

25. Acton, Forman S; Numerical Methods that Work, Harper and Row, New York, 1970.

26. Kuhn, Paul; Stresses in Aircraft and Shell Structures, McGraw Hill, New York, 1956.

27. Wah, Thein and Calcote, Lee R.; Structural Analysis by Finite Difference Calculus, Van Nostrand Reinhold Co., New York, 1970.

28. Wind Turbine Structural Dynamics, NASA Lewis, NASA Conference Publication 2034, DOE Publication CONF-771148.

29. Larrabee, E; Aerodynamic Design and Performance of Windmills, (Dept. of Commerce?) PB-256 198.

30. Morrison, J.G.; The Development of a Method for Measurement of Strains in a Windmill Rotor, The Electrical Research Association, Technical Report C/T117, 1957.

31. Wood as an Engineering Material, U.S. Forest Products Lab., 1974, Wood Hdbk.

32. McCormick, Barnes, W.; Technical Bibliography of Helicopters, AIAA Student Journal, Fall, 1975.

33. Rohrbach, Carl and Worobel, Rose; Performance Characteristics of Aerodynamically Optimum Turbines for Wind Energy Generators, 31st Annual National Forum of the American Helicopter Society, Washington, D.C., May, 1975, Preprint No. S-996.

34. Ormiston, Robert A.; Dynamic Response of Wind Turbine Rotor Systems, 31st Annual National Forum of the American Helicopter Society, Washington, D.C., May 1975, Preprint No. S-993.

35. Stoddard, Forrest S.; Discussion of Momentum Theory for Windmills, Energy Alternatives Program, University of Massachusetts, TR/76/2, APPENDIX IV.

36. Scanlan, Robert H. and Rosenbaum, Robert; Introduction to the Study of Aircraft Vibration and Flutter, the Macmillan Company, New York, 1951.

37. Proceedings, Specialists Meeting on Rotorcraft Dynamics, American Helicopter Society and NASA/Ames Research Center, James C. Biggers, M.S. 274-1, NASA-Ames Research Center, Moffett Field, California, 94035.

38. Wind Energy Conversion Systems, Workshop Proceedings, NSF-NASA, June 11-13, 1973, D.C., NSF/RA/W-73-006, Dec. 1973.

39. Golding, E.W.; The Generation of Electricity by Wind Power, E. & F.N. SPON LTD, London, 1976.

40. Helicopter Aerodynamics and Dynamics, Agard Lecture Series No. 63, Agard LS-63.

41. Young, Maurice I.; The Influence of Pitch and Twist on Blade Vibrations, Journal of Aircraft, 6:10, pg. 383.

42. Hohenemser, Kurt H. and Yin, Sheng Kuang; On the Question of Adequate Hingeless Rotor Modelling in Forward Flight, 29th Annual Forum of the American Helicopter Society, D.C., May, 1973, preprint No. 732.

A P P E N D I X A

COORDINATE SYSTEM CORRESPONDENCE

The differential equations for beam bending were taken from Rivello, Theory and Analysis of Flight Structures[A.1]. The coordinate systems correspond in the following manner. Primes refer to Rivello's system. All indicated directions are positive.

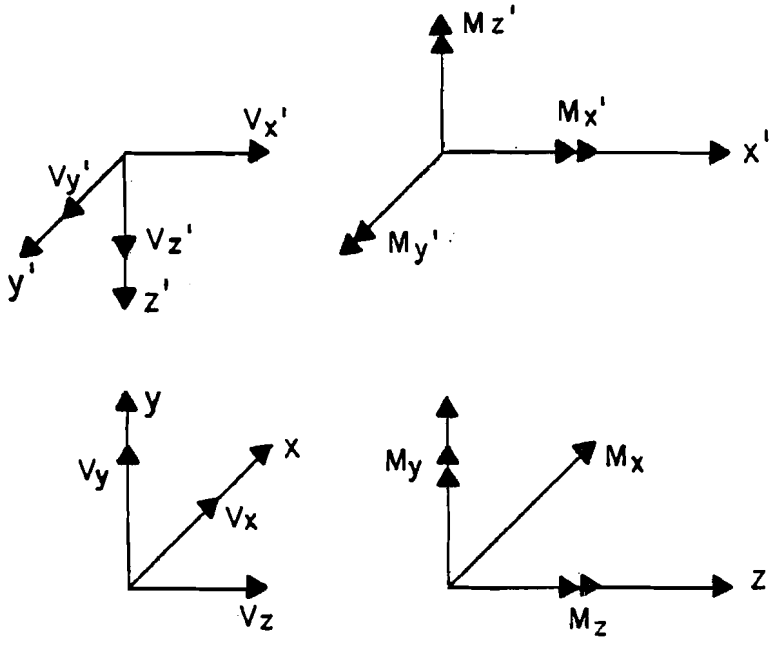

Hence the following correspondences

$x = - y'$	$M_x = - M_y'$	$V_x = - V_y'$
$y = - z'$	$M_y = M_z'$	$V_y = - V_z'$
$z = x'$	$M_z = M_x'$	$V_z = V_x'$

Rivello's equations for beam bending are

$$\frac{d^2w}{dz^2}\frac{1}{(1+(\frac{dw}{dx})^2)^{3/2}} = \frac{1}{E_1}\frac{M_yI_{zz}-M\ I_{yz}}{I_{yy}I_{zz}-I_{yz}^2}$$

$$\frac{d^2v}{dx^2}\frac{1}{(1+(\frac{dv}{dx})^2)^{3/2}} = \frac{1}{E_1}\frac{M_zI_{yy}-M_yI_{zz}}{I_{yy}I_{zz}-I_{yz}^2}$$

These become

$$\frac{d^2v}{dz^2}\frac{1}{(1\quad(\frac{dv}{dz})^2)^{3/2}} = -\frac{1}{E_1}\frac{M_xI_{yy}+M_yI_{xy}}{I_{xx}I_{yy}-(I_{xy})^2}$$

$$\frac{d^2u}{dz^2}\frac{1}{(1\quad(\frac{du}{dz})^2)^{3/2}} = \frac{1}{E_1}\frac{M_yI_{xx}+M_xI_{xy}}{I_{xx}I_{yy}-(I_{xy})^2}$$

Rivello's radial stress equation is

$$\sigma_{xx} = \frac{E}{E_1}\left[\frac{P}{A}+\frac{-(M_zI_{yy}-M_yI_{yz})y}{I_{yy}I_{zz}-(I_{yz})^2} - \frac{(M_yI_{zz}-M_zI_{yz})z}{I_{yy}I_{zz}-(I_{yz})^2}\right]$$

This becomes,

$$\sigma_{zz} = \frac{E}{E_1}\left[\frac{P}{A}+\frac{-(M_yI_{xx}+M_xI_{xy})x}{I_{xx}I_{yy}-(I_{xy})^2} + \frac{(M_xI_{yy}+M_yI_{xy})y}{I_{xx}I_{yy}-(I_{xy})^2}\right]$$

where

P is any radial load

A is the cross section area

M_i is a bending moment about the i^{th} axis

x,y,z are space coordinates

A P P E N D I X B

Equations of Motion

Figure B1 shows the transverse shear forces and bending moments acting on a slice of blade of length dz. This diagram neglects the influence of an off axis placement of the c.g., the inclusion of which would introduce torsional coupling. f_x and f_y are the D'alembert forces acting on the oscillating section.

Summing moments about the inferior edge, we have

$$x: \; -M_x + M_x + \frac{dM_x}{dz}\,dz + F_y\,\frac{dz}{2} - (V_y + \frac{dV_y}{dz}\,dz)dz = 0$$

Neglecting higher order terms in dz and cancelling

$$\frac{dM_x}{dz} = V_y \tag{1}$$

$$y: \; -M_y + M_y + \frac{dM_y}{dz}\,dz - f_x\,\frac{dz}{2} + (V_x + \frac{dV_x}{dz}\,dz)dz = 0$$

Neglecting higher order terms in dz and cancelling

$$\frac{dM_y}{dz} = -V_x \tag{2}$$

Summing forces acting on the element

FIG. B.1

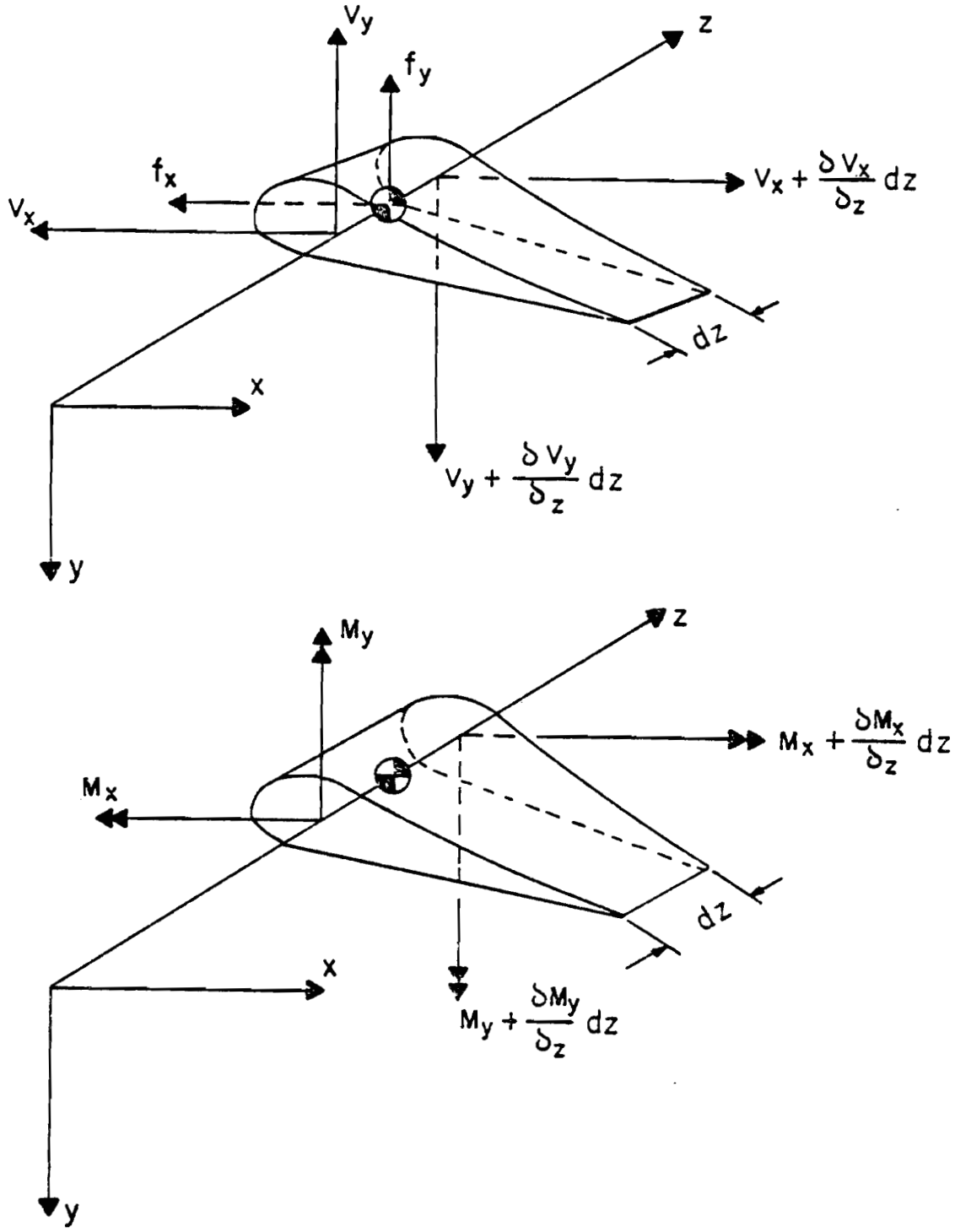
V_y
f_y
z
f_x
V_x
$V_x + \frac{\delta V_x}{\delta z} dz$
dz
x
$V_y + \frac{\delta V_y}{\delta z} dz$
y
M_y
z
$M_x + \frac{\delta M_x}{\delta z} dz$
M_x
dz
x
$M_y + \frac{\delta M_y}{\delta z} dz$
y

$$x: \quad -V_x - f_x + V_x + \frac{dV_x}{dz}\, dz = 0$$

$$f_x = \frac{dV_x}{dz}\, dz \tag{3a}$$

$$y: \quad -V_y - f_y + V_y + \frac{dV_y}{dz}\, dz = 0$$

$$f_y = \frac{dV_y}{dz}\, dz \tag{4a}$$

If m is the lineal mass density, u is a unit displacement in the x directions and v in the y direction, then

$$f_x = m\, \ddot{u}\, dz$$

$$f_y = m\, \ddot{v}\, dz$$

then from 3a and 4a, we have

$$m\, \ddot{u} = \frac{dV_x}{dz} \tag{3}$$

$$m\, \ddot{v} = \frac{dV_y}{dz} \tag{4}$$

For small displacements, we have from Rivello that

$$\frac{d^2u}{dz^2} = \frac{1}{E_1} \quad \frac{M_y I_{xx} + M_x I_{xy}}{I_{xx} I_{yy} - T_{xy}^2} \tag{5}$$

$$\frac{d^2v}{dz^2} = \frac{-1}{E_1} \quad \frac{M_x I_{yy} + M_y I_{xy}}{I_{xx} I_{yy} - I_{xy}^2} \tag{6}$$

where

a) E_1 is an arbitrary reference modulus

b) M_y is the bending moment about the y axis

c) M_x is the bending moment about the x axis

d) $$I_{xx} = \int_A \frac{E(x,y)}{E_1} y^2 \, dA$$

e) $$I_{yy} = \int_A \frac{E(x,y)}{E_1} x^2 \, dA$$

f) $$I_{xy} = \int_A \frac{E(x,y)}{E_1} xy \, dA$$

We can now solve for the bending moments at some point z in terms of the curvatures at that point. Let

$$\frac{d^2u}{dz^2} = u'' \quad , \quad \frac{d^2v}{dz^2} = v''$$

and

$$k = E_1 \, (I_{xx}I_{yy} - I_{xy}^2)$$

Rearranging 5 and 6,

$$\frac{k\,u'' - M_x I_{xy}}{I_{xx}} = M_y \tag{7}$$

$$\frac{-k\,v'' - M_y I_{xy}}{I_{yy}} = M_x \tag{8}$$

Substituting 8 into 7

$$\frac{k\ u''}{I_{xx}} + \frac{(k\ v'' + M_y I_{xy})}{I_{xx}I_{yy}}\ I_{xy} = M_y$$

$$k\ (\frac{u''}{I_{xx}} + \frac{I_{xy}\ v''}{I_{xx}I_{yy}}) + M_y\ (\frac{I_{xy}^2}{I_{xx}I_{yy}} - 1) = 0$$

$$M_y = \frac{k}{I_{xx}}\ (\frac{I_{xy}}{I_{yy}}\ v'' + u'')\ \ \frac{I_{xx}I_{yy}}{(I_{xx}I_{yy}-I_{xy}^2)}$$

Recalling the definition of k, this reduces to

$$M_y = E_1 I_{yy}\ (\frac{I_{xy}}{I_{yy}}\ v'' + u'')$$

Solving for M_x by insertion into 8

$$\frac{-k\ v''}{I_{yy}} - \frac{E_1 I_{yy}}{I_{yy}}\ (\frac{I_{xy}}{I_{yy}}\ v'' + u'')\ I_{xy} = M_x.$$

Expanding k and simplifying,

$$-E_1\ v''\ (I_{xx} - \frac{I_{xy}^2}{I_{yy}}) - E_1\ (\frac{I_{xy}}{I_{yy}}\ v'' + u''\ I_{xy}) = M_x$$

$$-E_1\ v''\ I_{xx} - E_1\ u''\ I_{xy} = M_x$$

$$M_x = -E_1 I_{xx}\ (\frac{u''\ I_{xy}}{I_{xx}} + v'')\ . \qquad (10)$$

Rewriting 1 in terms of 10 and 2 in terms of 9, we get

$$V_y = \frac{-d}{dz} E_1 I_{xx} \left(\frac{I_{xy}}{I_{xx}} \frac{d^2u}{dz^2} + \frac{d^2v}{dz^2}\right) \tag{11}$$

$$V_x = \frac{-d}{dz} E_1 I_{yy} \left(\frac{I_{xy}}{I_{yy}} \frac{d^2v}{dz^2} + \frac{d^2u}{dz^2}\right) . \tag{12}$$

Rewriting 3 in terms of 12 and 4 in terms of 11, we get

$$m \ddot{u} = \frac{-d^2}{dz^2} E_1 I_{xx} \left(\frac{I_{xy}}{I_{xx}} \frac{d^2u}{dz^2} + \frac{d^2v}{dz^2}\right) \tag{13}$$

$$m \ddot{v} = \frac{-d^2}{dz^2} E_1 I_{yy} \left(\frac{I_{xy}}{I_{yy}} \frac{d^2v}{dz^2} + \frac{d^2u}{dz^2}\right) \tag{14}$$

These are the equations of motion for the coupled flexural free vibrations of a beam of arbitrary mass distribution and construction. No closed form solution for these equations exists. Numerous simplifications are of engineering interest, however.

For example, if we consider a uniform homogeneous beam without twist, the equations 13 and 14 reduce to

$$m \ddot{u} = -EI_{xx} \left(\frac{I_{xy}}{I_{xx}} u^{iv} + v^{iv}\right) \tag{13a}$$

$$m \ddot{v} = -EI_{yy} \left(\frac{I_{xy}}{I_{yy}} v^{iv} + u^{iv}\right) \tag{14a}$$

where

$$f^{iv} \simeq \frac{d^4 f}{dz^4} .$$

If we further restrict attention to the case of bending about principal axes, then we have

$$m\ddot{u} = -EI_{xx}v^{iv} \tag{13b}$$

$$m\ddot{v} = -EI_{yy}u^{iv} \tag{14b}$$

These latter equations are commonly encountered in books on beam vibrations and structural dynamics.

A P P E N D I X C

C.1 Flow Chart Formalism

B_i	The subscript i implies that B is a data file with more than one number (potentially assigned to it).
$B_i[d_1,d_2,\ldots d_n]$	B_i is assigned all numbers included within the brackets.
$B_i[k]$	Only the k^{th} entry of B_i is considered.
	Input, Output or executable statement.
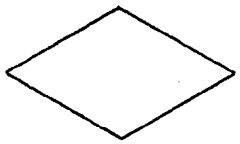	Decision or comparison.
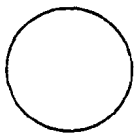	Program control transfer
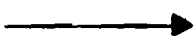	Machine control flow direction.

C.2 Program Moments

This is the main program of the static analysis. The program flow chart is included on the following pages.

The program first directs the presetting of pertinent variables, then the input of information necessary to the analysis. Once the input section is completed, the (modulus weighted) moments of inertia are transposed to the point at which the bending axis passes through the station. The program then rotates the section axes (hence the values of the moments of inertia) into the proper orientation for the bending analysis. Next the program computes the deflections due to bending by calling function DEF (see Appendix G). Finally, the stress levels in the skin are computed and reported.

The program then asks whether or not iteration is desired. If not, program execution ceases. If yes, the operator is asked for the starting value of the collective pitch, the increment by which the collective pitch is to be changed (this may be positive or negative) and the number of iterations desired. The load pattern is assumed to remain constant. The program then computes the bending stress distribution associated with each collective pitch setting.

There were few problems involved in writing the main program. The coordinate transformations are straightforward. One peculiarity of the algorithm is that the variable BMX is actually the negative of the bending moments about the x axis.

The iterative loop for reporting stresses was introduced to save computer time. That section of the program uses very little computer time when compared with the input section. Consequently, one input can result

FIG. C.1

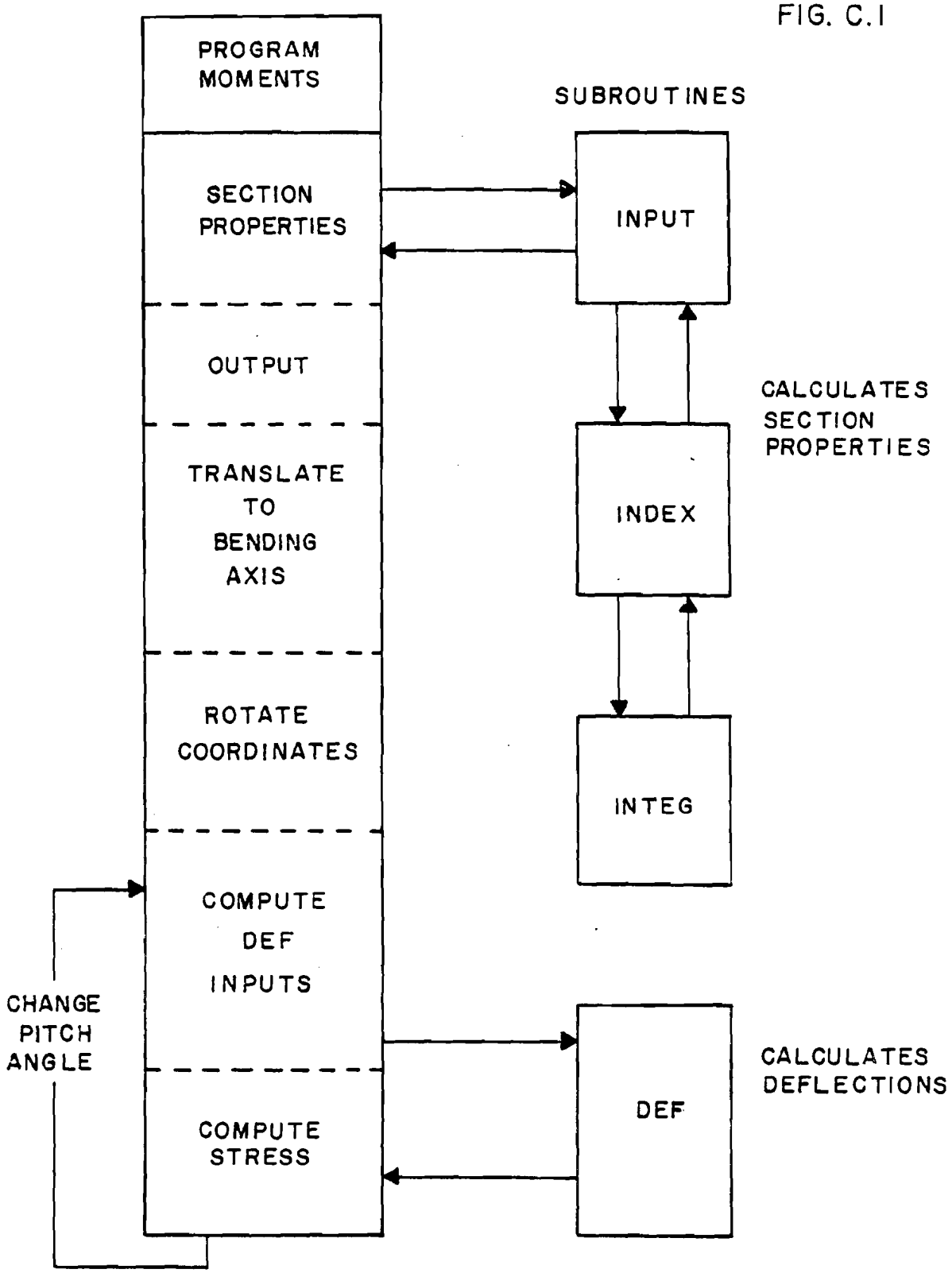

SCHEMATIC PROGRAM MOMENTS

in analysis of many different collective pitch settings. One obvious refinement, which has not been made, is to allow the introduction of different load patterns within the iterative loop. Presently, only collective pitch may be indexed.

Alternatively, the program can be very easily modified to allow the moments of inertia for particular designs to be stored in global memory. This would require the input section to be used only once for any particular blade design. The modification necessary is the removal of the variables concerned from the header line of MOMENTS.

PRINCIPAL VARIABLES

BETA	Local pitch angle
BETANOT	Collective pitch angle
THETA	1) Polar Mass Moment of Inertia about rotor axis 2) ANGLE of PRINCIPAL AXES w.r.t. chord at each station. (Positive is a rotation from Leading edge towards Low Pressure surface)
PR	Minor principal moment of inertia
PS	Major principal moment of Inertia
RHO	Local pitch angle w.r.t. wind mill axes
IXX	Section moment of inertia about windmill x axis
IYY	Section moment of inertia about windmill y axis
IXY	Mixed section moment of inertia about windmill axis
EUP	Bending modulus at low pressure surface skin
ELO	Bending modulus of high pressure surface skin
YU	Y coordinate distribution of low pressure surface
XC	X coordinate distribution of low pressure surface
YL	Y coordinate distribution of high pressure surface
XCL	X coordinate distribution of high pressure surface
C1	$-\frac{1}{E}\left(\frac{M_x I_{yy}+M_y I_{xy}}{I_{xx}I_{yy}-I_{xy}^2}\right)$
C2	$\frac{1}{E_1}\left(\frac{M_y I_{xx}+M_x I_{xy}}{I_{xx}I_{yy}-I_{xy}^2}\right)$
STRU	Stress distribution in Low Pressure surface skin

STRL	Stress distribution in High Pressure surface skin

PROGRAM LISTING

```
      ∇MOMENTS[□]∇
      ∇MOMENTS;IXXO;IYYO;IXYO;THETA;PR;PS;ROOT;YBAR;GEOAREA;BETA;RHO;YUP;YLO;C1;C2;
[1]    FOOL1                                                    XC;XCL;YU;YL;YUP1;YLO1
[2]    INPUT
[3]    ⍝
[4]    ⍝FIND IXXC,IYYC,IXYC
[5]    IXXC←IXXO-AREA×YBAR*2
[6]    IYYC←IYYO-AREA×XBAR1*2
[7]    IXYC←IXYO-AREA×XBAR1×YBAR
[8]    BETA←BETA+PHI
[9]    THETA←H×((2⊖PR)×INBORD+H×¯1+⍳⍴MASS)*2
[10]   THETA←THETA×MASS
[11]   THETA[1]←THETA[1]÷2
[12]   THETA[⍴THETA]←THETA[⍴THETA]÷2
[13]   'MASS MOMENT OF INERTIA ABOUT THE ROTOR AXIS (LB IN SEC*2) ';+/THETA÷32.2×12
[14]   ''
[15]   THETA←MASS×H
[16]   THETA[1]←THETA[1]÷2
[17]   THETA[⍴THETA]←THETA[⍴THETA]÷2
[18]   'BLADE WEIGHT, POUNDS ';+/THETA
[19]   ''
[20]   ''
[21]   ⍝
[22]   ⍝FIND PRINCIPAL ANGLE AND MOMENTS OF INERTIA
[23]   THETA←(¯3⊖(2×IXYC÷IYYC-IXXC))÷2
[24]   PR←((IXXC+IYYC)÷2)-ROOT←(((((IXXC-IYYC)÷2)*2)+IXYC*2)*0.5
[25]   PS←((IXXC+IYYC)÷2)+ROOT
[26]   'INCLINATION OF SECTION PRINCIPAL AXES FROM CHORD (CCW=+)'
[27]   9 2↑THETA×57.29578
[28]   ''
[29]   'MODULUS WEIGHTED CENTROID LOCATION'
[30]   '   XBAR     YBAR'
[31]   9 2↑⊖(2,⍴XBAR)⍴XBAR,YBAR
[32]   ''
[33]   'MODULUS WEIGHTED X  CENTROID LOCATION AS CHORD FRACTION'
[34]   9 3↑XBAR÷CHORD
[35]   ''
[36]   'MASS CENTROID COORDINATES'
[37]   '    XBAR     YBAR'
[38]   9 2↑⊖(2,⍴MASSX)⍴MASSX,MASST
[39]   ''
[40]   'MASS X CENTROID AS CHORD FRACTION'
[41]   9 3↑MASSX÷CHORD
[42]   ''
[43]   'BENDING STIFFNESSES ÷1E7'
[44]   'ABOUT THE MAJOR PRINCIPAL AXIS'
[45]   9 2↑PR
[46]   ''
[47]   'ABOUT THE MINOR PRINCIPAL AXIS'
[48]   9 2↑PS
[49]   ''
[50]   'TOTAL AREA OF MASS'
[51]   9 2↑GEOAREA
[52]   ''
[53]   'WEIGHT OF UNIT SPAN, POUNDS PER INCH'
[54]   9 4↑MASS
[55]   ⍝
[56]  P0:⍝COMPUTE MOMENTS OF INERTIA ABOUT WINDMILL AXES
[57]   ''
[58]   ''
[59]   ''
[60]   'BETA NAUGHT ';(¯1↑BETA)×180÷○1
[61]   ''
[62]   'BENDING STIFFNESSES (÷1E7) ABOUT WINDMILL AXES REFERRED TO BENDING AXIS'
```

```
[63]   RHO←BETA-@1
[64]   'ExIXX÷1E7'
[65]   9 2▼IXX←(IXXCx(2@RHO)*2)+(IYYCx(1@RHO)*2)-DD←2x(1@RHO)x(2@RHO)xIXYC
[66]   ''
[67]   'ExIYY÷1E7'
[68]   9 2▼IYY←(IXXCx(1@RHO)*2)+(IYYCx(2@RHO)*2)+DD
[69]   ''
[70]   'ExIXY÷1E7'
[71]   9 2▼IXY←(IXXCx(1@RHO)x2@RHO)-(IYYCx(1@RHO)x2@RHO)+IXYCx2@2xRHO
[72]   ''
[73]   YOUNG←10000000
[74]   C1←(÷YOUNG)x((BMXxIYY)-BMYxIXY)÷(IXXxIYY)-IXY*2
[75]   C2←(÷YOUNG)x((BMYxIXX)-BMXxIXY)÷(IXXxIYY)-IXY*2
[76]   ''
[77]   ''
[78]   'IN THE FLAP DIRECTION'
[79]   (H,⍴C1)DEF C1
[80]   ''
[81]   ''
[82]   'IN THE LEAD LAG DIRECTION'
[83]   (H,⍴C2)DEF C2
[84]   ⍝COMPUTE STRESSES IN THE SKIN
[85]   I←1
[86]   ⍝ITERATIVE LOOP FOR REPORTING OUT STRESSB
[87]   ⍝⍝AXIS ROTATION
[88]   EUP←YUP[1;1]
[89]   ELO←YLO[1;1]
[90]   XB←X
[91]   YUP1←(1 1)↓YUP
[92]   YLO1←(1 1)↓YLO
[93]   'ORDER OF READING IS BENDING STRESS ABOVE X, X/CHORD, BENDING STRESS BELOW X'
[94]  P1:⍝==========================================
[95]   YUP1[I;]←YUP1[I;]-YBAR[I]
[96]   YLO1[I;]←YLO1[I;]-YBAR[I]
[97]   X1←(¯1xXBAR1[I])+XB[I;]
[98]   YU←(¯1xX1x1@RHO[I])+YUP1[I;]∘.x2@RHO[I]
[99]   YL←(¯1xX1x1@RHO[I])+YLO1[I;]∘.x2@RHO[I]
[100]  XC←(X1x2@RHO[I])+YUP1[I;]∘.x1@RHO[I]
[101]  XCL←(X1x2@RHO[I])+YLO1[I;]∘.x1@RHO[I]
[102]  ⍝
[103]  ⍝STRESS FORMULATION AND SOLUTION
[104]  STRU←STRL←(⍴YUP)⍴1
[105]  STRU←EUPx(C1[I]∘.xYU)+C2[I]∘.xXC
[106]  STRL←ELOx(C1[I]∘.xYL)+C2[I]∘.xXCL
[107]  ''
[108]  ''
[109]  'STATION NUMBER ';I
[110]  7 0▼STRU
[111]  7 2▼(X1+XBAR1[I])÷CHORD[I]
[112]  7 0▼STRL
[113]  ''
[114]  I←I+1
[115]  →(I)⍴C1)/P2
[116]  →P1
[117] P2:→(ITIND≠0)/P3
[118]  ''
[119]  ''
[120]  'DO YOU WANT TO ITERATE WITH ME?'
[121]  ITIND←∧/''YES'=3⍴□
[122]  →(ITIND=0)/P4
[123]  ITIND←0
[124]  'NUMBER OF ITERATIONS'
[125]  NIT←□
[126]  'INCREMENT'
[127]  ITINC←(@÷180)x□
[128]  'STARTING POINT'
```

```
[129]   ITSTAR←(Θ÷180)×□
[130]   ITSTAR←ITSTAR-ITINC
[131]   BETA←PHI+ITSTAR
[132] P3:ITIND←ITIND+1
[133]   →(ITIND>NIT)/P4
[134]   BETA←BETA+ITINC
[135]   →P0
[136] P4:'END OF PROGRAM'
      ∇
```

FUNCTION MOMENTS

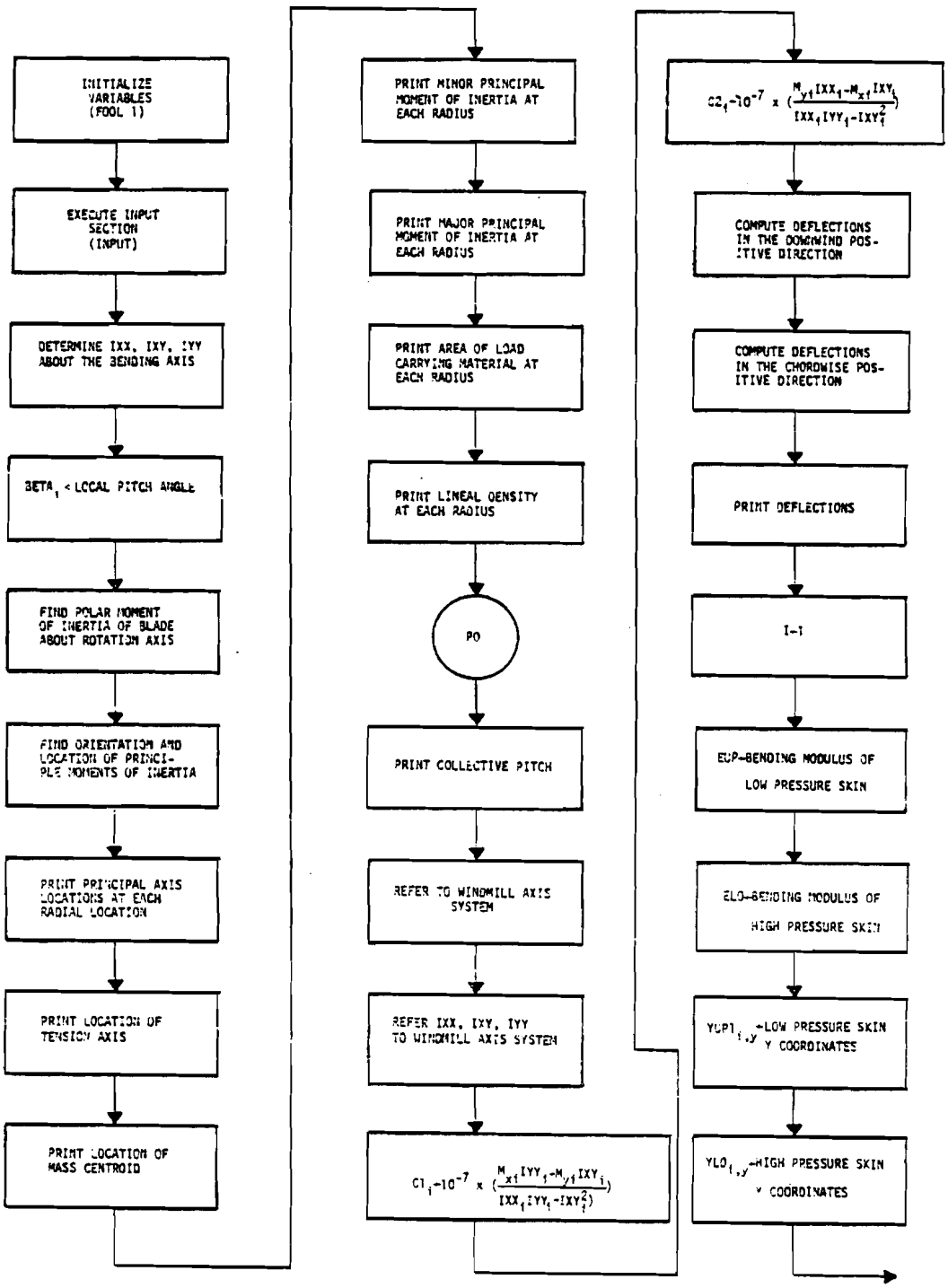

MOMENTS (Continued)

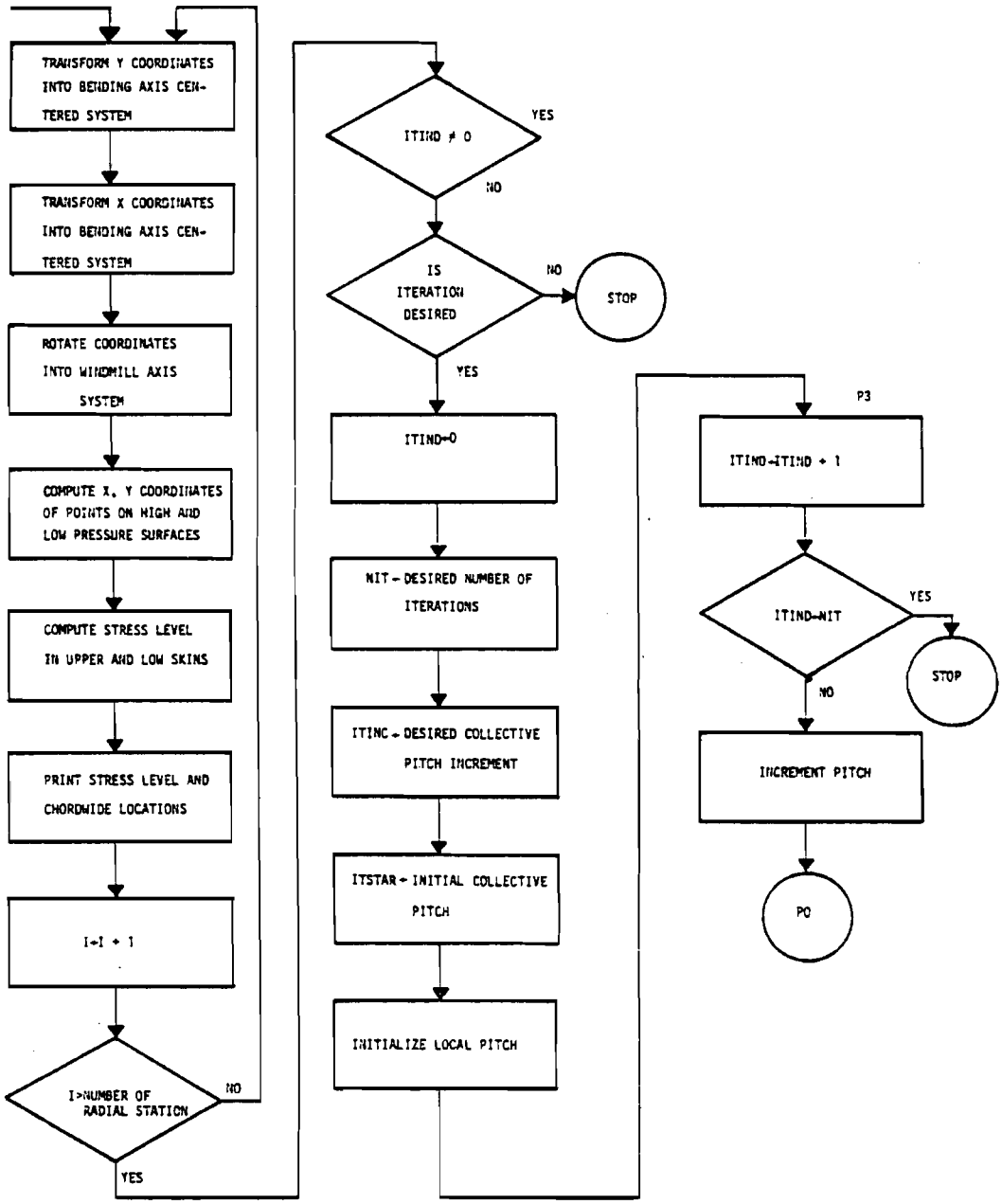

TERMINAL SESSION

```
      MOMENTS

ENTER THE NUMBER OF DATA SETS
□:
      8
ENTER THE UPPER SKIN Y CO-ORDINATES
□:
      NEWF1
ENTER THE SKIN X CO-ORD
□:
      NEWF12X
ENTER THE LOWER SKIN Y CO-ORD
□:
      NEWF2

ENTER THE Y MATRIX
□:
      NEWF3
X MATRIX
□:
      NEWF34X

ENTER THE Y MATRIX
□:
      NEWF4
X MATRIX
□:
      NEWF34X

ENTER THE Y MATRIX
□:
      NEWF5
X MATRIX
□:
      NEWF56X

ENTER THE Y MATRIX
□:
      NEWF6
X MATRIX
□:
      NEWF56X

ENTER THE Y MATRIX
□:
      NEWF7
X MATRIX
□:
      NEWF78X

ENTER THE Y MATRIX
□:
      NEWF8
X MATRIX
□:
      NEWF78X
```

```
READ VECTOR PHI, THE REL. TWIST IN DEGREES
□:
      NEWPHI
ENTER BETA NAUGHT
□:
      0
ENTER THE RADIAL STATION SPACING, H
□:
      19.5
ENTER THE LOCATION OF THE BENDING AXIS
□:
      .25xCHORD
SHEAR FORCE PER SPANWISE SECTION IN THE X DIRECTION
□:
      0 0 0 0 0 0 0 0 0
SHEAR FORCE IN THE Y DIRECTION
□:
      0 0 0 0 0 0 0 0 15+9÷16
ENTER THE RADIUS OF THE MOST INBOARD STATION.
□:
      19.5


CONING ANGLE?
□:
      10

MASS MOMENT OF INERTIA ABOUT THE ROTOR AXIS (LB IN SEC*2) 664.6

BLADE WEIGHT, POUNDS 34.06

INCLINATION OF SECTION PRINCIPAL AXES FROM CHORD (CCW=+)
   ¯10.89     5.59     5.06     4.58     3.50     4.77    17.23     7.33     8.78     6.24

MODULUS WEIGHTED CENTROID LOCATION
   XBAR     YBAR
     3.61     1.04
     4.29     0.63
     3.77     0.55
     3.01     0.45
     2.43     0.38
     2.07     0.34
     2.03     0.38
     1.56     0.27
     1.33     0.24
     1.16     0.15

MODULUS WEIGHTED X  CENTROID LOCATION AS CHORD FRACTION
    0.223    0.245    0.249    0.246    0.238    0.236    0.269    0.236    0.246    0.276

MASS CENTROID COORDINATES
    XBAR     YBAR
     3.80     1.02
     4.62     0.62
     4.08     0.54
     3.28     0.45
     2.66     0.38
     2.25     0.34
     2.15     0.36
     1.70     0.27
     1.47     0.25
```

```
     1.31      0.16

MASS X CENTROID AS CHORD FRACTION
    0.234     0.264     0.270     0.268     0.261     0.256     0.285     0.258     0.272     0.311

BENDING STIFFNESSES ÷1E7
ABOUT THE MAJOR PRINCIPAL AXIS
     4.09      2.96      1.67      1.01      0.65      0.39      0.16      0.13      0.06      0.01

ABOUT THE MINOR PRINCIPAL AXIS
    13.89     15.13     10.23      5.50      3.18      1.51      0.91      0.44      0.27      0.15

TOTAL AREA OF MASS
    10.32      6.33      4.94      4.16      3.57      2.76      2.42      1.51      1.06      0.55

WEIGHT OF UNIT SPAN, POUNDS PER INCH
   0.5633    0.3431    0.2671    0.2254    0.1940    0.1507    0.1298    0.0825    0.0574    0.0295


BETA NAUGHT 0

BENDING STIFFNESSES (÷1E7) ABOUT WINDMILL AXES REFERRED TO BENDING AXIS
EXIXX÷1E7
     7.17      4.39      1.97      1.05      0.67      0.39      0.21      0.13      0.07      0.01

EXIYY÷1E7
    10.81     13.71      9.93      5.45      3.17      1.51      0.86      0.44      0.27      0.15

EXIXY÷1E7
     4.55     -5.39     -2.86     -1.12     -0.47     -0.18     -0.24     -0.05     -0.03     -0.02


IN THE FLAP DIRECTION
DEFLECTION
   0.000     0.016     0.077     0.205     0.415     0.723     1.162     1.766     2.513     3.339


IN THE LEAD LAG DIRECTION
DEFLECTION
   0.000     0.002     0.015     0.047     0.097     0.161     0.249     0.373     0.520     0.678

ORDER OF READING IS BENDING STRESS ABOVE X, X/CHORD, BENDING STRESS BELOW X


STATION NUMBER 1
    -447      -444      -379      -220       -37       163       375       596       824      1179      1551
    0.00      0.05      0.10      0.20      0.30      0.40      0.50      0.60      0.70      0.85      1.00
    -447      -293      -181        22       215       406       597       787       977      1265      1551


STATION NUMBER 2
      84      -203      -297      -391      -411      -377      -306      -207       -85       140       418
    0.00      0.05      0.10      0.20      0.30      0.40      0.50      0.60      0.70      0.85      1.00
      84       273       327       370       382       389       395       398       400       410       418


STATION NUMBER 3
     241      -187      -344      -525      -602      -604      -552      -462      -340       -96       222
    0.00      0.05      0.10      0.20      0.30      0.40      0.50      0.60      0.70      0.85      1.00
     241       484       536       547       515       476       434       389       343       285       222
```

```
STATION NUMBER 4
    257    -173    -334    -525    -612    -625    -585    -507    -396    -172     128
   0.00    0.05    0.10    0.20    0.30    0.40    0.50    0.60    0.70    0.85    1.00
    257     492     538     537     495     445     393     337     281     206     128


STATION NUMBER 5
    232    -189    -346    -530    -613    -623    -580    -501    -390    -165     134
   0.00    0.05    0.10    0.20    0.30    0.40    0.50    0.60    0.70    0.85    1.00
    232     464     511     513     474     428     380     328     275     206     134


STATION NUMBER 6
    285    -178    -354    -567    -669    -692    -658    -584    -476    -250      56
   0.00    0.05    0.10    0.20    0.30    0.40    0.50    0.60    0.70    0.85    1.00
    285     531     576     566     512     449     385     316     247     153      56


STATION NUMBER 7
    966     172    -184    -680   -1006   -1211   -1329   -1386   -1391   -1300   -1087
   0.00    0.05    0.10    0.20    0.30    0.40    0.50    0.60    0.70    0.85    1.00
    966    1258    1241    1056     802     537     267      -8    -284    -683   -1087


STATION NUMBER 8
    320    -116    -289    -506    -621    -664    -655    -608    -530    -355    -107
   0.00    0.05    0.10    0.20    0.30    0.40    0.50    0.60    0.70    0.85    1.00
    320     535     565     535     463     384     303     219     133      15    -107


STATION NUMBER 9
    212     -47    -152    -286    -362    -395    -398    -379    -342    -252    -120
   0.00    0.05    0.10    0.20    0.30    0.40    0.50    0.60    0.70    0.85    1.00
    212     333     346     320     270     216     160     103      45     -37    -120


STATION NUMBER 10
      0       0       0       0       0       0       0       0       0       0       0
   0.00    0.05    0.10    0.20    0.30    0.40    0.50    0.60    0.70    0.85    1.00
      0       0       0       0       0       0       0       0       0       0       0


DO YOU WANT TO ITERATE WITH ME?
YES
NUMBER OF ITERATIONS
0:
      2
INCREMENT
0:
      2
STARTING POINT
0:
      2


BETA NAUGHT 2
```

BENDING STIFFNESSES (÷1E7) ABOUT WINDMILL AXES REFERRED TO BENDING AXIS

ExIXX÷1E7

6.86	4.67	2.09	1.09	0.68	0.39	0.20	0.13	0.07	0.01

ExIYY÷1E7

11.12	13.42	9.81	5.41	3.15	1.51	0.87	0.44	0.27	0.15

ExIXY÷1E7

4.67	-5.57	-3.07	-1.25	-0.55	-0.22	-0.26	-0.06	-0.04	-0.02

IN THE FLAP DIRECTION

DEFLECTION

0.000	0.016	0.076	0.205	0.419	0.731	1.186	1.826	2.621	3.501

IN THE LEAD LAG DIRECTION

DEFLECTION

0.000	0.002	0.016	0.050	0.104	0.176	0.278	0.424	0.601	0.790

ORDER OF READING IS BENDING STRESS ABOVE X, X/CHORD, BENDING STRESS BELOW X

STATION NUMBER 1

-491	-477	-403	-226	-26	191	420	658	902	1282	1679
0.00	0.05	0.10	0.20	0.30	0.40	0.50	0.60	0.70	0.85	1.00
-491	-329	-209	11	222	430	639	846	1053	1367	1679

STATION NUMBER 2

63	-211	-299	-382	-394	-354	-278	-175	-50	179	459
0.00	0.05	0.10	0.20	0.30	0.40	0.50	0.60	0.70	0.85	1.00
63	250	306	354	374	388	400	410	420	441	459

STATION NUMBER 3

228	-207	-364	-543	-613	-607	-547	-447	-314	-52	286
0.00	0.05	0.10	0.20	0.30	0.40	0.50	0.60	0.70	0.85	1.00
228	481	538	556	532	499	465	426	387	338	286

STATION NUMBER 4

250	-192	-355	-546	-630	-637	-589	-502	-382	-140	179
0.00	0.05	0.10	0.20	0.30	0.40	0.50	0.60	0.70	0.85	1.00
250	496	547	552	515	470	422	371	319	251	179

STATION NUMBER 5

225	-204	-362	-546	-625	-629	-581	-494	-375	-137	176
0.00	0.05	0.10	0.20	0.30	0.40	0.50	0.60	0.70	0.85	1.00
225	465	515	523	488	446	402	354	306	243	176

STATION NUMBER 6

277	-196	-374	-586	-684	-701	-660	-577	-459	-217	107
0.00	0.05	0.10	0.20	0.30	0.40	0.50	0.60	0.70	0.85	1.00
277	533	582	578	529	472	412	348	283	197	107

STATION NUMBER 7

1097	164	-249	-817	-1184	-1408	-1529	-1576	-1561	-1423	-1140
0.00	0.05	0.10	0.20	0.30	0.40	0.50	0.60	0.70	0.85	1.00
1097	1453	1443	1244	963	668	368	61	-247	-690	-1140

STATION NUMBER 8

316	-134	-310	-529	-642	-679	-663	-608	-520	-328	-61
0.00	0.05	0.10	0.20	0.30	0.40	0.50	0.60	0.70	0.85	1.00
316	542	577	552	484	409	332	250	169	56	-61

STATION NUMBER 9

217	-56	-167	-307	-384	-416	-416	-392	-349	-249	-103
0.00	0.05	0.10	0.20	0.30	0.40	0.50	0.60	0.70	0.85	1.00
217	348	364	340	290	235	179	121	63	-19	-103

STATION NUMBER 10

0	0	0	0	0	0	0	0	0	0	0
0.00	0.05	0.10	0.20	0.30	0.40	0.50	0.60	0.70	0.85	1.00
0	0	0	0	0	0	0	0	0	0	0

BETA NAUGHT 4

BENDING STIFFNESSES (÷1E7) ABOUT WINDMILL AXES REFERRED TO BENDING AXIS

ExIXX÷1E7

6.55	4.98	2.23	1.14	0.70	0.39	0.19	0.13	0.06	0.01

ExIYY÷1E7

11.42	13.12	9.67	5.37	3.13	1.51	0.88	0.44	0.27	0.15

ExIXY÷1E7

4.76	-5.73	-3.27	-1.38	-0.63	-0.25	-0.28	-0.07	-0.05	-0.02

IN THE FLAP DIRECTION

DEFLECTION

0.000	0.016	0.076	0.204	0.419	0.734	1.205	1.887	2.740	3.681

IN THE LEAD LAG DIRECTION

DEFLECTION

0.000	0.002	0.016	0.052	0.111	0.190	0.306	0.478	0.688	0.912

ORDER OF READING IS BENDING STRESS ABOVE X, X/CHORD, BENDING STRESS BELOW X

STATION NUMBER 1

-537	-512	-429	-232	-13	222	468	723	985	1391	1813
0.00	0.05	0.10	0.20	0.30	0.40	0.50	0.60	0.70	0.85	1.00
-537	-367	-238	-1	228	455	681	907	1132	1473	1813

STATION NUMBER 2

42	-217	-297	-370	-374	-329	-248	-143	-16	215	494
0.00	0.05	0.10	0.20	0.30	0.40	0.50	0.60	0.70	0.85	1.00
42	225	283	336	362	383	402	418	435	466	494

STATION NUMBER 3

211	-226	-381	-554	-617	-603	-533	-424	-281	-4	351
0.00	0.05	0.10	0.20	0.30	0.40	0.50	0.60	0.70	0.85	1.00
211	470	532	560	543	518	491	461	429	392	351

STATION NUMBER 4

240	-211	-376	-565	-644	-645	-588	-492	-362	-102	236
0.00	0.05	0.10	0.20	0.30	0.40	0.50	0.60	0.70	0.85	1.00
240	496	552	565	533	493	451	405	359	299	236

STATION NUMBER 5

215	-219	-378	-560	-635	-634	-579	-485	-358	-106	222
0.00	0.05	0.10	0.20	0.30	0.40	0.50	0.60	0.70	0.85	1.00
215	463	517	531	501	464	425	381	337	282	222

STATION NUMBER 6

266	-215	-394	-604	-697	-708	-658	-567	-439	-180	162
0.00	0.05	0.10	0.20	0.30	0.40	0.50	0.60	0.70	0.85	1.00
266	532	586	589	546	494	440	381	322	244	162

STATION NUMBER 7

1258	145	-339	-999	-1415	-1659	-1778	-1810	-1765	-1560	-1180
0.00	0.05	0.10	0.20	0.30	0.40	0.50	0.60	0.70	0.85	1.00
1258	1701	1702	1487	1174	844	509	165	-181	-676	-1180

STATION NUMBER 8

309	-154	-333	-552	-661	-693	-669	-605	-507	-297	-8
0.00	0.05	0.10	0.20	0.30	0.40	0.50	0.60	0.70	0.85	1.00
309	547	587	568	506	435	362	285	208	102	-8

STATION NUMBER 9

222	-68	-183	-329	-407	-438	-433	-405	-355	-242	-81
0.00	0.05	0.10	0.20	0.30	0.40	0.50	0.60	0.70	0.85	1.00
222	363	382	360	311	256	201	143	84	3	-81

STATION NUMBER 10

0	0	0	0	0	0	0	0	0	0	0
0.00	0.05	0.10	0.20	0.30	0.40	0.50	0.60	0.70	0.85	1.00
0	0	0	0	0	0	0	0	0	0	0

END OF PROGRAM

APPENDIX D

FUNCTION INPUT

Function input reads the data necessary for all subsequent calculations. The function also calls the routines which compute the sections' structural characteristics.

The calculations actually performed by the subroutine are limited to incrementing indices and the reduction of first moments to centroids by division by the appropriately weighted areas. Specifically,

$$\text{XBAR} \quad \frac{\int_A (E(x,y) \div E_1) x \, dA}{\int_A (E(x,y) \div E_1) \, dA}$$

$$\text{YBAR} \quad \frac{\int_A (E(x,y) \div E_1) y \, dA}{\int_A (E(x,y) \div E_1) \, dA}$$

$$\text{MASSX} \quad \frac{\int_A \rho(x,y) x \, dA}{\int_A \rho(x,y) \, dA}$$

$$\text{MASSY} \quad \frac{\int_A \rho(x,y) y \, dA}{\int_A \rho(x,y) \, dA}$$

where

$\int_A \phi \, dA$ is the integral of the function over all load carrying area,

$E(x,y)$ is the local bending modulus,

E_1 is an arbitrary reference modulus,

$\rho(x,y)$ is the local density.

The function checks to insure that the correct number of transverse loads have been entered in both the x and y directions.

By the time the vectorial inputs are required (line 28 and beyond) the vector CHORD has already been established. This is useful if, for example, the bending axis is scaled with the chord. Thus, when the program asks for the location of the bending axis, one need only type '.25 x CHORD' and all of the bending will be referred to the quarter chord line. If scaled any other way, this can also be entered as long as the scale has the same shape as CHORD.

MASSX and XBAR have also been established at this point. They could be exploited in a similar manner.

(The characterization of the rotor as a cantilever beam supported at the most inboard station is accomplished at this point by the function BEND. This will be described explicitly in Appendix H. Any other beam type can be accomplished by modification of this Function.)

The variable CHORD, the values of the chord length for the various sections, is assigned by operation on the first entered file of x coordinates. If any data file is entered which does not contain this information, the values stored in CHORD will be incorrect. Subsequent calculations based on the chord will be adversely effected.

PRINCIPAL VARIABLES

YUP	A record of the Low pressure skin Y coordinates and bending modulus
YLO	A record of the high pressure skin Y coordinates and bending modulus
X	A Record of the X coordinates associated with the above
XBAR	The X component of the modulus weighted centroid for each station
YBAR	The Y component of the modulus weighted centriod for each station
MASSX	The X components of the mass centroid locations
MASSY	The Y components of the mass centroid locations

PROGRAM LISTING

```
∇INPUT[□]∇
      ∇INPUT;N;JJ;MM1;MM
[1]     ''
[2]     ''
[3]     'ENTER THE NUMBER OF DATA SETS'
[4]     N←□
[5]     JJ←0
[6]     'ENTER THE UPPER SKIN Y CO-ORDINATES '
[7]     MM1←YUP←□
[8]     'ENTER THE SKIN X CO-ORD'
[9]     MM←X←□
[10]    CHORD←⌈/MM
[11]    →DALTON
[12]   LENOX:'ENTER THE LOWER SKIN Y CO-ORD'
[13]    YLO←MM1←□
[14]    →DALTON
[15]    ''
[16]    ''
[17]   L1:''
[18]    ''
[19]    'ENTER THE Y MATRIX'
[20]    MM1←□
[21]    'X MATRIX'
[22]    MM←□
[23]   DALTON:MM INDEX MM1
[24]    JJ←JJ+1
[25]    →(JJ=N)/ALBANY
[26]    →(JJ=1)/LENOX
[27]    →L1
[28]   ALBANY:'READ VECTOR PHI, THE REL. TWIST IN DEGREES'
[29]    XBAR←XBAR÷AREA
[30]    YBAR←YBAR÷AREA
[31]    MASSX←MASSX÷MASS
[32]    MASSY←MASSY÷MASS
[33]    PHI←(0÷180)×□
[34]    'ENTER BETA NAUGHT'
[35]    BETA←(0÷180)×□
[36]    'ENTER THE RADIAL STATION SPACING, H'
[37]    H←□
[38]    'ENTER THE LOCATION OF THE BENDING AXIS'
[39]    XBAR1←□
[40]   CX1:'SHEAR FORCE PER SPANWISE SECTION IN THE X DIRECTION'
[41]    BMY←H BEND □
[42]    →((⍴BMY)=⍴CHORD)/CX2
[43]    'INCORRECT SHEAR INPUT, TRY AGAIN.'
[44]    →CX1
[45]   CX2:'SHEAR FORCE IN THE Y DIRECTION'
[46]    BMX←H BEND □
[47]    →((⍴BMX)=⍴CHORD)/CX3
[48]    'INCORRECT SHEAR INPUT, TRY AGAIN.'
[49]    →CX2
[50]   CX3:'ENTER THE RADIUS OF THE MOST INBOARD STATION.'
[51]    INBORD←□
[52]    'CONING ANGLE? '
[53]    PR←(0÷180)×□
[54]    ''
[55]    ''
      ∇
```

FUNCTION INPUT

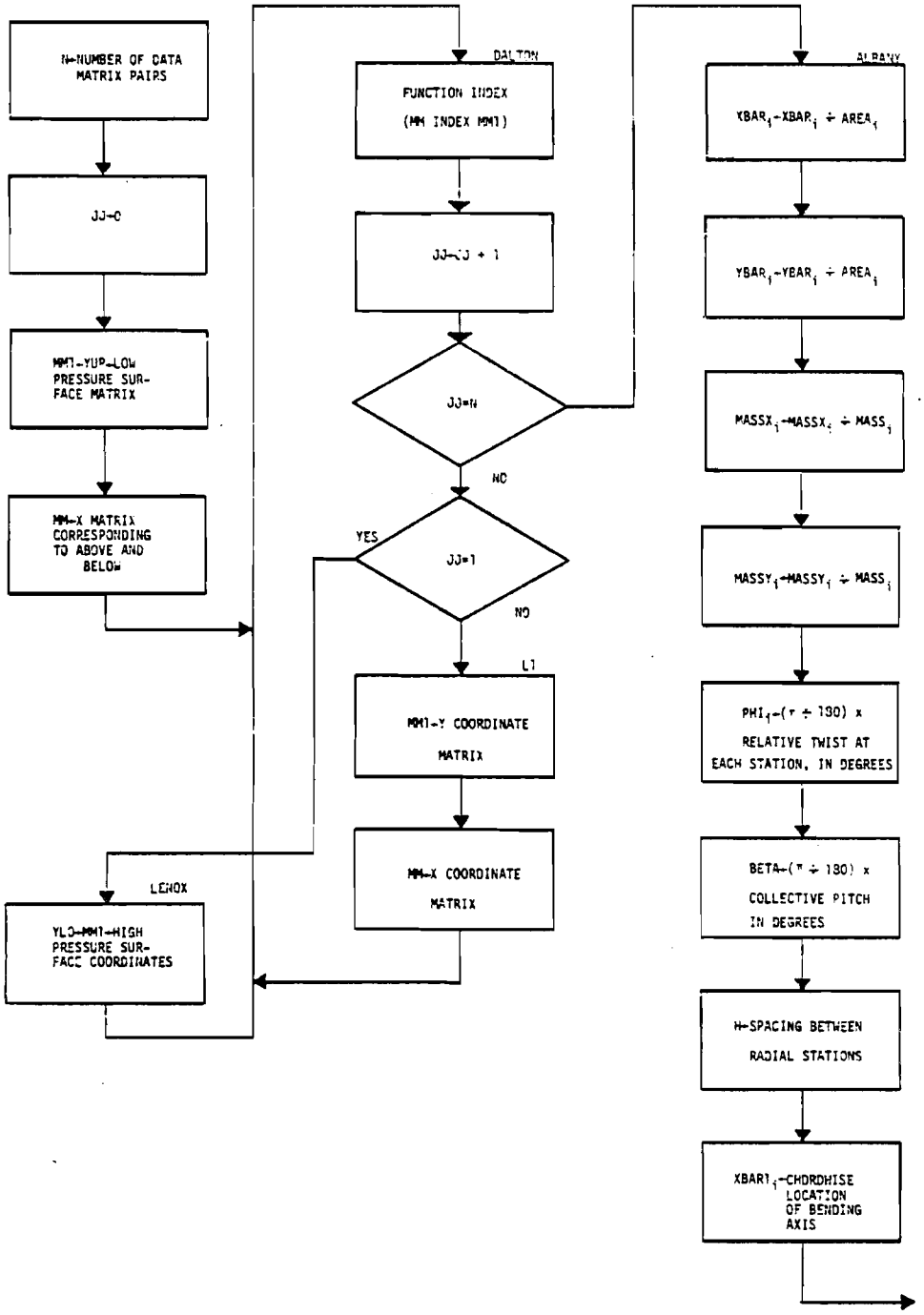

INPUT (Continued)

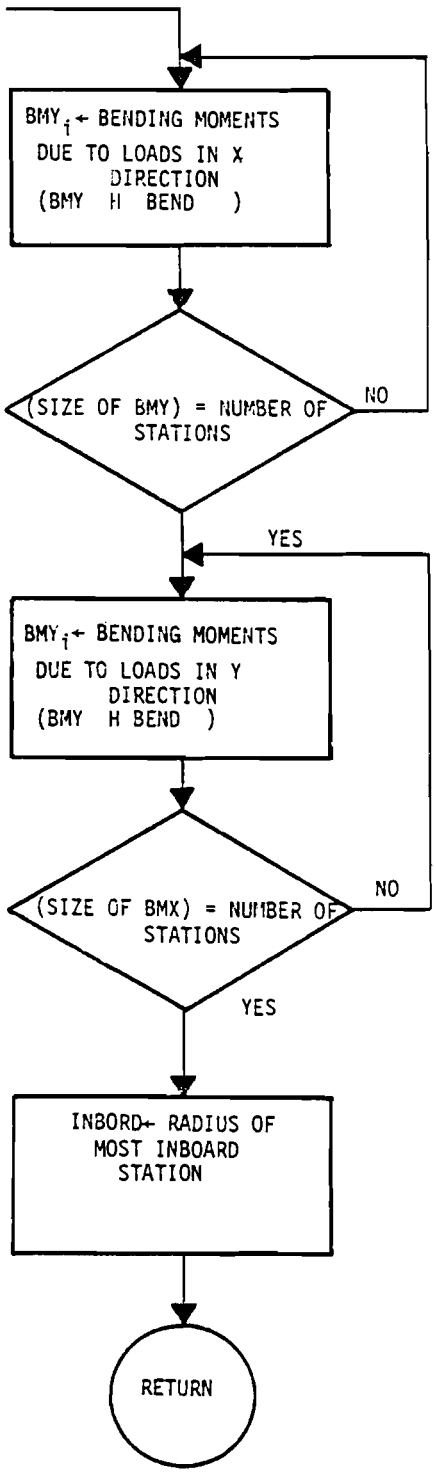

A P P E N D I X E

FUNCTION INDEX

This function reads the data files MM and MM1 and directs their integration.

The only arithmetic activity is the addition of the results of function INTEG to the appropriate variables.

The vector X consists of the x coordinates, the local bending modulus, and the local density. The vector Y consists of the thickness of the section being considered, and three y coordinates corresponding to the above x coordinates. The function INTEG is then called to operate on x and y.

On the first pass, that is when the first data file is being processed, the size of the variables in lines 15 through 24 is established. When other data files are being processed, the newly integrated quantities are summed with the appropriate elements of the already established vectors. The unique advantage of this arrangement is that any size data files may be used in the analysis. The algorithm automatically adapts itself, as long as every data file pertains to the same number of stations.

The program first moves across the columns, then down the rows. Because the program always picks out three points at a time, there are some requirements on the shape of MM and MM1. Since each row of MM1 except the first contains thickness and coordinate information, each row must have an even number of numerals included. Each row of MM must have an odd number of entries. MM1 must have one more row than MM, because the first row of MM contains only bending modulus and density information.

PRINCIPAL VARIABLES

$IXXO_i$ $\int_{A_i} \frac{E(x,y)y^2\, dA_i}{E_1}$ measured from chord line

$IYYO_i$ $\int_{A_i} \frac{E(x,y)x^2\, dA_i}{E_1}$ measured from the leading edge

$IXYO_i$ $\int_{A_i} \frac{E(x,y)xy\, dA_i}{E_1}$

$AREA_i$ $\int_{A_i} \frac{E(x,y)\, dA_i}{E_1}$

$YBAR_i$ $\int_{A_i} \frac{E(x,y)x\, dA_i}{E_1}$

$MASS_i$ $\int_{A_i} \rho(x,y)\, dA_i$

$MASSX_i$ $\int_{A_i} x\rho(x,y)\, dA_i$

$MASSY_i$ $\int_{A_i} y\rho(x,y)\, dA_i$

$GEOAREA_i$ $\int_{A_i} dA_i$

PROGRAM LISTING

```
      ∇INDEX[□]∇
      ∇MM INDEX MM1;EREF;J;K;M;N;X;Y;F;I1;I2;I3;BASE1;MODWTX
[1]    EREF←10000000          ;MODWTY;MAS;RHOWTX;RHOWTY;AREA1
[2]    J←0
[3]    K←0
[4]    RESET
[5]    M←1↑⍴MM
[6]    N←¯1↑⍴MM
[7]   FIRST:X←MM[J;K-1],MM[J;K],MM[J;K+1],MM1[1;1],MM1[1;2]
[8]    F←J+1
[9]    Y←MM1[F;K],MM1[F;K+1],MM1[F;K+2],MM1[F;1]
[10]   X INTEG Y
[11]   →(K=N-1)/SECOND
[12]   K←K+2
[13]   →FIRST
[14]  SECOND:→(JJ≠0)/THIRD
[15]   IXXO←IXXO,I3
[16]   IXYO←IXYO,I2
[17]   IYYO←IYYO,I1
[18]   AREA←AREA,BASE1
[19]   YBAR←YBAR,MODWTY
[20]   XBAR←XBAR,MODWTX
[21]   MASS←MASS,MAS
[22]   MASSX←MASSX,RHOWTX
[23]   MASSY←MASSY,RHOWTY
[24]   GEOAREA←GEOAREA,AREA1
[25]   →(J=M)/ASWAN
[26]   RESET
[27]   →FIRST
[28]  THIRD:IXXO[J]←IXXO[J]+I3
[29]   IXYO[J]←IXYO[J]+I2
[30]   IYYO[J]←IYYO[J]+I1
[31]   AREA[J]←AREA[J]+BASE1
[32]   YBAR[J]←YBAR[J]+MODWTY
[33]   XBAR[J]←XBAR[J]+MODWTX
[34]   MASS[J]←MASS[J]+MAS
[35]   MASSX[J]←MASSX[J]+RHOWTX
[36]   MASSY[J]←MASSY[J]+RHOWTY
[37]   GEOAREA[J]←GEOAREA[J]+AREA1
[38]   →(J=M)/ASWAN
[39]   RESET
[40]   →FIRST
[41]  ASWAN:⍬
      ∇
```

FUNCTION INDEX

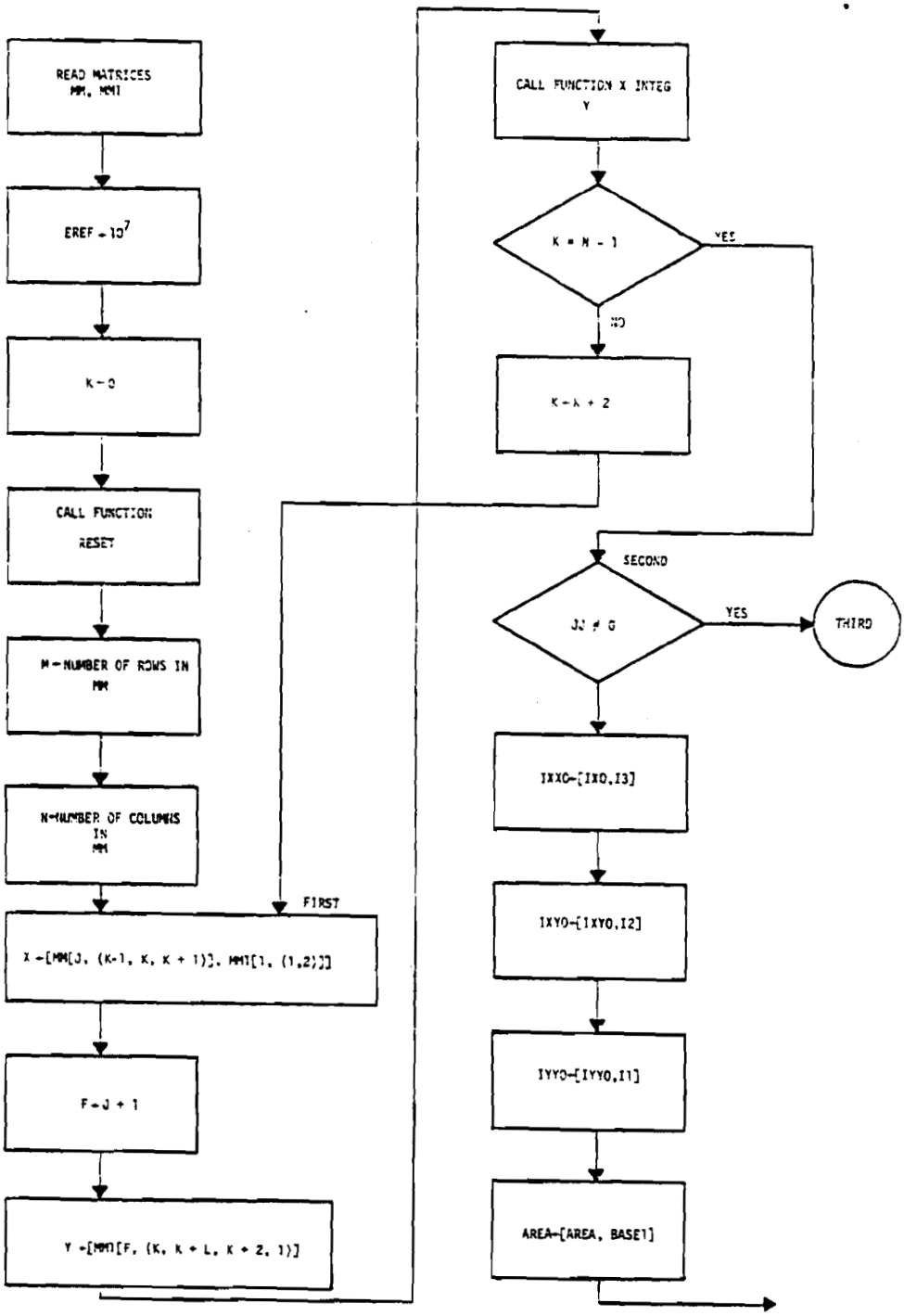

INDEX (Continued)

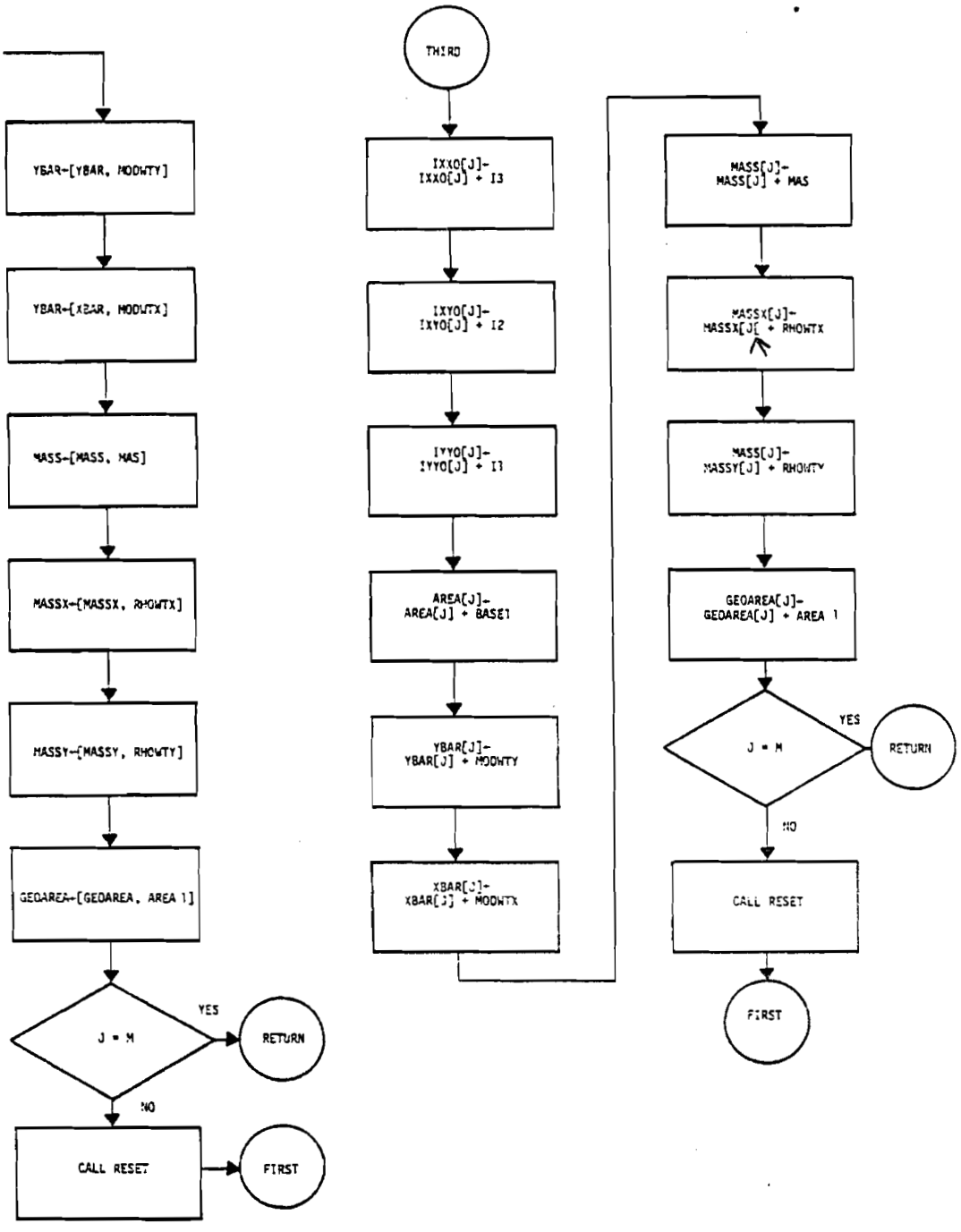

A P P E N D I X F

FUNCTION INTEG

Function INTEG performs summations of the section properties to approximate the integrals detailed in Appendix E.

If the specified thickness for the summation is zero, the logic assumes that the specified section is solid. In this case, most of the integrable section characteristics are computed directly (lines 17 through 29). Otherwise, the section is broken up into many rectangles and the centroid coordinates of these rectangles used.

The input requires the specification of three points on the surface. A parabola is fit through these points, and evenly spaced intervals are proscribed onto that curve. Thus, we get ten intervals evenly spaced between the largest and smallest value of x. The centroidal x coordinates are then determined for each of the intervals. The values of y associated with these x values are then determined.

If the section is solid, the included section properties are then determined. If the section is not solid, then the projected thickness is subtracted from the previous value of y and the intermediates between these values of y are found. This establishes the coordinates of the centroid of the section considered. This information is then operated on in lines 41 through 53 to establish the summation of interest.

PRINCIPAL VARIABLES

RHO	density
E	local bending modulus
x	x components of selected points
y	y components of selected points
co	coefficients of the best fit parabola $co_0 + co_1 x + co_2 x^2 = y$
I1	$\sum_i \frac{E_i}{E_1} x_i^2 \Delta A_i$
I2	$\sum_i \frac{E_i}{E_1} x_i y_i \Delta A_i$
I3	$\sum_i \frac{E_i}{E_1} y_i^2 \Delta A_i$
MODWTY	$\sum_i \frac{E_i}{E_1} y_i \Delta A_i$
MODWTX	$\sum_i \frac{E_i}{E_1} x_i \Delta A_i$
MAS	$\sum_i \rho_i \Delta A_i$
RHOWTX	$\sum_i \rho_i x_i \Delta A_i$
RHOWTY	$\sum_i \rho_i y_i \Delta A_i$
AREA1	$\sum_i \Delta A_i$

where

ρ = density

E = local bending modulus

ΔA = small section of area

E_1 = 10^7

PROGRAM LISTING

```
      ∇INTEG[□]∇
      ∇X INTEG Y;RHO;E;T;CO;THET;A;Y1;AA;DX;DY;XB;YB;NEW
[1]    ⍝ THIS ROUTINE DOES THE PIECEWISE SUMMATION OF THE
[2]    ⍝VARIOUS PROPERTIES OF THE CROSS SECTIONS. MOST OF THE
[3]    ⍝QUANTITIES SHOULD BE READILY IDENTIFIABLE.
[4]    ⍝I1, I2, I3 HAVE TO DO WITH THE SECTION'S IYY, IXY, AND
[5]    ⍝IXX RESPECTIVELY.
[6]    RHO←X[5]
[7]    E←X[4]
[8]    T←Y[4]
[9]    E←E÷EREF
[10]   X←X[⍳3]
[11]   Y←Y[⍳3]
[12]   CO←,X ⌹ Y
[13]   X←X[1]+(DX←2)+(((⍳10)-1)×DX←0.1×X[3]-X[1]
[14]   Y←CO[1]+(CO[2]×X)+CO[3]×X*2
[15]   →(T≠0)/HECK
[16]   I1←I1++/E×Y×DX×0.25×X*2
[17]   I2←I2++/E×0.5×DX×X×Y*2
[18]   I3←I3++/E×(DX÷3)×Y*3
[19]   BASE1←BASE1++/E×DX×Y
[20]   MODWTY←MODWTY++/E×DX×0.5×Y*2
[21]   MODWTX←MODWTX++/E×DX×Y×X
[22]   MAS←MAS++/DX×Y×RHO
[23]   RHOWTX←RHOWTX++/RHO×X×DX×Y
[24]   RHOWTY←RHOWTY++/RHO×DX×0.5×Y*2
[25]   AREA1←AREA1++/DX×Y
[26]   →1000
[27]  HECK:THET←¯3○CO[2]+2×CO[3]×X
[28]   Y1←Y-0.5×(×Y[2])×T÷2○THET
[29]   AA←(×Y1)=×Y[2]
[30]   YB←(AA×Y1)+0.5×Y×~AA
[31]   DY←((CO[2]×X-DX÷2)+CO[3]×(X-DX÷2)*2)-(CO[2]×X+DX÷2)+CO[3]
[32]   A←Y×((DX*2)+DY*2)*0.5                    ×(X+DX÷2)*2
[33]   →(10=|+/AA)/WORK
[34]   A←(AA×A)+(~AA)×|DX×Y
[35]  WORK:⍝ THE BUTTER
[36]   XB←X
[37]   I1←I1++/E×A×XB*2
[38]   I2←I2++/E×A×XB×YB
[39]   I3←I3++/E×A×YB*2
[40]   BASE1←BASE1++/E×A
[41]   MODWTY←MODWTY++/E×YB×A
[42]   MODWTX←MODWTX++/E×XB×A
[43]   MAS←MAS+RHO×+/A
[44]   RHOWTX←RHOWTX++/RHO×XB×A
[45]   RHOWTY←RHOWTY++/RHO×YB×A
[46]   AREA1←AREA1++/A
       ∇
```

FUNCTION INTEG

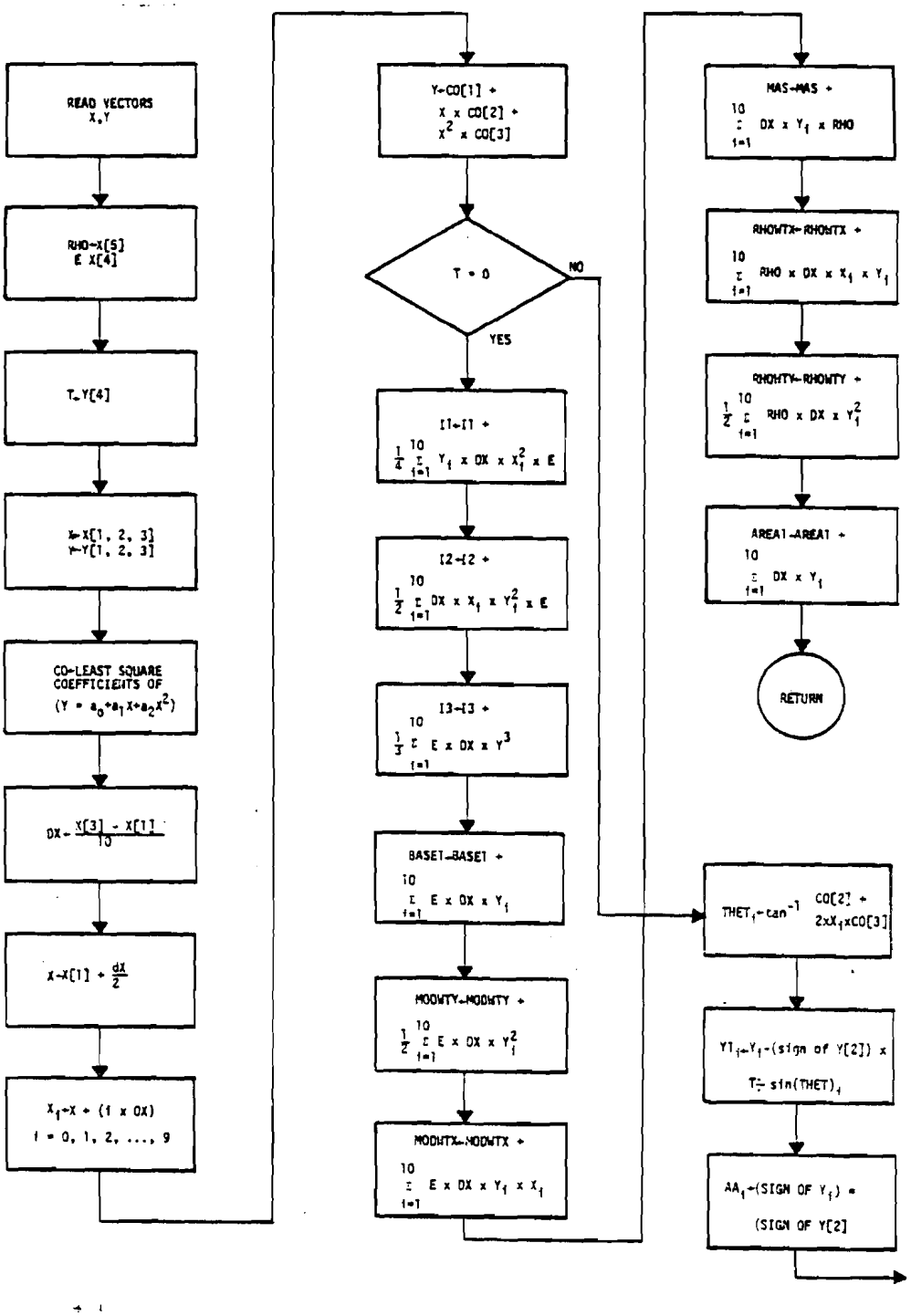

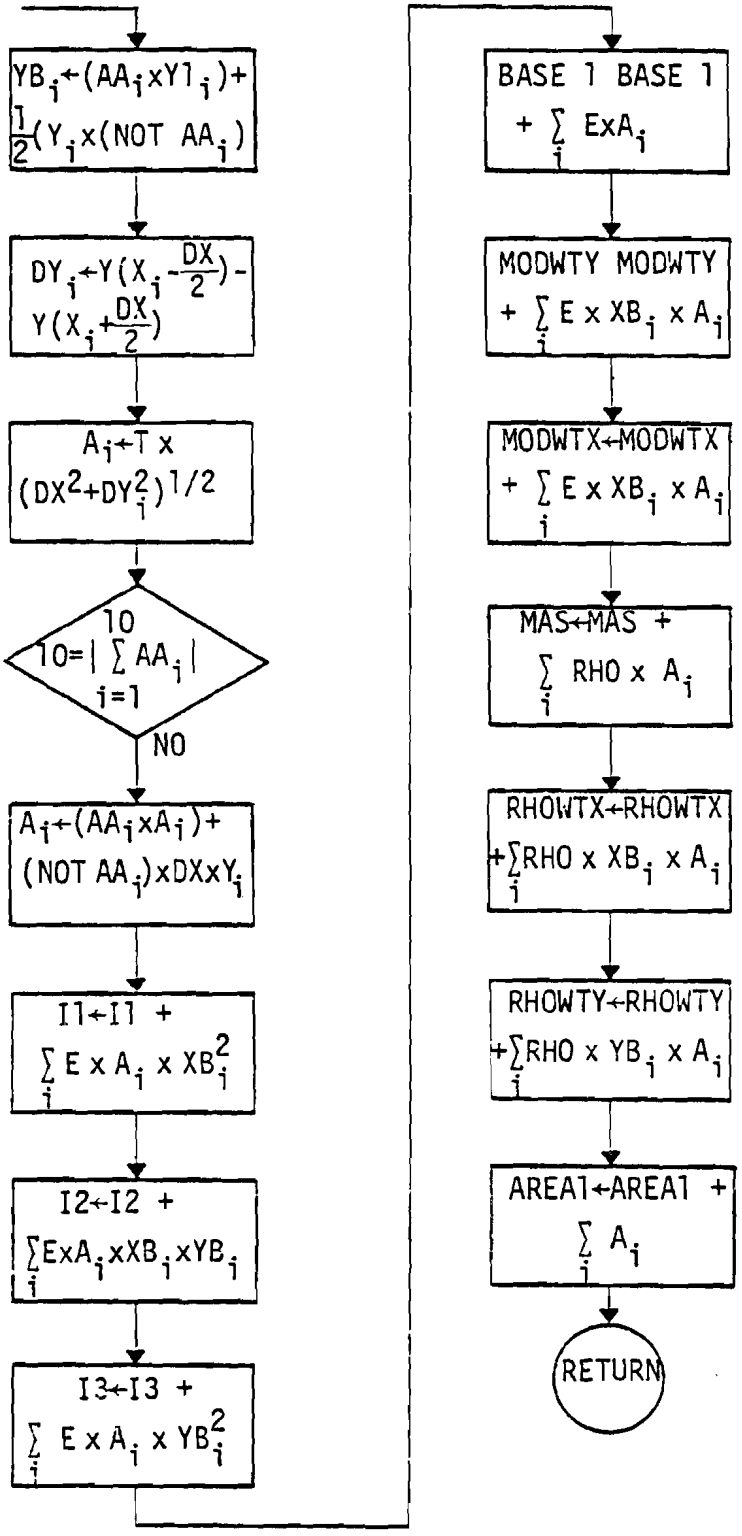
$YB_i \leftarrow (AA_i \times Y1_i) + \frac{1}{2}(Y_i \times (NOT\ AA_i))$
$DY_i \leftarrow Y(X_i - \frac{DX}{2}) - Y(X_i + \frac{DX}{2})$
$A_i \leftarrow T \times (DX^2 + DY_i^2)^{1/2}$
$IO = |\sum_{i=1}^{IO} AA_i|$
NO
$A_i \leftarrow (AA_i \times A_i) + (NOT\ AA_i) \times DX \times Y_i$
$I1 \leftarrow I1 + \sum_i E \times A_i \times XB_i^2$
$I2 \leftarrow I2 + \sum_i ExA_i \times XB_i \times YB_i$
$I3 \leftarrow I3 + \sum_i E \times A_i \times YB_i^2$
BASE 1 BASE 1 + $\sum_i ExA_i$
MODWTY MODWTY + $\sum_i E \times XB_i \times A_i$
MODWTX←MODWTX + $\sum_i E \times XB_i \times A_i$
MAS←MAS + $\sum_i RHO \times A_i$
RHOWTX←RHOWTX + $\sum_i RHO \times XB_i \times A_i$
RHOWTY←RHOWTY + $\sum_i RHO \times YB_i \times A_i$
AREA1←AREA1 + $\sum_i A_i$
RETURN

APPENDIX G

FUNCTION DEF

Function DEF solves the Equation of bending given in Chapter 3. It utilizes a fourth order Runge-Kutta method for the solution (Chapter 4). Its operation is straightforward. Integration begins at the most inboard station and proceeds toward the tip. The deflection of the most inboard station is assumed to be zero in both directions.

The initial slope is assigned the value zero. This must be changed to some other value if some rotor support other than a cantilever is to be considered.

PRINCIPAL VARIABLES

H station spacing

N number of stations

F slope

FF a record of slope as a function of radius

RET deflection

C the quantity being integrated, for example

$$\frac{-1}{E_1}\left(\frac{M_x I_{yy} + M_y I_{xy}}{I_{xx} I_{yy} - I_{xy}^2}\right)$$

PROGRAM LISTING

```
      ∇DEF[□]∇
      ∇IN DEF C;H;N;F;FF;RET;IT;K;K2;K3;K4;L1;L2;L3;L4
[1]    H←IN[1]
[2]    N←IN[2]
[3]    F←FF←0
[4]    RET←0
[5]    IT←1
[6]   L0:K←0.5×C[IT]+C[IT+1]
[7]    K1←H×K×(1+F*2)*1.5
[8]    L1←H×F
[9]    L2←H×BB←F+K1÷2
[10]   K2←H×K×(1+BB*2)*1.5
[11]   L3←H×BB←F+K2÷2
[12]   K3←H×K×(1+BB*2)*1.5
[13]   L4←H×BB←F+K3
[14]   K4←H×K×(1+BB*2)*1.5
[15]   FF←FF,F+(÷6)×K1+K4+2×K2+K3
[16]   RET←RET,(¯1↑RET)+(÷6)×L1+L4+2×L2+L3
[17]   →(IT=N-1)/L11
[18]   IT←IT+1
[19]   F←¯1↑FF
[20]   →L0
[21]  L11:'DEFLECTION'
[22]   8 3↑RET
[23]   ''
      ∇
```

FUNCTION DEF

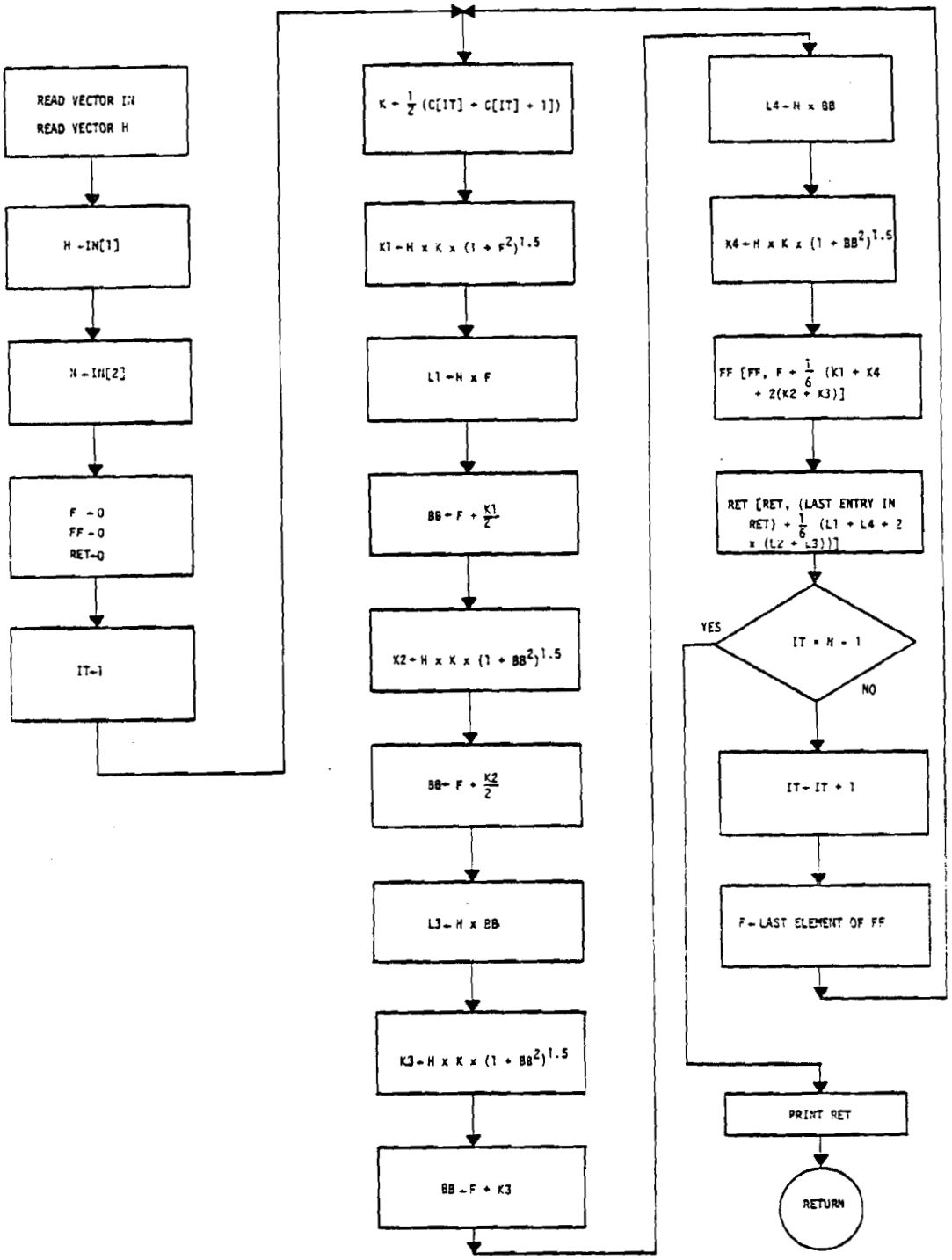

APPENDIX H

MINOR ROUTINES

Function Bend

Function Bend computes bending moments due to the loads F according to the spacing defined by H. For positive H and positive F the computer bending moments will all be positive. Care must therefore be taken that the sign of the bending moments thus calculated are adjusted correctly in the calling program.

Function RESET

RESET assigns variable type (empty vector) to the listed vectors. It also assigns initial values to the listed scalars.

Function FOOL 1

FOOL 1 assigns variable type to the listed vectors and initial values to the listed scalars.

PROGRAM LISTING

```
      ∇BEND[□]∇
      ∇M←H BEND F;I;K
[1]    M←F
[2]    I←1
[3]   NEW:K←I+(⌊1+(⍴F)-I)-1
[4]    M[I]←Hx+/(0.5+K-I)xF[K]
[5]    →(I=⍴F)/L
[6]    I←I+1
[7]    →NEW
[8]   L:M←M,0
      ∇
```

```
   ∇RESET[□]∇
      ∇RESET
[1]    MODWTX←MODWTY←I1←I2←I3←BASE1←AREA1←0
[2]    RHOWTX←RHOWTY←MAS←0
[3]    K←2
[4]    J←J+1
[5]    I11←I22←I33←0
      ∇
```

```
      ∇FOOL1[□]∇
      ∇FOOL1
[1]    IXXO←IXYO←IYYO←AREA←YBAR←XBAR←MASS←MASSX
[2]    I11←I22←I33←⌊0                ←MASSY←GEOAREA←⌊0
[3]    IXM←IXYM←IYM←⌊0
[4]    ITIND←0
      ∇
```

FUNCTION BEND

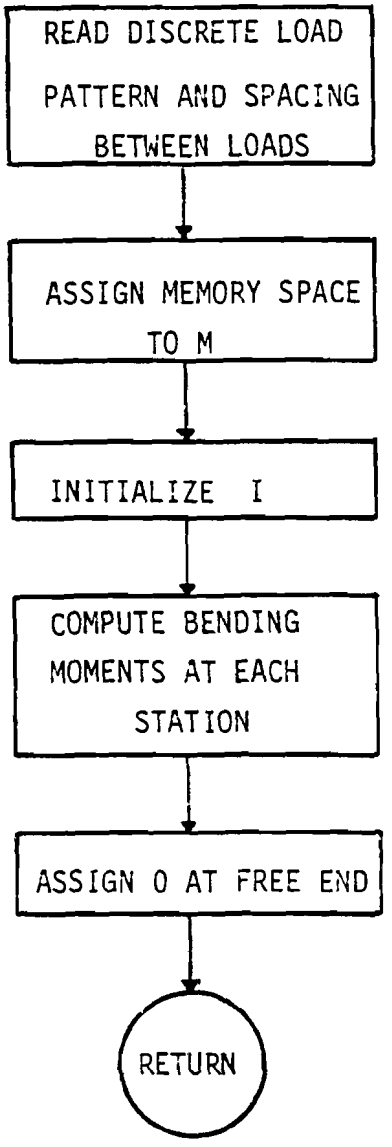

FUNCTION
FOOL I

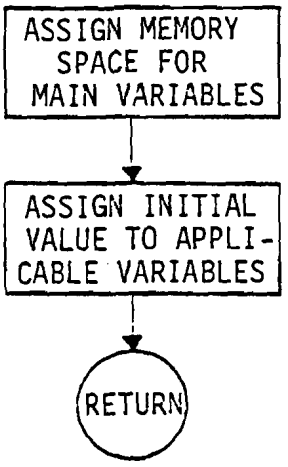

FUNCTION
RESET

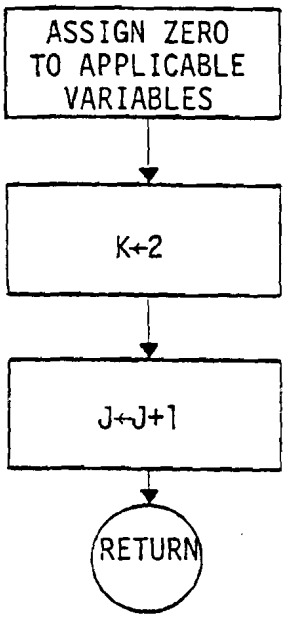

APPENDIX I

PROGRAM FREQ

FREQ calculates the natural frequencies and mode shapes of a freely vibrating beam. The beam considered may be of completely arbitrary construction, material distribution, twist and taper so long as coupling between flexural and any other non-flexural vibratory modes may be neglected.

FREQ is written such that the required input to the program is supplied during the normal execution of the program MOMENTS. The pertinent constants are calculated by MOMENTS and stored in global memory. To execute FREQ you need only type the name.

FREQ uses the Rayleigh Ritz method of assumed solution to find the frequencies and mode shapes. The beam is first allowed deflections with no constraints. The method converges to the fundamental.

The next operation is to assume a mode shape which is the negative transpose of the fundamental mode shape. This assumed mode shape is 90° out of phase with the fundamental mode shape at each radial station. The inertial load due to this assumed mode shape is determined. The deflections, mode shape, and frequency due to this inertial load are computed and reported.

(The function DOG is used to compute the deflections.)

Higher modes are now sought. The function ORTHOG is used to subtract the influence of lower modes on the assumed solution by Schmitt Orthogonalization. When applied iteratively, the assumed solution converges on the next higher mode shape. Once convergence has been noted,

the frequency is computed, and the frequency and mode shape are printed.

Once again the negative transpose of the mode shape is used to compute a yet higher mode. The process is the same as described above.

The program as presently written now stops. The program will find arbritrarily higher modes (up to the limit imposed by the size of the data entered) if the 2 in line 77 is changed to some arbitrary larger integer. (In a test, a uniform beam defined by 11 stations was entered. The modes predicted agreed with the exact result up to the third mode. Above that agreement was progressively worse.)

If the operations on the lower modes by ORTHOG do not converge to a single assumed mode after 10 iterations, a different scheme is used. First, a node is assumed at the sixth station. (The support is defined to be station 1.) A sine function having a node at the support and at the assumed mode is established. The fundamental mode shape is multiplied by the imposed sine. This becomes the assumed solution. The frequency is computed on this basis. Next, a node is assumed at the free end and the same operations are carried out. Next, a node is assumed halfway between station six and the free end. The same operations are carried out again.

These three steps are the first in a bisection search routine. The search seeks the node position and frequency corresponding to a frequency maximum. (This is the same in intent as the Schmitt Orthogonalization of an assumed solution with just the fundamental.) This frequency maximum corresponds to a well defined spanwise node. The frequency and mode shape so determined are reported and the program stops.

This program can be used for any boundary conditions once suitable modifications have been made to functions BEND and DEF1 (DEF1 is logically identical to DEF, Appendix G), such that they reflect the bending moments and initial slope due to the changed boundary conditions.

The deflected mode shapes and moments of inertia are all referred to the most recent pitch setting in MOMENTS.

PRINCIPAL VARIABLES

$MASS_i$	Lineal weight density, lbs/in.
IXX_i	Modulus weighted moment of inertia
IYY_i	Modulus weighted moment of inertia
IXY_i	Modulus weighted moment of inertia
$ACCX_{i,j}$	X components of lower mode shapes
$ACCY_{i,j}$	Y components of lower mode shapes
MAS_i	MASS of radial segments
$PHIX_i$	X component of assumed mode shape
$PHIY_i$	Y component of assumed mode shape
PX_i	X component of inertial load
PY_i	Y component of inertial load
A	Amplitude (lines 25-80)
A	Node position (lines 81 on)
AAAA	Amplitude (lines 81 on)
$PHIXA_i$	Calculated mode shape, x
$PHIX1_i$	Calculated mode shape, x
$PHIYA_i$	calculated mode shape, y
$PHIY1_i$	Calculated mode shape, y
$PHIXB_i$	Calculated mode shape, x
$PHIYB_i$	Calculated mode shape, y
B	Circular frequency

A1	Previous node position
A2	Previous node position
B1	Previous circular frequency
B2	Previous circular frequency
u	Deflection in the +x direction
v	Deflection in the +y direction

PROGRAM LISTING

```
      ∇FREQ[□]∇
      ∇FREQ;ACCX;ACCY;PX;PY;PHIX;PHIY;PHIX1;PHIY1;A1;RMS;IN;PSI;I;PHIXA;PHIYA;MAS;D
[1]    'INPUT RECORD'
[2]    'MASS  ';6 3⍕MASS
[3]    'IXX   ';6 2⍕IXX
[4]    'IYY   ';6 2⍕IYY
[5]    'IXY   ';6 2⍕IXY
[6]    'M     ';6 3⍕M
[7]    ''
[8]    ''
[9]    COUNT←0
[10]   ACCX←ACCY←(0,⍴IXX)⍴''
[11]   IN←0
[12]   PX←PY←((⍴IXX)-1)⍴1
[13]   M1←M,⍴IXX
[14]   I←⍳¯1+⍴MASS
[15]   MAS←(MASS[I]+MASS[I+1])÷2
[16]   MAS←M×MAS÷386.4
[17]   DOG
[18]   PHIX←(⍴U)⍴1
[19]   PHIY←PHIX
[20]  AA:→(IN=0)/AAA
[21]   ORTHOG
[22]   PX←MAS×(PHIX[I]+PHIX[I+1])÷2
[23]   PY←MAS×(PHIY[I]+PHIY[I+1])÷2
[24]   DOG
[25]   A←⌈/((U*2)+V*2)*0.5
[26]   PHIX←U÷A
[27]   PHIY←V÷A
[28]   ORTHOG
[29]   COUNT←COUNT+1
[30]   →(COUNT=10)/AC
[31]  AAA:PX←MAS×(PHIX[I]+PHIX[I+1])÷2
[32]   PY←MAS×(PHIY[I]+PHIY[I+1])÷2
[33]   DOG
[34]   A1←⌈/((U*2)+V*2)*0.5
[35]   PHIX1←U÷A1
[36]   PHIY1←V÷A1
[37]   RMS←(+/(PHIX-PHIX1)*2)*0.5
[38]   RMS←RMS+(+/(PHIY-PHIY1)*2)*0.5
[39]   →(RMS<0.001)/AB
[40]   PHIX←PHIX1
[41]   PHIY←PHIY1
[42]   →AA
[43]  AB:ACCX←ACCX,PHIX1
[44]   ACCY←ACCY,PHIY1
[45]   'OMEGA'
[46]   PHIXA←(PHIX[I]+PHIX[I+1])÷2
[47]   PHIX1←(PHIX1[I]+PHIX1[I+1])÷2
[48]   PHIYA←(PHIY[I]+PHIY[I+1])÷2
[49]   PHIY1←(PHIY1[I]+PHIY1[I+1])÷2
[50]   6 2⍕B←((+/MAS×(PHIXA×PHIX1)+(PHIYA×PHIY1))÷A1×+/MAS×(PHIY1*2)+PHIX1*2)*0.5
[51]   'FREQENCY, HERTZ ';6 2⍕B÷6.2
[52]   'MODE SHAPE'
[53]   'U ';6 2⍕PHIX
[54]   'V ';6 2⍕PHIY
[55]   ''
[56]   ''
[57]   ''
[58]   PHIXA←PHIY1
[59]   PHIYA←¯1×PHIX1
[60]   PX←MAS×PHIXA
[61]   PY←MAS×PHIYA
[62]   DOG
```

```
[63]    A←⌈/(⌈/|U),⌈/|V
[64]    PHIXB←U÷A
[65]    PHIYB←V÷A
[66]    PHIX1←(PHIXB[I]+PHIXB[I+1])÷2
[67]    PHIY1←(PHIYB[I]+PHIYB[I+1])÷2
[68]    'OMEGA ';6 2▼B←((+/MASx(PHIX1xPHIXA)+(PHIY1xPHIYA))÷Ax+/MASx(PHIX1*2)+PHIY1*2)*0.5
[69]    'FREQENCY, HERTZ ';6 2▼B÷@2
[70]    'MODE SHAPE '
[71]    'U ';6 2▼PHIXB
[72]    'V ';6 2▼PHIYB
[73]    ''
[74]    ''
[75]    ''
[76]    IN←IN+1
[77]    →(IN=2)/1000
[78]    PHIX←xPHIY←(⍴U)⍴1
[79]    →AA
[80]   AC:'NO CONVERGENCE OF ORTHOGONAL VECTORS'
[81]    A←6
[82]    IN←1
[83]   ABA:⍝ SEARCH FOR FREQUENCY
[84]    PHIX←ACCX[1;]x1@@(⌽H1[2])÷A
[85]    PHIY←ACCY[1;]x1@@(⌽H1[2])÷A
[86]    AAAA←⌈/((PHIX*2)+PHIY*2)*0.5
[87]    PHIX←PHIX÷AAAA
[88]    PHIY←PHIY÷AAAA
[89]    PX←MASx(PHIX[I]+PHIX[I+1])÷2
[90]    PY←(PHIY[I]+PHIY[I+1])xMAS÷2
[91]    DOG
[92]    AAAA←⌈/((U*2)+V*2)*0.5
[93]    PHIX1←U÷AAAA
[94]    PHIY1←V÷AAAA
[95]    PHIX1←(PHIX1[I]+PHIX1[I+1])÷2
[96]    PHIX←(PHIX[I]+PHIX[I+1])÷2
[97]    PHIY1←(PHIY1[I]+PHIY1[I+1])÷2
[98]    PHIY←(PHIY[I]+PHIY[I+1])÷2
[99]    B←((+/MASx(PHIX1xPHIX)+PHIYxPHIY1)÷AAAAx+/MASx(PHIX1*2)+PHIY1*2)*0.5
[100]   IN←IN+1
[101]   →(IN)2)/ABB
[102]   A1←A
[103]   A←⍎IXX
[104]   B1←B
[105]   →ABA
[106]  ABB:→(IN)3)/ABC
[107]   A2←A
[108]   B2←B
[109]   A←0.5xA1+A
[110]   →ABA
[111]  ABC:→((1⌶B-B1)^0.12⌶A-A1)/ABD
[112]   →((BxB2)(BxB1)/ABE
[113]   B1←B
[114]   A1←A
[115]   A←0.5xA2+A
[116]   →ABA
[117]  ABE:B2←B
[118]   A2←A
[119]   A←0.5xA1+A
[120]   →ABA
[121]  ABD:'OMEGA ';B
[122]   'HERTZ ';B÷@2
[123]   'U ';6 2▼PHIX
[124]   'V ';6 2▼PHIY
        ▽
```

PROGRAM FREQ

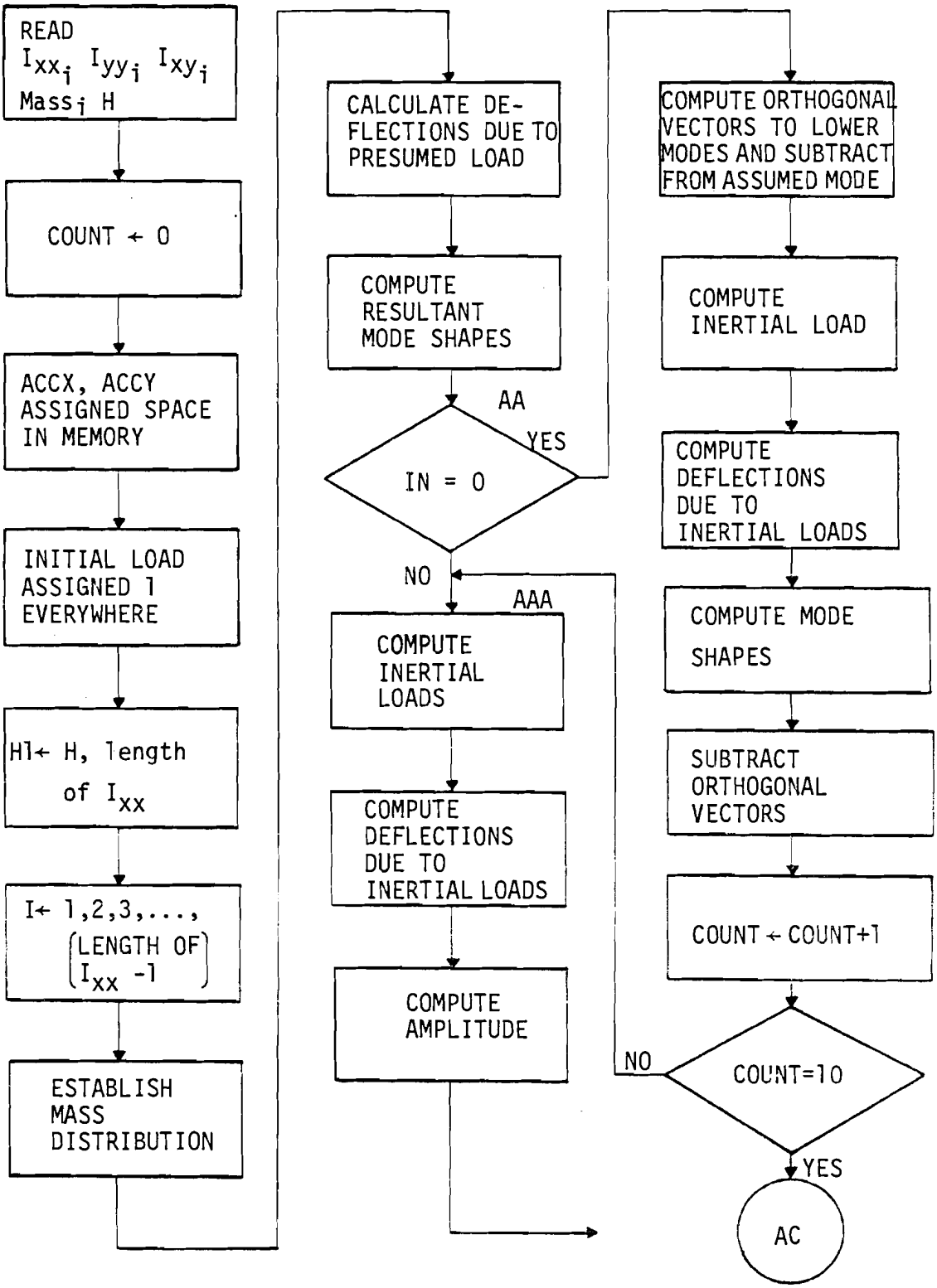

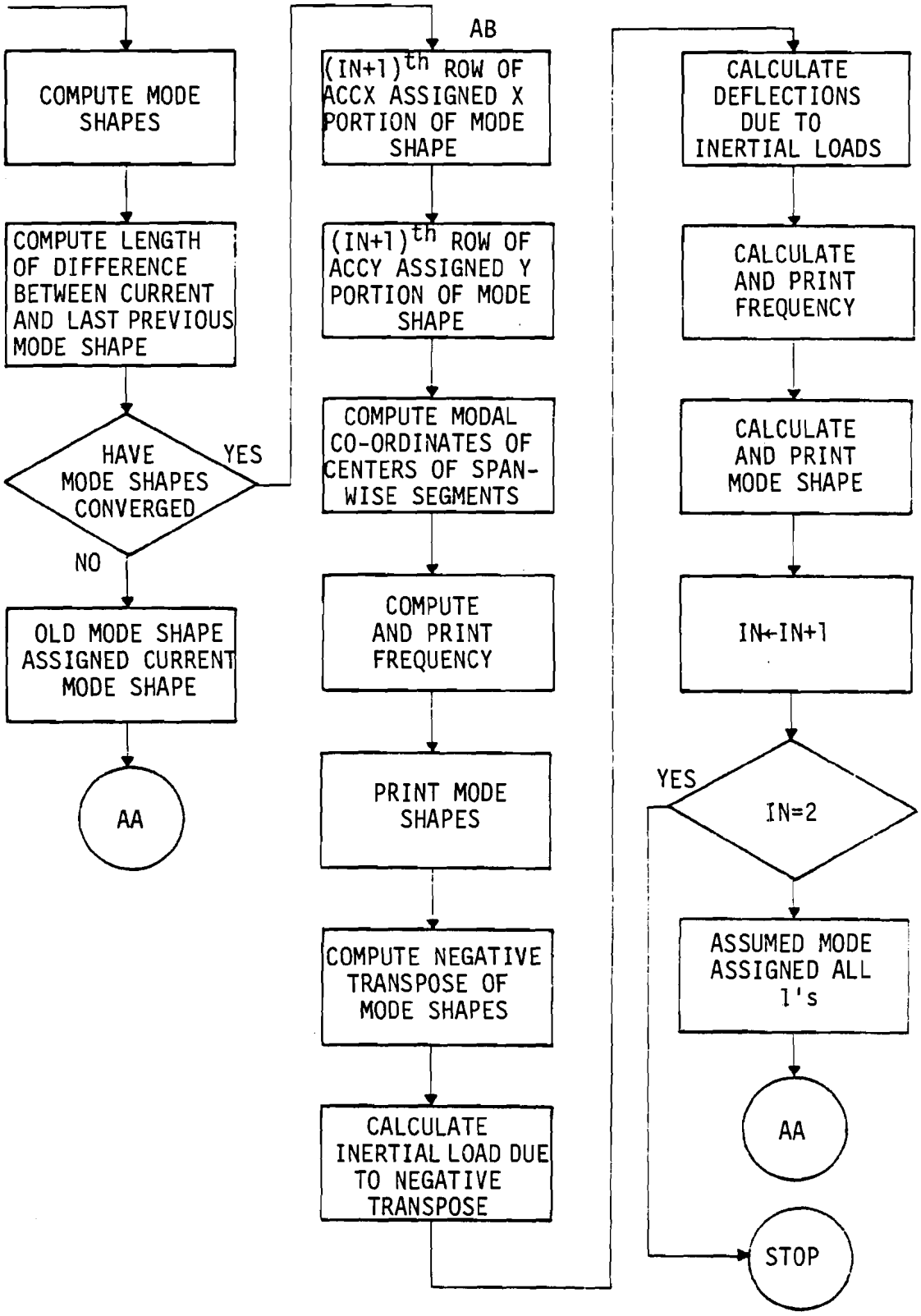
COMPUTE MODE SHAPES
COMPUTE LENGTH OF DIFFERENCE BETWEEN CURRENT AND LAST PREVIOUS MODE SHAPE
HAVE MODE SHAPES CONVERGED
YES
NO
OLD MODE SHAPE ASSIGNED CURRENT MODE SHAPE
AA
AB
(IN+1)th ROW OF ACCX ASSIGNED X PORTION OF MODE SHAPE
(IN+1)th ROW OF ACCY ASSIGNED Y PORTION OF MODE SHAPE
COMPUTE MODAL CO-ORDINATES OF CENTERS OF SPAN-WISE SEGMENTS
COMPUTE AND PRINT FREQUENCY
PRINT MODE SHAPES
COMPUTE NEGATIVE TRANSPOSE OF MODE SHAPES
CALCULATE INERTIAL LOAD DUE TO NEGATIVE TRANSPOSE
CALCULATE DEFLECTIONS DUE TO INERTIAL LOADS
CALCULATE AND PRINT FREQUENCY
CALCULATE AND PRINT MODE SHAPE
IN←IN+1
YES
IN=2
ASSUMED MODE ASSIGNED ALL 1's
AA
STOP

PROGRAM FREQ
Page 3

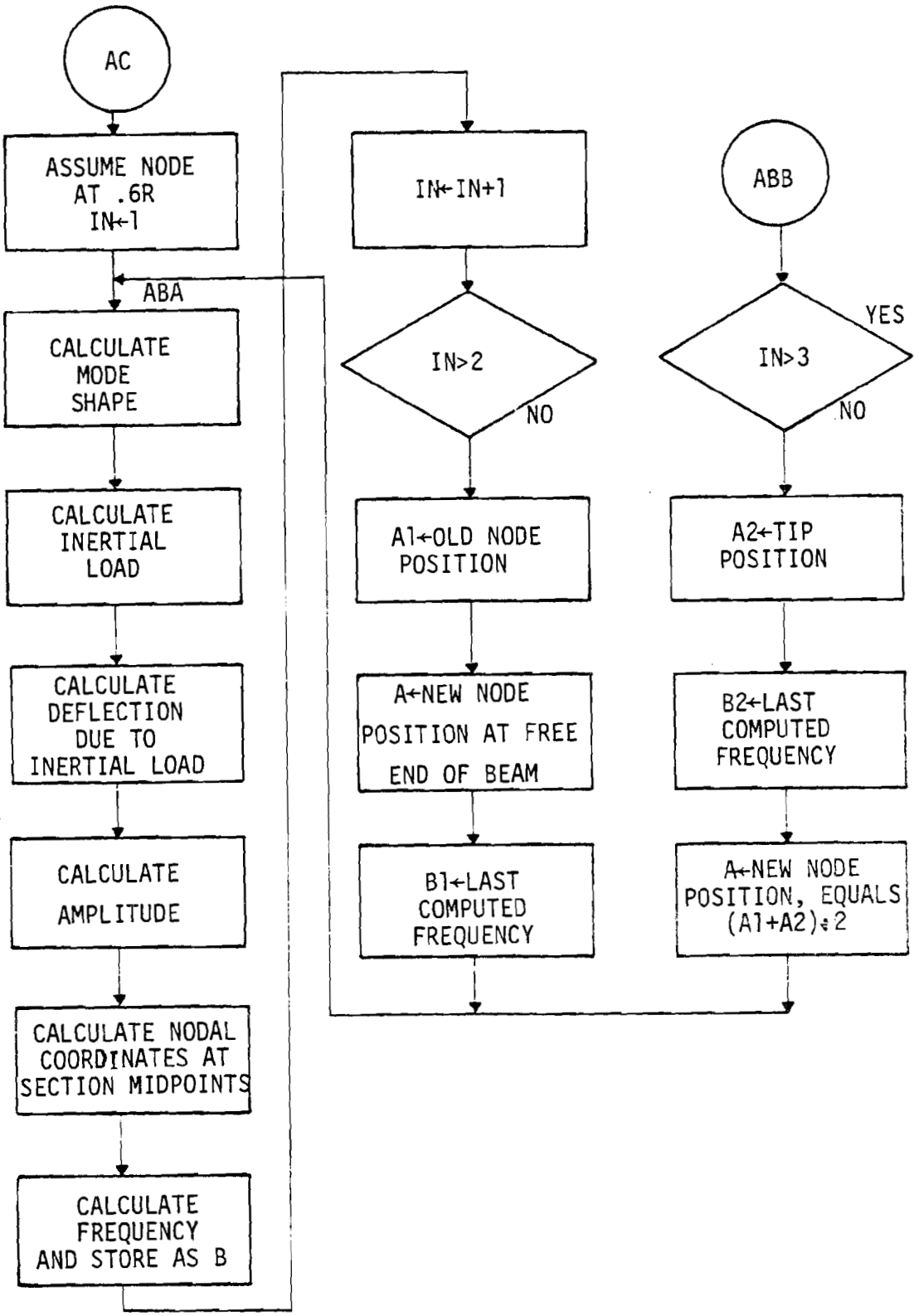

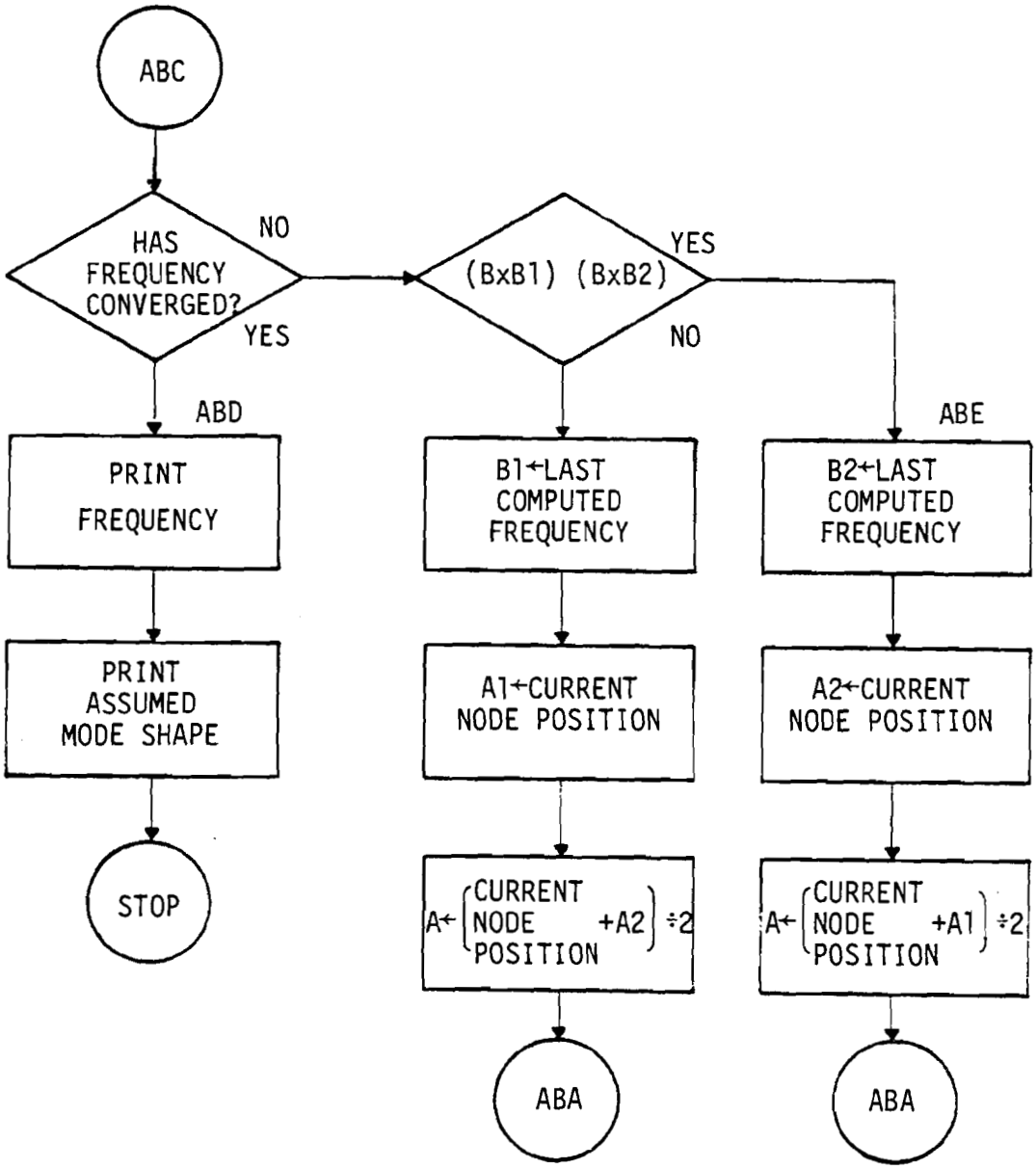
ABC
HAS FREQUENCY CONVERGED?
NO
YES
(BxB1) (BxB2)
YES
NO
ABD
PRINT FREQUENCY
PRINT ASSUMED MODE SHAPE
STOP
B1←LAST COMPUTED FREQUENCY
A1←CURRENT NODE POSITION
A←(CURRENT NODE POSITION +A2)÷2
ABA
ABE
B2←LAST COMPUTED FREQUENCY
A2←CURRENT NODE POSITION
A←(CURRENT NODE POSITION +A1)÷2
ABA

TERMINAL SESSION

```
      FREQ
INPUT RECORD
MASS  0.563 0.343 0.267 0.225 0.194 0.151 0.130 0.082 0.057 0.030
IXX    6.55  4.98  2.23  1.14  0.70  0.39  0.19  0.13  0.06  0.01
IYY   11.42 13.12  9.67  5.37  3.13  1.51  0.88  0.44  0.27  0.15
IXY    4.76 -5.73 -3.27 -1.38 -0.63 -0.25 -0.28 -0.07 -0.05 -0.02
H     19.500


OMEGA
 26.80
FREGENCY, HERTZ   4.26
MODE SHAPE
U   0.00  0.00 -0.01 -0.02 -0.05 -0.08 -0.12 -0.17 -0.23 -0.30
V   0.00  0.01  0.03  0.07  0.15  0.25  0.38  0.55  0.75  0.96


OMEGA  63.07
FREGENCY, HERTZ  10.04
MODE SHAPE
U   0.00  0.01  0.05  0.11  0.19  0.30  0.43  0.60  0.79  1.00
V   0.00  0.01  0.02  0.03  0.05  0.08  0.13  0.19  0.26  0.34



NO CONVERGENCE OF ORTHOGONAL VECTORS
OMEGA 89.76
HERTZ 14.29
U   0.00 -0.01 -0.02 -0.05 -0.08 -0.09 -0.05  0.05  0.20
V   0.00  0.02  0.08  0.17  0.25  0.27  0.16 -0.15 -0.66
```

APPENDIX J

FUNCTION DOG

DOG reads the radial spacing of stations, the loads in two planes and the section properties to compute the deflections in two planes. The values of deflection are returned to the calling program.

The program uses the function DEF1. This function is logically identical to DEF (Appendix G).

PRINCIPAL VARIABLES

MX_i	Bending moment about x axis
MY_i	Bending moment about y axis
$C1_i$, $C2_i$, $C3_i$	Bending constants
u	Deflection in x direction
v	Deflection in y direction

PROGRAM LISTING

```
      ∇DOG[□]∇
      ∇DOG;MX;MY;C1;C2;C3
[1]    MX←¯1×H BEND PY
[2]    MY←H BEND PX
[3]    C1←(MY×IXX)-MX×IXY
[4]    C2←(MX×IYY)-MY×IXY
[5]    C3←(IXX×IYY)-IXY*2
[6]    U←H1 DEF1 C1÷C3×10000000
[7]    V←¯1×(H1 DEF1 C2÷C3×10000000)
      ∇
```

FUNCTION DOG

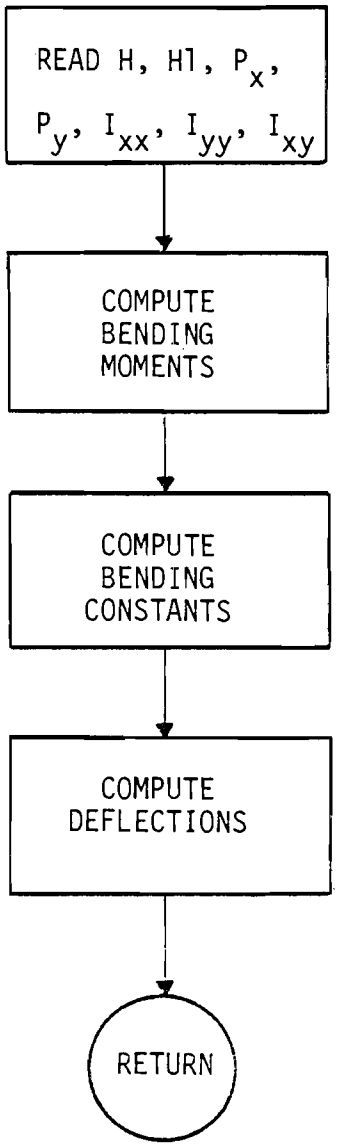

APPENDIX K

FUNCTION ORTHOG

ORTHOG accomplishes the Schmitt Orthogonalization of the current assumed mode shape with previously determined (lower) modes. The function requires only the mass distribution, assumed mode shape and past mode shapes for input. (The procedure is explained in Chapter IV.)

Each of the previously determined mode shapes is represented by one line in both ACCX and ACCY. The program first repeats the assumed mode shape row by row until there is one row of the current mode shape stored in memory for each previously determined mode. The coordinates are then compressed into the modal coordinates of the section mid-spans. The matrices are then operated on row by row to find the participation factor(s) for each mode. The participation factors are then multiplied into the respective mode shapes and the influence of each mode subtracted station by station from the assumed mode shape. The modified assumed mode shape is then returned to the calling program.

PRINCIPAL VARIABLES

$ACCX_{i,j}$	Accumulated x components of mode shapes
$ACCY_{i,j}$	Accumulated y components of mode shapes
$F1_{i,j}$	Matrix with the same shape as ACCX filled with assumed mode components (lines 5-15)
$F2_{i,j}$	As above for y components
$AC1_{i,j}$	Midspan components from ACCX
$AC2_{i,j}$	Midspan components from ACCY
$M1_{i,j}$	Mass per segment corresponding to AC1 or AC2
$PHIXX_{i,j}$	Midspan coordinates from F1
$PHIYY_{i,j}$	Midspan coordinates from F2
$PSIX_{i}$	X components' participation factor
$PSIY_{i}$	Y components' participation factor
$F1_{i,j}$	Matrix of x lower mode coordinates times their respective participation factors
$F2_{i,j}$	As above for y
$PHIX_{j}$	Assumed mode shape, x component
$PHIY_{j}$	Assumed mode shape, y component

PROGRAM LISTING

```
      ∇ORTHOG[□]∇
      ∇ORTHOG;PHIXX;PHIYY;M1;AC1;AC2;II;F1;F2;P1;PSIX;PSIY
[1]    ⍝ THIS SUBROUTINE ACCOMPLISHES SCHMITT ORTHOGONALIZATION
[2]    ⍝OF THE PRESUMED MODE SHAPE WITH ALL PAST MODE SHAPES,  SEE
[3]    ⍝BIGGS, STRUCTURAL DYNAMICS FOR AN EXPLANATION OF THE PROCE-
[4]    ⍝DURE, BYE FOR NOW.
[5]    F1←PHIXX←(⍴ACCX)⍴PHIX
[6]    F2←PHIYY←(⍴ACCX)⍴PHIY
[7]    PHIXX←(PHIXX[;I]+PHIXX[;I+1])÷2
[8]    PHIYY←(PHIYY[;I]+PHIYY[;I+1])÷2
[9]    AC1←(ACCX[;I]+ACCX[;I+1])÷2
[10]   AC2←(ACCY[;I]+ACCY[;I+1])÷2
[11]   M1←(⍴AC1)⍴MASS
[12]   PSIX←(+/M1×AC1×PHIXX)÷+/M1×AC1*2
[13]   PSIY←(+/M1×AC2×PHIYY)÷+/M1×AC2*2
[14]   F1←ACCX×⍉(⍴⍉ACCX)⍴PSIX
[15]   F2←ACCY×⍉(⍴⍉ACCY)⍴PSIY
[16]   PHIX←PHIX-+⌿F1
[17]   PHIY←PHIY-+⌿F2
      ∇
```

FUNCTION ORTHOG

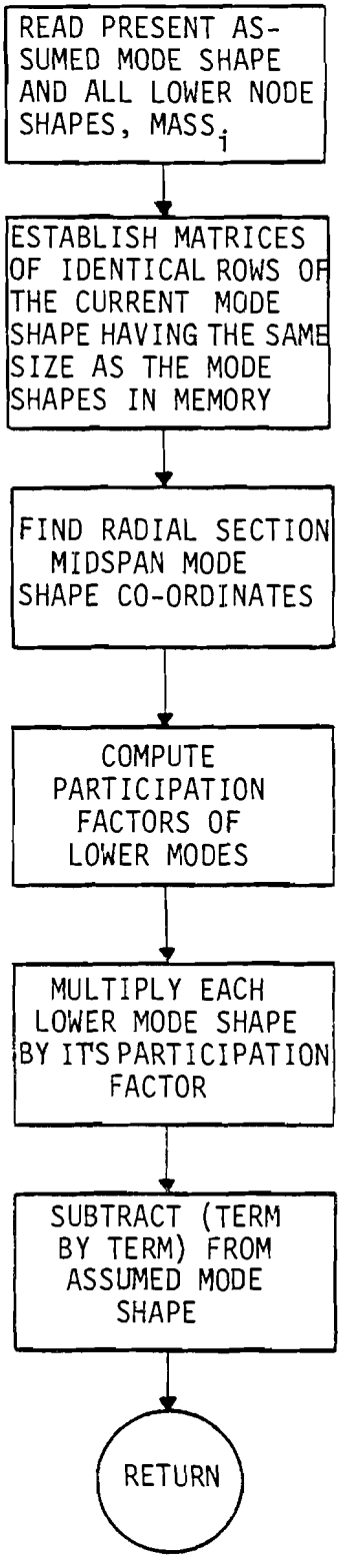

APPENDIX L

DATA FILES

The data files all have a number of well defined characteristics. The y matrices contain the following information:

1) local bending modulus (in the [1;1] position)
2) local weight density (in the [1;2] position)
3) the material thickness at each station (in the first position of each row)
4) the extreme co-ordinate relative to the chord (starting at the second column of each row from the second row down)

The x matrix contains one entry for each of the y co-ordinates in the corresponding y matrix and nothing else. The y matrix thus has one more row and one more column than the x matrix.

The thickness listed in the first column of the y matrix is the minimum distance from one side of the skin to the other. The integrating routines which operate on these data files automatically correct for the curvature of the skin relative to the section axes. If the listed thickness is zero, the integrating routines assume that the considered section is solid.

For example, consider the following files: NEWF1, NEWF12X, NEWF3, and NEWF34X. NEWF1 and NEWF3 are y matrices. NEWF12X and NEWF34X are x matrices. NEWF1 refers to the exterior skin. NEWF3 refers to the spar. They both refer to the low pressure surface of the stations. They both have an even number of columns. (The routines require an odd number of data points. Adding the thickness, in the first column, the total

number of columns becomes even.) They both have the same number of rows (one per station plus the bending and density information in the first row).

The x matrices have only one row per station. The number of columns will always be odd. The number of columns will always be one less than the number of columns in the y matrix, the same for the number of rows.

As written, NEWF1, NEWF2, and NEWF12X refer to the exterior skin. NEWF3, NEWF4, NEWF34X refer to the spar. NEWF5, NEWF6, NEWF56X refer to the spar web. NEWF7, NEWF8, NEWF78X refer to the trailing edge bond.

If any other data were entered, for example, a concentrated mass, other data files could be developed. For example, a y matrix filled with zeros would contribute nothing to the total. If any row contained non-zero elements, its properties would be integrated as a lumped parameter. (However, it would be much more conservative of computer time if such lumped parameters were introduced subsequent to integration as an addition to the appropriate element of some vector. This could be (and has been) done by interrupting function INPUT.)

NEWPHI contains the twist information of the blade design. There is one entry for each station. The reference point for β, the collective pitch setting, is arbitrary. The tip has been used here.

All of the above information is stored in global memory. This makes the information easily available. The local pitch setting could easily be typed in by the operator during the data input stage of the program.

DATA FILES

```
      NEWF1
2.200E6  0.0502 1       1       1       1       1       1       1       1       1       1
3.543E-2 0       1.916   2.616   3.421   3.755   3.755   3.514   3.104   2.546   1.442   0
3.543E-2 0       1.146   1.566   2.047   2.247   2.247   2.103   1.857   1.524   0.8628  0
3.543E-2 0       0.9893  1.351   1.767   1.939   1.939   1.815   1.603   1.315   0.7445  0
3.543E-2 0       0.8572  1.171   1.531   1.68    1.68    1.572   1.389   1.139   0.6451  0
3.543E-2 0       0.767   1.048   1.37    1.503   1.503   1.407   1.243   1.02    0.5773  0
2.756E-2 0       0.6738  0.9203  1.203   1.321   1.321   1.236   1.092   0.8956  0.5071  0
2.756E-2 0       0.5771  0.7882  1.03    1.131   1.131   1.059   0.935   0.7671  0.4343  0
1.969E-2 0       0.5265  0.7191  0.9401  1.032   1.032   0.9658  0.853   0.6998  0.3962  0
1.969E-2 0       0.4558  0.6225  0.8139  0.8933  0.8933  0.8361  0.7384  0.6058  0.343   0
1.969E-2 0       0.2484  0.3392  0.4435  0.4868  0.4868  0.4556  0.4024  0.3301  0.1869  0
```

```
      NEWF12X
0 0.81    1.62    3.24    4.86    6.48    8.1     9.72    11.34   13.77   16.2
0 0.876   1.752   3.504   5.256   7.008   8.76    10.51   12.26   14.89   17.52
0 0.7559  1.512   3.024   4.535   6.047   7.559   9.071   10.58   12.85   15.12
0 0.612   1.224   2.448   3.672   4.896   6.12    7.344   8.568   10.4    12.24
0 0.51    1.02    2.04    3.06    4.08    5.1     6.12    7.141   8.671   10.2
0 0.438   0.876   1.752   2.628   3.504   4.38    5.256   6.132   7.446   8.76
0 0.378   0.7559  1.512   2.268   3.024   3.78    4.535   5.291   6.425   7.559
0 0.3299  0.6598  1.32    1.98    2.639   3.299   3.959   4.619   5.609   6.598
0 0.2701  0.5402  1.08    1.62    2.161   2.701   3.241   3.781   4.591   5.402
0 0.21    0.4201  0.8402  1.26    1.68    2.1     2.52    2.941   3.571   4.201
```

```
      NEWF2
2.200E6  0.0502  1       1       1       1       1       1       1       1       1       1
3.543E-2 0       -1.091  -1.328  -1.385  -1.252  -1.085  -0.9078 -0.7142 -0.5173 -0.267  0
3.543E-2 0       -0.6531 -0.7949 -0.8289 -0.749  -0.6491 -0.5433 -0.4274 -0.3096 -0.1598 0
3.543E-2 0       -0.5636 -0.6859 -0.7152 -0.6463 -0.5601 -0.4688 -0.3688 -0.2671 -0.1379 0
3.543E-2 0       -0.4883 -0.5943 -0.6197 -0.56   -0.4853 -0.4062 -0.3196 -0.2315 -0.1195 0
3.543E-2 0       -0.437  -0.5318 -0.5546 -0.5011 -0.4343 -0.3635 -0.286  -0.2071 -0.1069 0
2.756E-2 0       -0.3838 -0.4672 -0.4871 -0.4402 -0.3815 -0.3193 -0.2512 -0.1819 -0.09391 0
2.756E-2 0       -0.3288 -0.4001 -0.4172 -0.377  -0.3267 -0.2735 -0.2151 -0.1558 -0.08043 0
1.969E-2 0       -0.2999 -0.365  -0.3806 -0.3439 -0.2981 -0.2495 -0.1963 -0.1422 -0.07337 0
1.969E-2 0       -0.2596 -0.316  -0.3295 -0.2978 -0.2581 -0.216  -0.1699 -0.1231 -0.06352 0
1.969E-2 0       -0.1415 -0.1722 -0.1796 -0.1623 -0.1406 -0.1177 -0.09259 -0.06707 -0.03461 0
```

```
      NEWF3
4.400E6  0.0556 1       1       1       1
5.920E-1 0        2.53    3.348   3.681   3.681
3.276E-1 0        1.521   2.006   2.208   2.208
2.872E-1 0        1.306   1.728   1.899   1.899
3.074E-1 0        1.119   1.489   1.638   1.638
3.301E-1 0        0.9954  1.325   1.454   1.454
3.113E-1 0        0.8757  1.166   1.282   1.282
2.566E-1 0        0.7435  0.9949  1.094   1.094
2.189E-1 0        0.6895  0.9139  1.007   1.007
1.736E-1 0        0.5903  0.7871  0.8623  0.8623
1.014E-1 0        0.3163  0.4217  0.4663  0.4663
```

```
      NEWF34X
0 1.622  3.24    4.862 6.48
0 1.752  3.504   5.256 7.008
0 1.512  3.024   4.535 6.047
0 1.224  2.449   3.673 4.898
0 1.02   2.039   3.059 4.079
0 0.878  1.752   2.63  3.504
0 0.7559 1.512   2.268 3.024
0 0.6614 1.319   1.98  2.638
0 0.5394 1.079   1.622 2.161
0 0.4213 0.8386  1.26  1.681
```

```
      NEWF4
4.400E6  0.0556  1        1        1        1
5.920E-1 0       -1.257   -1.314   -1.176   -1.014
3.276E-1 0       -0.754   -0.7899  -0.7091  -0.6104
2.872E-1 0       -0.6463  -0.6732  -0.6059  -0.5206
3.074E-1 0       -0.5524  -0.5764  -0.5187  -0.4419
3.301E-1 0       -0.4848  -0.5106  -0.4539  -0.3868
3.113E-1 0       -0.4326  -0.4484  -0.4009  -0.3429
2.566E-1 0       -0.3613  -0.3822  -0.3404  -0.288
2.189E-1 0       -0.3393  -0.3557  -0.3174  -0.2681
1.736E-1 0       -0.2894  -0.3009  -0.2662  -0.2315
1.014E-1 0       -0.15    -0.1581  -0.1419  -0.1217
```

NEWF5

4.4E6	0.0502	1	1
0.0E0	3.681	3.681	3.681
0.0E0	2.208	2.208	2.208
0.0E0	1.899	1.899	1.899
0.0E0	1.638	1.638	1.638
0.0E0	1.454	1.454	1.454
0.0E0	1.282	1.282	1.282
0.0E0	1.094	1.094	1.094
0.0E0	1.007	1.007	1.007
0.0E0	0.8623	0.8623	0.8623
0.0E0	0.4663	0.4663	0.4663

NEWF56X

6.362	6.48	6.598
6.89	7.008	7.126
5.937	6.047	6.157
4.823	4.898	4.972
4.055	4.079	4.102
3.48	3.504	3.528
2.776	3.024	3.276
2.614	2.638	2.661
2.138	2.161	2.185
1.657	1.681	1.705

NEWF6

4.4E6	0.0502	1	1
0.0E0	-1.014	-1.014	-1.014
0.0E0	-0.6104	-0.6104	-0.6104
0.0E0	-0.5206	-0.5206	-0.5206
0.0E0	-0.4419	-0.4419	-0.4419
0.0E0	-0.3868	-0.3868	-0.3868
0.0E0	-0.3429	-0.3429	-0.3429
0.0E0	-0.288	-0.288	-0.288
0.0E0	-0.2681	-0.2681	-0.2681
0.0E0	-0.2315	-0.2315	-0.2315
0.0E0	-0.1217	-0.1217	-0.1217

```
      NEWF7
 2.2E6 0.0502 0      0
 0.0E0 0.25   0.125 0
 0.0E0 0.25   0.125 0
 0.0E0 0.25   0.125 0
 0.0E0 0.25   0.125 0
 0.0E0 0.25   0.125 0
 0.0E0 0.25   0.125 0
 0.0E0 0.25   0.125 0
 0.0E0 0.25   0.125 0
 0.0E0 0.25   0.125 0
 0.0E0 0.25   0.125 0
```

```
      NEWF78X
15.2  15.7  16.2
16.15 16.83 17.52
13.87 14.5  15.12
11.24 11.74 12.24
 9.2   9.7  10.2
 7.76  8.26  8.76
 6.56  7.06  7.56
 5.6   6.1   6.6
 3.9   4.65  5.4
 2.95  3.58  4.2
```

```
      NEWF8
 2.2E6  0.0502  0      0
 0.0E0 -0.25   -0.125 0
 0.0E0 -0.25   -0.125 0
 0.0E0 -0.25   -0.125 0
 0.0E0 -0.125  -0.125 0
 0.0E0 -0.125  -0.125 0
 0.0E0 -0.125  -0.125 0
 0.0E0 -0.125  -0.125 0
 0.0E0 -0.125  -0.125 0
 0.0E0 -0.125  -0.125 0
 0.0E0 -0.125  -0.125 0
```

```
      NEWPHI
45 25.6 15.9 10.4 7.4 4.5 2.7 1.4 0.4 0
```

APPENDIX M

SAMPLE CALCULATION FOR RAYLEIGH'S METHOD

This example is taken from Biggs, Structural Dynamics, p. 170.

The simply supported beam of figure 1 has three regions. The central span has a mass intensity of

$$M_2 = .10 \frac{\text{lb sec}^2}{\text{in}^2}$$

and a bending stiffness of

$$EI_2 = 20 \times 10^9 \text{ lb in}^2.$$

The two ends have mass intensities of

$$M_1 = .050 \frac{\text{lb sec}^2}{\text{in}^2}$$

and bending stiffnesses of

$$EI_1 = 5 \times 10^9 \text{ lb in}^2.$$

The beam deflections are calculated by the conjugate beam method, in which the bending moment due to the elastic load is equal to the deflection. For the purpose of analysis, the beam is broken up into twenty equal segments. Since this is a simply supported beam, only the symmetric modes will be important. Each section is assigned a mass

FIG. M I

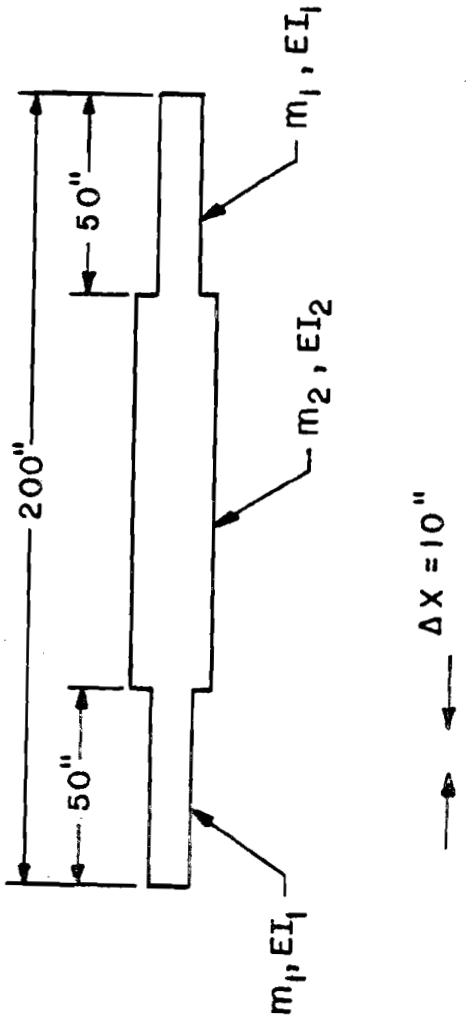

$$M_r = M(X)\Delta X.$$

Because of symmetry, only one half of the beam need be considered. For this half beam, five of the segments have an assigned mass of

$$M_r = .5 \frac{\text{lb sec}^2}{\text{in}}$$

and the other five an assigned mass of

$$M_r = 1.0 \frac{\text{lb sec}^2}{\text{in}}$$

since $\Delta X = 10$ inches.

The frequency is given by

$$\omega^2 = \frac{\sum_r M_r \phi_r' \phi_r''}{A'' \sum_r M_r (\phi_r'')^2}$$

where M_r = the mass at r,

ϕ_r' = the assumed mode shape at r,

ϕ_r'' = computed mode shape at r,

A'' = computed amplitude.

The computations leading to the frequency are shown in table 1. Any other method of computing the beam deflections would have led to the same result. The initial assumed mode shape is a sine curve. The left half of the beam is used for analysis.

TABLE MI.

		Sec. 1	Sec. 2	Sec. 3	Sec. 4	Sec. 5	Sec. 6	Sec. 7	Sec. 8	Sec. 9	Sec. 10	Σ
Cycle 1	M_r	0.5	0.5	0.5	0.5	0.5	1.0	1.0	1.0	1.0	1.0	
	Assumed shape, ϕ_r'	0.078	0.234	0.382	0.522	0.650	0.760	0.852	0.924	0.973	0.996	
	$P_{ri} = M_r\phi_r'$	0.039	0.117	0.191	0.261	0.325	0.760	0.852	0.924	0.973	0.996	
	Inertia shear, V_r (at left of load)	5.438	5.399	5.282	5.091	4.830	4.505	3.745	2.893	1.969	0.996	
	Inertia moment, $\mathfrak{M}$ (at midsection)	27.19	81.16	134.00	184.91	233.21	279.26	316.71	344.64	364.33	374.29	
	Elastic load, $(\mathfrak{M}/EI)\,\Delta x \times 10^6$	54.38	162.36	268.00	369.82	466.42	139.13	167.85	172.32	182.16	187.14	
	Elastic shear $\times 10^6$	2150	2105	1943	1675	1305	839	699	543	369	187	
	Elastic moment, $A''\phi_r'' \times 10^6$	10,800	31,850	51,280	68,030	81,060	89,470	96,460	101,880	105,570	107,440	
	ϕ_r'' $(A'' = 107{,}440 \times 10^{-6})$	0.100	0.296	0.477	0.633	0.755	0.831	0.898	0.948	0.982	1.000	
	$P_{ri}\phi_r''$	0.004	0.035	0.091	0.165	0.245	0.631	0.764	0.875	0.956	0.996	$\Sigma P_{ri}\phi_r'' = 4.782$
	$M_r(\phi_r'')^2$	0.005	0.044	0.114	0.200	0.288	0.691	0.894	0.895	0.908	1.000	$\Sigma M_r(\phi_r'')^2 = 5.003$
Cycle 2	Assumed shape, ϕ_r'	0.100	0.296	0.477	0.633	0.755	0.831	0.898	0.948	0.982	1.000	
	$P_{ri} = M_r\phi_r'$	0.050	0.148	0.238	0.316	0.378	0.831	0.898	0.948	0.982	1.000	
	Inertia shear, V_r (at left of load)	5.765	5.735	5.597	5.349	5.033	4.655	3.824	2.928	1.982	1.000	
	Inertia moment $\mathfrak{M}$ (at mid-section)	28.92	86.27	142.14	195.63	245.96	292.51	330.75	360.03	379.85	389.85	
	Elastic load, $(\mathfrak{M}/EI)\,\Delta x \times 10^6$	57.84	172.54	284.28	391.26	491.92	146.26	165.37	180.01	189.92	194.92	
	Elastic shear $\times 10^6$	2274	2216	2044	1760	1368	870	730	565	385	195	
	Elastic moment, $A''\phi_r'' \times 10^6$	11,370	33,530	53,970	71,670	86,250	94,010	101,310	106,960	110,810	112,760	
	ϕ_r'' $(A'' = 112{,}760 \times 10^{-6})$	0.101	0.298	0.479	0.636	0.757	0.835	0.900	0.950	0.984	1.000	
	$P_{ri}\phi_r''$	0.005	0.044	0.114	0.201	0.286	0.695	0.807	0.899	0.966	1.000	$\Sigma P_{ri}\phi_r'' = 5.017$
	$M_r(\phi_r'')^2$	0.005	0.044	0.115	0.202	0.287	0.697	0.810	0.902	0.968	1.000	$\Sigma M_r(\phi_r'')^2 = 5.030$
	$P_{ri}\phi_r''$	1.01p_1	2.98p_1	4.79p_1	6.38p_1	7.57p_1	8.35p_1	9.00p_1	9.50p_1	9.84p_1	10.00p_1	$\Sigma P_{ri}\phi_r'' = 69.46p_1$

TAKEN FROM BIGGS, STRUCTURAL DYNAMICS

The computed natural frequency at the end of the first cycle is

$$\omega_1 = 94.13 \text{ radians/sec.}$$

At the end of the second cycle, the computed frequency is

$$\omega_2 = 94.05 \text{ radians/sec.}$$